การพัฒนาตัวรับรู้ไอออนโลหะจากอนุพันธ์คราวน์อีเทอร์เทียมที่มีหมู่ไดเอโซ

นายอธิป อนุพันธ์

วิทยานิพนธ์นี้เป็นส่วนหนึ่งของการศึกษาตามหลักสูตรปริญญาวิทยาศาสตรมหาบัณฑิต
สาขาวิชาเคมี ภาควิชาเคมี
คณะวิทยาศาสตร์ จุฬาลงกรณ์มหาวิทยาลัย
ปีการศึกษา 2558

DEVELOPMENT OF METAL ION SENSORS

BASED ON DIAZO PSEUDOCROWN ETHER DERIVATIVES

Mr. Athip Anupan

A Thesis Submitted in Partial Fulfillment of the Requirements

for the Degree of Master of Science Program in Chemistry

Department of Chemistry

Faculty of Science

Chulalongkorn University

Academic Year 2015

Thesis Title	DEVELOPMENT OF METAL ION SENSORS BASED ON DIAZO PSEUDOCROWN ETHER DERIVATIVES
By	Mr. Athip Anupan
Field of Study	Chemistry
Thesis Advisor	Assistant Professor Saowarux Fuangswasdi, Ph.D.

Accepted by the Faculty of Science, Chulalongkorn University in Partial Fulfillment of the Requirements for the Master's Degree

.....Dean of the Faculty of Science
(Associate Professor Polkit Sangvanich, Ph.D.)

THESIS COMMITTEE

.....Chairman
(Associate Professor Vudhichai Parasuk, Ph.D.)

.....Thesis Advisor
(Assistant Professor Saowarux Fuangswasdi, Ph.D.)

.....Examiner
(Numpon Insin, Ph.D.)

.....Examiner
(Assistant Professor Anawat Ajavakom, Ph.D.)

.....External Examiner
(Gamolwan Tumcharern, Ph.D.)

อธิป อนุพันธ์ : การพัฒนาตัวรับรู้ไอออนโลหะจากอนุพันธ์คราวน์อีเทอร์เทียมที่มีหมู่ไดเอโซ (DEVELOPMENT OF METAL ION SENSORS BASED ON DIAZO PSEUDOCROWN ETHER DERIVATIVES) อ.ที่ปรึกษาวิทยานิพนธ์หลัก: ผศ. ดร.เสาวรักษ์ เฟื่องสวัสดิ์, 79 หน้า.

ทำการสังเคราะห์อนุพันธ์คราวน์อีเทอร์เทียมที่ต่อกับหมู่เอโซเบนซีนชนิดใหม่ 5 อนุพันธ์ โดยใช้ปฏิกิริยาควบคู่เอโซของโอลิโกเอทิลลีนไดอะมิโนเบนซีนกับเอทิล-2-อะมิโนเบนโซเอตหรือ 4-ไนโตรอะนิลีน ทำการพิสูจน์เอกลักษณ์โดยเทคนิค ^{1}H, ^{13}C-NMR และแมสสเปกโตรสโกปี ผลศึกษาสมบัติการตรวจวัดพบว่า แม้สารละลายของอนุพันธ์เอสเทอร์ไม่แสดงการเปลี่ยนสีที่ชัดเจนในภาวะที่มีไอออนโลหะ แต่การเติมไอออนโลหะหนักหรือทรานสิชัน (Cu^{2+}, Zn^{2+}, Cd^{2+}, Hg^{2+}, Pb^{2+}) สามารถทำให้สารละลายของอนุพันธ์ไนโตร D3N ใน DMSO เปลี่ยนสีจากสีน้ำตาลอ่อน (λ_{max} 404 nm) เป็นสีส้มอ่อนที่มีสัญญาณการดูดกลืนแสงใหม่ที่ 490 nm ได้ การเติมไอออนลบที่มีความเป็นเบสสูงอย่าง OH^-, F^-, CN^- ยังเปลี่ยนสีของสารละลาย D3N ให้เป็นสีม่วงเข้มที่แสดงการดูดกลืนแสงใหม่ช่วง 570-576 nm ซึ่งสามารถเปลี่ยนเป็นสีส้มเมื่อเติมไอออนโลหะหนักหรือทรานสิชันลงไป ผลการเปลี่ยนสีเหล่านี้ทำให้ใช้สารละลาย D3N ที่มีการเติมไฮดรอกไซด์จำนวน 2 เท่าเพื่อใช้ตรวจวัดไอออนโลหะเหล่านี้ด้วยตาเปล่า ทั้งนี้แม้ D3N ไม่แสดงการเปลี่ยนสีแบบจำเพาะต่อไอออนชนิดใดชนิดหนึ่ง แต่ยังสร้างกราฟมาตรฐานสำหรับการวิเคราะห์ปริมาณไอออนต่างๆ ในระดับน้อยมากได้ อาทิ ใช้การดูดกลืนแสงของสารละลาย D3N 20 μM ใน DMSO ที่ความยาวคลื่น 574 nm เพื่อวัดปริมาณ CN^- ในช่วงเส้นตรงระหว่าง 2 ถึง 10 μM ที่มีค่าสัมประสิทธิ์สหสัมพันธ์ R^2 = 0.9956 นอกจากนี้ยังพบว่ากราฟมาตรฐานสำหรับการวัดปริมาณไอออนโลหะหนักหรือทรานสิชันในภาวะที่เป็นเบสให้ค่า R^2 ในระดับดีมาก เช่น R^2 0.9968 ในกรณีของ Cd^{2+} เป็นต้น ผลทั้งหมดนี้แสดงถึงการประยุกต์ D3N เป็นตัวรับรู้ที่มีสีสำหรับไอออนลบที่มีความเป็นเบสสูงรวมถึงไอออนโลหะหนักและทรานสิชัน

ภาควิชา เคมี ลายมือชื่อนิสิต .....

สาขาวิชา เคมี ลายมือชื่อ อ.ที่ปรึกษาหลัก .....

ปีการศึกษา 2558

5572194823 : MAJOR CHEMISTRY

KEYWORDS: DIAZO PSEUDOCROWN ETHER, TRANSITION METAL IONS, HEAVY METAL IONS CYANIDE ION, CHROMOGENIC SENSOR

ATHIP ANUPAN: DEVELOPMENT OF METAL ION SENSORS BASED ON DIAZO PSEUDOCROWN ETHER DERIVATIVES. ADVISOR: ASST. PROF. SAOWARUX FUANGSWASDI, Ph.D., 79 pp.

Five novel pseudocrown ether derivatives terminating with azobenzene moieties were synthesized via azo coupling of oligoethylenediaminobenzene with ethyl-2-aminobenzoate or 4-nitroaniline, and characterized by ^{1}H, ^{13}C-NMR, and mass spectroscopies. The presence of metal ions in the solution of ester derivatives displayed indistinguishable color changes whereas D3N, a nitro derivative showing light brown in DMSO with λ_{max} at 404 nm, turned to light orange with a new peak around 490 nm in the presence of transition or heavy metal ions (Cu^{2+}, Zn^{2+}, Cd^{2+}, Hg^{2+}, Pb^{2+}). The presence of strong basic anion (OH^-, F^-, CN^-) also produced dark purple solution with a new absorption band around 570-576 nm, which turned to orange upon adding transition or heavy metal ions. These color changes could be used for naked-eye detection of these metal ions in the presence of 2 equivalents of hydroxide ion. Although D3N solution could not selectively change color toward any particular ion, a calibration curve employing the absorption intensity of 20 μM D3N in DMSO at 574 nm could be constructed to determine trace quantity of CN^- with a linear range between 2 to 10 μM with R^2 = 0.9956. In addition, calibration curves for transition or heavy metal ions were constructed under a basic condition with excellent correlation coefficient, e.g. R^2 = 0.9968 for Cd^{2+}. Thus D3N could be employed as chromogenic sensor for strong basic anions and transition or heavy metal ions.

Department: Chemistry Student's Signature .....

Field of Study: Chemistry Advisor's Signature .....

Academic Year: 2015

ACKNOWLEDGEMENTS

This thesis would have never been completed without the support from many people. During the period of the research study, I encountered lots of good and bad times, which made me grow stronger and know how to enjoy my life in every moment.

First of all, I would like to honestly and appreciatively acknowledge my kind-hearted research advisor Assistant Professor Dr. Saowarux Fuangswasdi for encouraging me to overcome all obstacles in this thesis and my life. Although I was hardly a good student in her expectation, she had never neglected me. All of my gratitude, I thus give to my beloved teacher.

It is a sincere pleasure to express my deep sense thanks to the committee (Assoc. Prof. Dr. Vudhichai Parasuk, Assist. Prof. Dr. Anawat Ajavakom, Dr. Numpon Insin, and Dr. Gamolwan Tumcharern) for the kindness and enthusiasm suggestions, which were very helpful.

Furthermore, I am grateful to the partial financial support from Thailand Research Fund (RTA5380003) and Teaching Assistant scholarship.

In addition, it is my privilege to thank Supramolecular Chemistry Research Unit (SCRU) for leading me to meet the wonderful relationship between me and my seniors, juniors and friends. These lovely SCRU members and their friends of friends had helped me many times while I was doing my experiments. Thank you for giving me the useful advices for solving several problems in my work and life.

Finally, I cannot find the proper word to thank for the precious support from my beloved family who always cheers up and stands beside me when I feel down. I am not able to imagine how I can finish this thesis in the absence of their loves.

Athip Aupan

CONTENTS

Page

Page

Page

LIST OF FIGURES

LIST OF SCHEMES

LIST OF ABBREVIATIONS AND SYMBOLS

g	gram
mg	milligram
ml	milliliter
cm	centimeter
nm	nanometer
mmol	millimole
M	molar
mM	millimolar
μM	micromolar
eq	equivalent
ppm	part per million
MHz	megahertz
°C	degree Celsius
δ	chemical shift
m/z	mass-to-charge ratio
λ_{max}	maximum absorption
R^2	correlation coefficient
o, p	position of substituent on aryl group (ortho, para)
s, d, t, m	splitting patterns of ^{1}H-NMR (singlet, doublet, triplet, multiplet)
Ar	aryl moiety
Et	ethyl moiety
Me	methyl moiety
Ts	tosyl moiety
TsCl	tosylchloride
CCA	cinnamic acid
DMAP	4-dimethylaminopyridine
Et_3N	triethylamine
HCl	hydrochloric acid
$NaBH_4$	sodium borohydride

NaOH	sodium hydroxide
$NaNO_2$	sodium nitrite
CH_2Cl_2	dichloromethane
DI H_2O	deionized water
DMSO	dimethylsulfoxide
EtOH	ethanol
EtOAc	ethyl acetate
MeOH	methanol
THF	tetrahydrofuran
TLC	Thin-Layer Chromatography
ESI	Electrospray Ionization Mass Spectrometry
MALDI-TOF	Matrix-Assisted Laser Desorption/Ionization Time-of-Flight Mass Spectrometry
^{1}H-NMR	Proton Nuclear Magnetic Resonance Spectrometry
^{13}C-NMR	Carbon-13 Nuclear Magnetic Resonance Spectrometry
IR	Infrared Spectroscopy
UV-vis	UV-visible Spectrometry
ICT	Intra-molecular Charge Transfer

CHAPTER I
INTRODUCTION

1.1 Overview of supramolecular chemistry

"Supramolecular chemistry", named by Prof. Lehn (Nobel laureates in chemistry in 1987), is about intermolecular bond, including structures and functions of the entities composed by association of two or more chemical substrates. Molecular associations have been known and studied for several decades [1, 2] and the term of "übermoleküle or supermolecule" was invented by Karl Lothar Wolf *et al* to refer the higher organized entities caused by the association coordinatively saturated species [2-4]. Supramolecular species can be formed by the selective binding of a "molecular receptor" toward a "substrate" [3, 4]. This molecular interaction creates the basis of extremely specific processes such as recognition, regulation, transportation, etc. already found in nature, for example, as in protein receptor-substrate binding, protein-protein assembling, enzymatic reaction, cellular recognition [4]. These natural processes are an inspiration for the design of molecular recognition for specific application using chemical knowledge. The strategy for creating receptor molecules capable of featuring performances of best efficiency and selectivity requires the correct manipulation of the stereochemical and energetic complements of the non-covalent being known as intermolecular force, *i.e.*, hydrogen bonding, van der Waals force, electrostatic interaction, etc. within an indicated molecular architecture [1, 2]. So, the structure of supermolecule is the consequence of both additive and cooperative interactions, including hydrogen bonding, hydrophobic interaction, and coordination, and their properties are different, often better, than the sum of the properties of each individual element.

1.2 Molecular recognition design of metal sensor: Chromogenic sensor

In several decades after the introduction of "supramolecular chemistry", the researches in this field have risen especially for metal ion sensing devices because

metal ions are found in several important processes in industries, environment and biological systems which involve regulatory parts of life processes [5-8]. However some metal ions such as cadmium, mercury, and lead can induce a fatal illness when only a little amount of these metals gets into organism and these toxic metal ions can be found in the environment via contamination of industrial wastes [8-10].

Among several concepts for metal ion determination, the development of chromoionophore is one of the highly active studied fields [11-13] because it can be applied to naked-eye sensor, which is a simple technique providing a real-time and inexpensive detection [6, 9, 13-15]. The *chromoionophore* consists of two functional parts: one is ion recognition or *ionophore*; which is able to bind with ions via non-covalent bond induced by the contrast of (partial) charge between binding site and ions; and the other is optical signal reporter or *chromophore*, which is able to transform the electronic phenomena in molecule to optical signals [5, 6, 8-10, 15-22].

There are many classes of ionophore for metal ions such as acyclic ligands, macrocyclic molecules, and three dimensional molecular hosts. One of the artificial host molecule being known as "crown ether" was coincidentally discovered by Pedersen from the by-product in the preparation of complexing agent for divalent cations [1, 17, 23, 24]. This cyclic hexaether compound was able to increase the solubility of potassium permanganate in benzene or chloroform and displayed a very stable potassium ion inclusion complex like the antibiotic "valinomycin", the first reported natural ionophore for the transport of potassium ions though the organism membrane by complexation [1, 23, 25, 26]. The study of the mechanism of complex formation of alkali and alkaline earth metal ions with crown ethers revealed that oxygen atoms could act as binding sites for metal ions and the crown size was critical to selective metal ion binding behavior. According to the basic structure of crown ether consisting of a ring of alternate oxygen atoms and ethylene moieties, *i.e.* $-OCH_2CH_2OCH_2CH_2-$, Weber and Vögtle were interested in the ring opening and subsequent addition at the terminal oxygen atoms to study the changes in the complexation behavior [27, 28]. They gave the term "podands" to refer a class of acyclic artificial hosts with pendent binding sites, *e.g.* polyamines, polyethers or

polyethylene glycols [24, 29]. Although these acyclic hosts usually show less cation affinity than their cyclic analogues because of their higher degree of flexibility, leading to lacking of preorganization, they can exhibit wrapping conformations like pseudocrown ethers in the presence of proper metal ions, which create cavities of appropriate sizes during interaction with metal ions or neutral molecules in a unique manner. The opened-chain ligands are able to increase their binding efficiency via the modification at the terminal chains with the rigid moieties (*e.g.* aryl, ester, and amide) for the extra degree of organization of host molecules [27-37].

In the part of chromophores, the color expression of the molecule occurs by the absence of some wavelengths of the visible region toward the absorption of visible light energy, which corresponds to the required energy for promoting π electrons in the molecule from the ground state to the excited state (a lower energy state to a higher energy state) by specific bonds in the molecule involving the π electrons delocalization [38, 39]. The required energy for this transition can decrease if the conjugated double bonds exist in the molecule. For example, the presence of aromatic rings is able to make the excitation of the electron easier due to the enhanced delocalization of the π electrons. The chromogenic organic compounds also consist of aromatic rings with an extensive conjugated double bond system bearing unsaturated moieties as chromophores, *i.e.* azobenzene (aromatic rings with N=N moieties), nitronaphthalene (bicyclic aromatic rings with NO_2 moieties, benzodifuranone (polycyclic aromatic rings with C=O moieties), etc. [38-41]. Furthermore, the color of the molecule can be more intense by an addition of auxochromes, the electron-donating functional groups, into the aromatic rings such as oxy (-O-) and amino ($-NH_2$, -NHR, $-NR_2$) moieties [38, 39].

The sensing property of the chromoionphoric sensor can be improved in several ways such as the modification of binding site of ligand, the development of signaling part of ligand. The design of chromoionophoric sensor as a ditopic receptor is an interesting concept because of a selective binding. After binding with the first target, the ditopic molecules can form an appropriate structure for the second target recognization. This ditopic receptor phenomenon is similar to biochemical enzyme

processes known as allosteric effect, of which the enzyme bind with the protein target at allosteric site (non-active site for the protein target) causing the inhibition or catalysis of biochemical processes [24, 42-44] as shown in Figure 1.1.

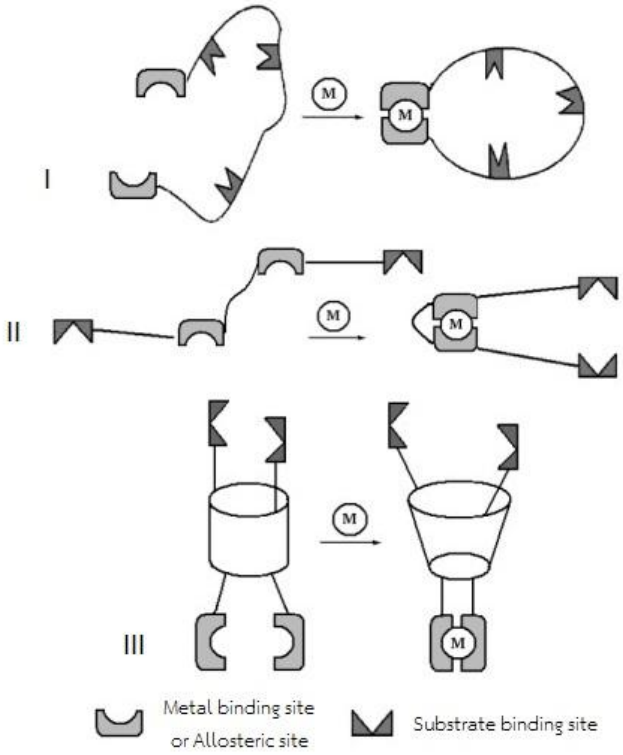

Figure 1.1 Allosteric effect on three kinds of ditopic sensor [42]

1.3 Allosteric effect on chromoionophoric molecules

In 1993, Nabeshima *et al.* [19] found a novel derivative of polyether as pseudo crown ether, which was able to bind alkali metal ion like crown ether via allosteric effect (Figure 1.2). When introducing Cu^{+} to this polyether, Cu^{+} interacted with two bipyridine moieties and induced preorganization of polyether linkage to exhibit the alkali metal ions binding site like crown ether. This event was followed by ^{1}H-NMR and UV-visible spectroscopies. The binding of alkali metal ions could be controlled by crown ether size and repulsion from Cu^{+}.

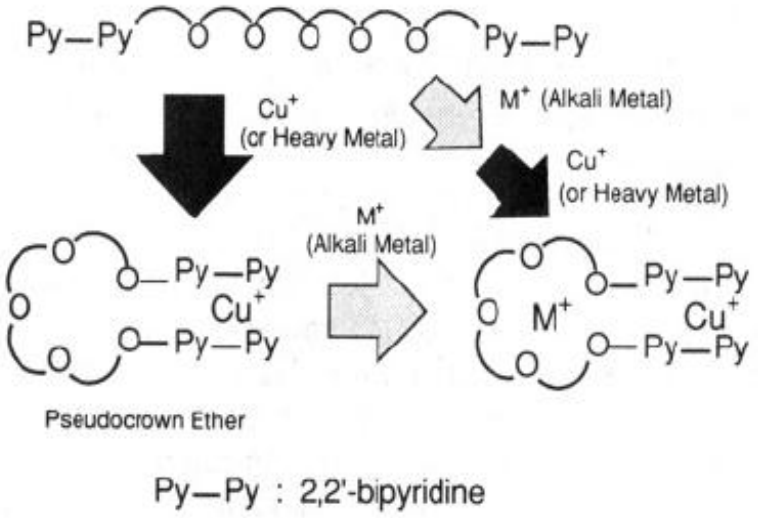

Figure 1.2 The presence of allosteric effect on psuedocrown ether based on 2,2'-pyridine toward Cu^{+} [19]

In 2005, Liu and coworkers [45] synthesized 4,4'-[(ethylenedioxy) bis(ethyleneoxy)]bis[1-(2-imidazo[4,5-*f*]-1,10-phenanthroline)-benzene] which gave blue fluorescent emission and was able to form complex with Mg^{2+} to generate green fluorescent emission via stacking of phenanthroline moieties. This phenomenon occurred from a result of a rearrangement of polyether to crown ether-like bridge when Mg^{2+} was introduced to this molecule as shown in Figure 1.3.

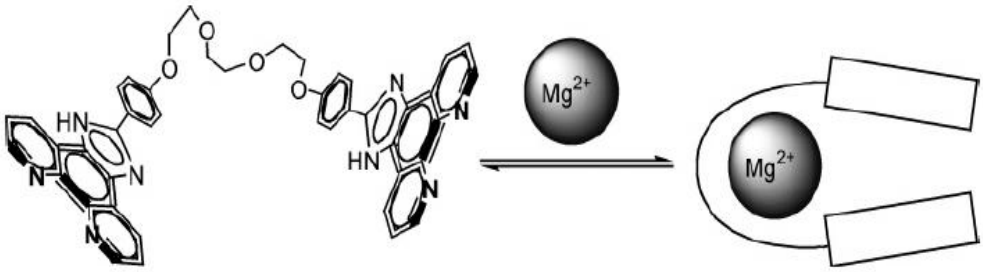

Figure 1.3 Complexation of 4,4'-[(ethylenedioxy)bis(ethyleneoxy)]bis[1-(2-imidazo [4,5-*f*]-1,10-phenanthroline)-benzene] with Mg^{2+} [45]

In 2002, Nishimura *et al.* [46] reported that an excellent selectivity of novel pseudo thiacrown ether toward Ag^{+} due to a pseudo cyclic structure formed by hydrophobic interaction of its lipophilic moieties in water (Figure 1.4), which was

confirmed by ^{1}H-NMR spectroscopy. Only the presence of Ag^{+} could decrease fluorescence and the stability constant in logarithm unit (log K) followed by fluorometric titration was approximately 4.2, which was similar to that by cyclic dithia-18-crown-6.

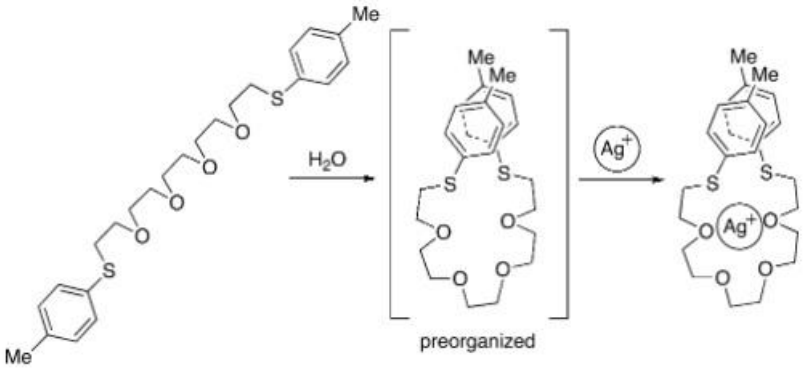

Figure 1.4 Preorganized of amphiphilic thioether bearing two methylbenzene moieties in water and its Ag^{+} complex [46]

In 2009, Kumar and coworkers [44] studied the allosteric effect on three novel thiacalix[4]-crown ditopic sensors using ^{1}H-NMR, fluorescence, and UV-visible spectroscopies. Although these molecules were able to firstly bind with K^{+} using crown ether moiety, the presence of a second metal ion such as Ag^{+}, Pb^{2+}, Cu^{2+} could chase K^{+} off and interacted with the hosts with a higher stability constant. The allosteric effect from K^{+} binding to allow a second metal ion interaction then prevented K^{+} to rebind with crown ether moiety because it could not go through a regulating gate formed by this second metal ion (Figure 1.5).

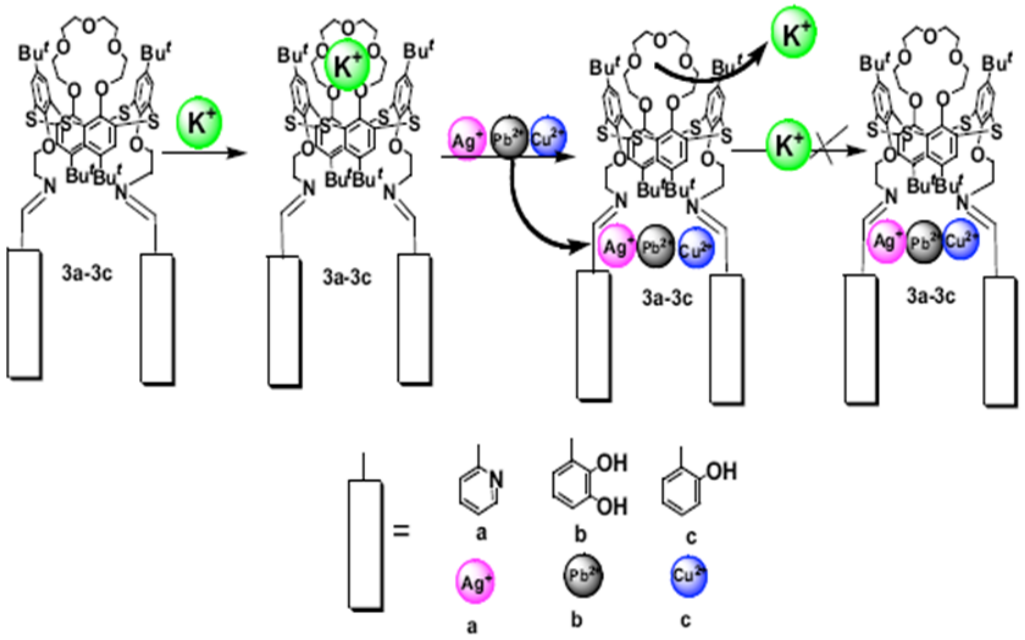

Figure 1.5 The presence of allosteric effect on three thiacalix[4]-crown ether derivatives upon the addition of metal ions [44]

1.4 Chomogengic metal sensors based on azo-dye

In 2009, Nuriman *et al*. [11] reported that a new chromogenic sensor based on tris[2-(4-phenyldiazenyl)phenylaminoethoxy]cyclotriveratrylene (TPPECTV) changed color from yellow (450 nm) to red-orange (490 nm) toward Hg^{2+} in 10% MeOH-H_2O solution. Moreover, the selectivity and sensitivity of this ligand, compared to its corresponding azo dye 4-aminoazobenzene, toward Hg^{2+} was enhanced by a factor of 10 because the three arms in cyclotriveratrylene platform were preorganized to give tripodalchromophore which bound with Hg^{2+} firmly (Figure 1.6).

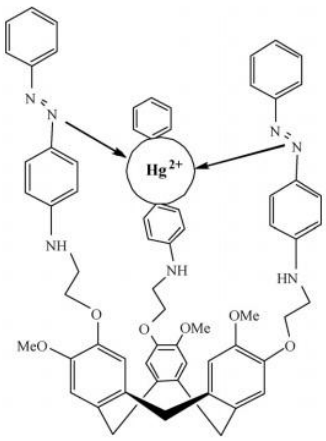

Figure 1.6 Interaction mode between TPPECTV and Hg^{2+} [11]

In 2011, Cheng *et al*. [47] designed two novel naked-eye chemosensors for Hg^{2+} based on azobenzene and dithioacetal. These sensors were able to detect Hg^{2+} via Hg^{2+}-promoted deprotection of the dithioacetal, leading to an intra-molecular charge transfer (ICT) as signaling mechanism. Using IR and ESI mass spectroscopies, it was revealed that Hg^{2+} could form an N-bound Hg^{2+} complex (Figure 1.7).

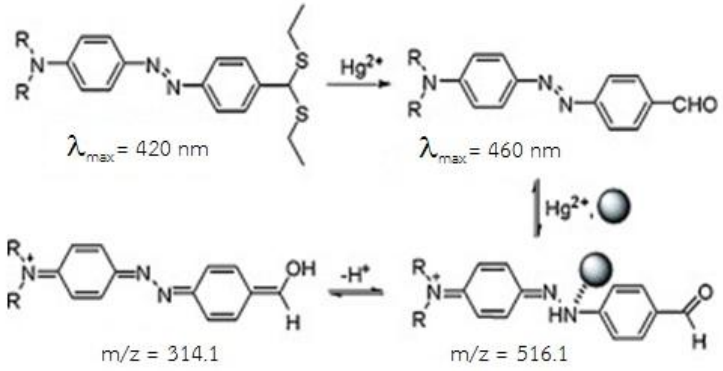

Figure 1.7 Postulated interaction of **2** toward Hg^{2+} [47]

In 2012, Yang and coworker [48] reported sensing properties of a novel *o*-hydroxybenzoyl-(N-butyl-4,6-naphthamimide) hydrazone **1** for Cu^{2+} and F^{-} by UV-visible, fluorescence, and ^{1}H-NMR spectroscopies (Figure 1.8). This chromogenic and fluorogenic sensor **1** showed the suppression of the absorption and fluorescent intensities upon the addition of Cu^{2+} due to a decreasing in electron density of the nitrogen atom on the NH moiety in the hydrazone tautomer and intra-molecular

charge transfer (ICT) process caused by Cu^{2+} interaction. In the case of F^{-}, the maximum absorption of **1** was shifted from 441 nm to 572 nm (red shift) and the fluorescent intensity was quenched because of the deprotonation of NH and OH moieties.

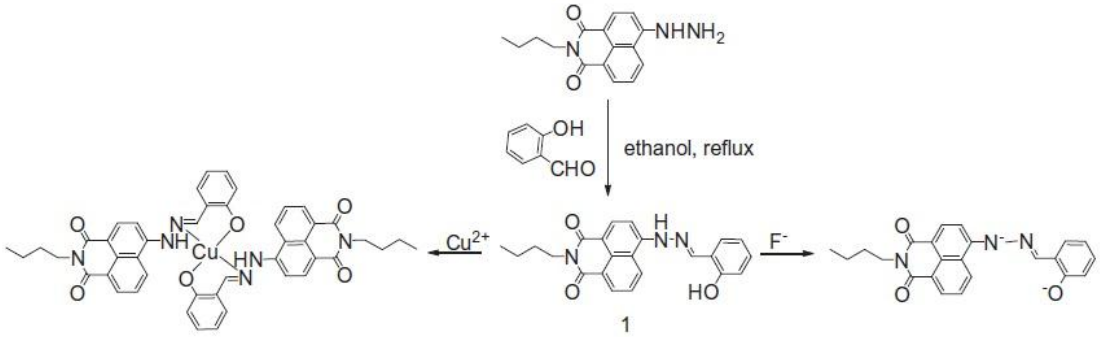

Figure 1.8 Preparation and concept for bifunctional sensor of *o*-hydroxybenzoyl-(N-butyl-4,6-naphthamimide) hydrazone [48]

1.5 Azo-hydrazone tautomerism

In 1960, Lewis [49] studied the tautomerism of 4-aminoazobenzene derivatives in solution using IR and UV-visible spectroscopies and found that these molecules coexisted as hydrozone ($\mathbf{I_a}\leftrightarrow\mathbf{I_b}$) and azo (**II**) in tautomeric equilibrium.

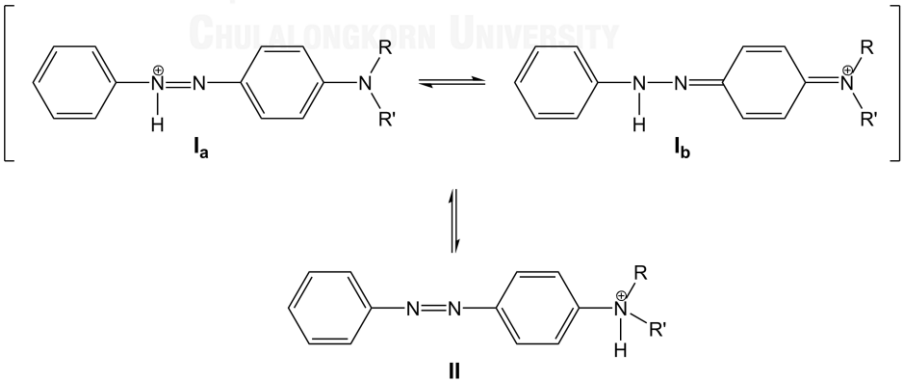

Figure 1.9 General tautomeric structure of 4-aminoazobenzene derivatives [49]

In 2008, Matazo and coworkers [50] followed the protonation on aminoazobenzene derivatives by UV-visible and resonance Raman spectroscopies, and discussed the outcomes using quantum-chemical calculations. The calculations

revealed that the azo-hydrazone tautomeric equilibrium of the protonated species (Figure 1.10) could involve the chromophoric moieties supported by the resonance Raman enhancement patterns. The hydrazone form showed a maximum absorption to a longer wavelength, with a difference of around 120 nm from that of the azo form. This phenomenon was caused by a large difference in electronic dipole moment between ground and excited states due to the enhancement of the electron delocalization of the quinoid structure in hydrazone form.

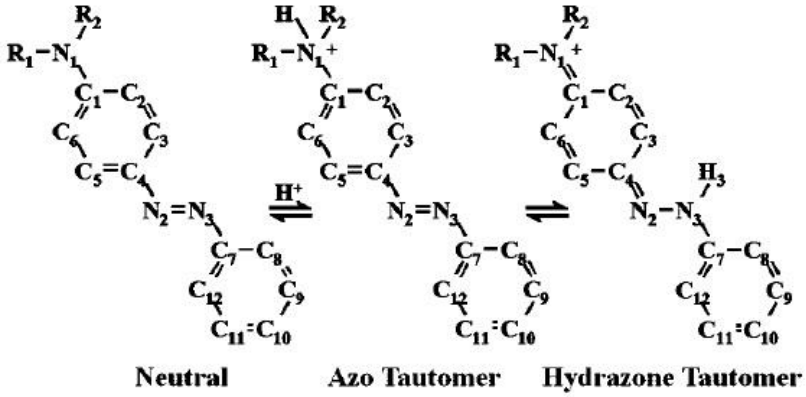

Figure 1.10 Structures of the neutral and protonated species of 4-amino (R = H) and 4-(dimethylamino)azobenzene (R =CH_3) involving the azo-hydrazone tautomeric equilibrium [50]

In 2012, Chen *et al.* [51] reported that the azo-hydrazone tautomerism of pyridine-2,6-dione-based Disperse Yellow Dyes was controlled by pH and metal ion complexation (Figure 1.11), which were investigate by UV-visible spectroscopy, ^{1}H-NMR spectroscopy, and X-ray single-crystal diffraction technique. The two dyes exhibited the equilibrium between azo ($HL_{1\text{-}A}$ and $HL_{2\text{-}A}$) and hydrazone ($HL_{1\text{-}H}$ and $HL_{2\text{-}H}$) forms. The hydrazone form was dominant at pH < 9 due to the cooperative effect of the hydrazone proton to induce a six-membered ring from intramolecular hydrogen bond. This hydrazone form displayed the maximum absorption at longer wavelength of around 100 nm from that of azo form. The azo form, however, was dominant during the complexation of dinuclear Cu^{2+} complexes ($Cu_2(L_{2\text{-}A})_4$) due to the fixation of coordinative bonds and favorable configuration for Cu^{2+} binding, which

showed the maximum absorption in the shorter wavelength shift of 34 nm compared to the signal of free $HL_{2\text{-}H}$.

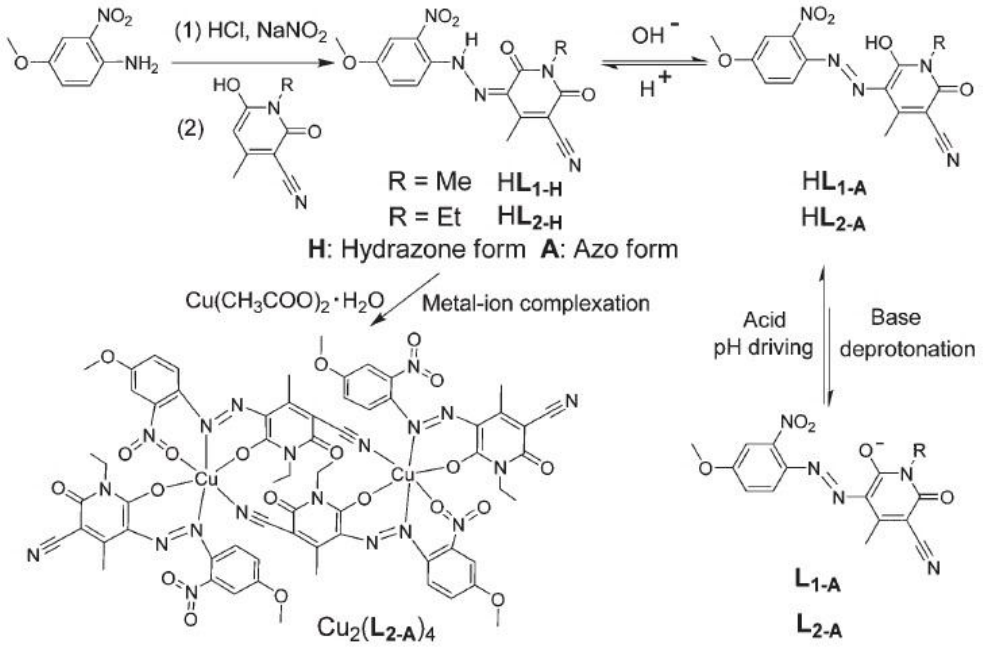

Figure 1.11 Preparation and azo–hydrazonetautomerism of pyridine-2,6-dione based Disperse Yellow dyes and their metal ion complexes [51]

1.6 Polyether azobenzene derivatives

In 2008, Harikrishnan and Menon [52] synthesized a series of crown ethers bearing azo dye moiety (Figure 1.12) which exhibited bright color from deep red (λ_{max} 546 nm) to yellow (λ_{max} 384 nm). This series of azo dyes were thermally stable up to 200 °C and resistant to acidic circumstance. So, these dyes were proper to use in all kinds of inks, especially as printing ink for uncoated paper due to good light and water fastness properties.

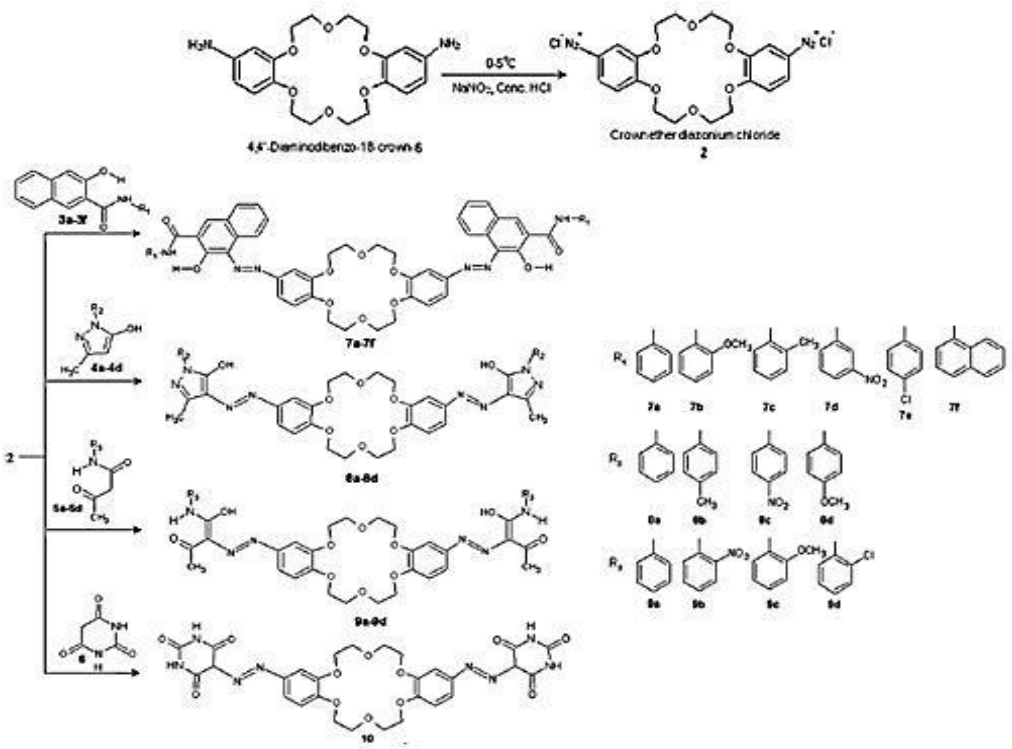

Figure 1.12 Synthetic pathway of crown ethers based azo dye [52]

In 2011, Langmuir films on the air-water interface of a series of liquid-crystalline azo dyes consisting of oligoethylene glycol terminated by amino and nitro subsitituted azobenzene units displayed blue shifted absorbance at λ = 394-410 nm due to the formation of H-aggregates as shown in Figure 1.13 [53].

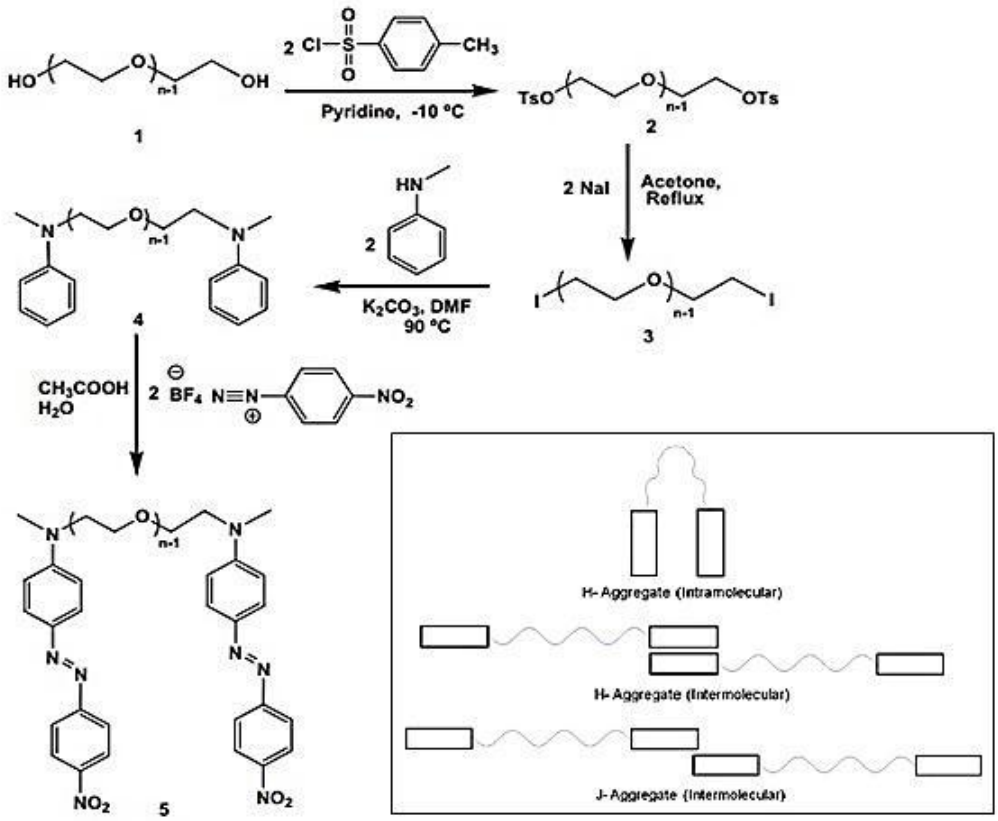

Figure 1.13 Synthetic pathway of two amino-nitro azobenzene units linked by oligoethylene glycol and aggregate formation of dyes in Langmuir films (in box) [53]

1.7 Concept of this research

There are many metal ion sensors based on several techniques such as fluorescence spectroscopy, cyclic voltammetry, etc. Unfortunately, some of these techniques need expensive and complicated instruments, which must to be used by the experts leading to a high price for analysis. To reduce the cost of the determination of metal ions in trace amounts, the design of naked-eye sensor for metal ion is interesting because it provides an easy, inexpensive and real-time analysis. Choromogenic sensor can also employ simple UV-visible spectrophotometer for detailed quantitative and qualitative analyses. A ditopic receptor is even more promising because of the allosteric effect. The designed chromoionophores in this research thus consisted of a diaza-pseudo crown ether units acting as the first ionophore linked to π-conjugated diazo aromatic bonds acting as both ionophore

and chromophore. Ester units were also introduced to assist the binding with metal ions. The synthesis of the design sensors would benefit from the fact that the precursor of required components such as polyethylene glycol and nitrite salt are common and inexpensive and the azo coupling reaction is a known and rather simple reaction.

The design of ligands in this research was varied in several positions in hope for the optimization of metal ion sensing property. The first set of the ligands in this study was ester derivatives. The expected ionophores in this set were (a) aza-polyether chain and (b) ester units. Polyglycol chain containing oxygen atoms is known to be good acceptor for alkali or alkaline earth metal ions and could arrange its conformation to wrap around suitable metal ions like pseudocrown ether. The ester moieties on benzene rings at the end of both chains were hoped to bind with heavy or transition metal ions [11, 54, 55] like forceps.

The second set of the ligand in this research was designed to vary the functional group on the ending benzene rings from ester to nitro group. A series of nitro pseudocrown ether derivatives was in focus based on the expectation that improving the efficiency of electron distribution in π conjugated system would be good for optical expressions. In a good π electron distribution system, the presence of the interaction between ligand and metal ions should affect the direction of electron flow causing the suppression or enhancement of the charge transfer interactions between electron-rich and electron-deficient substituents on aryl groups, which could induce the great change of required energy for the excitation of π electron leading the obvious appearance of new UV-visible absorption spectra and color expression. The architecture of the good π electron distribution system consists of good electron donor and electron acceptor components in opposite direction for the productive charge transfer. Generally, a good couple of electron donor and electron acceptor was known as amino and nitro groups, respectively, due to the lone pair on nitrogen atom in amino moiety as the electron-rich part and the partial positive charge on nitro moiety as the electron-deficient part [41, 56-59]. In

this series, the nitrogen atoms in diazacrown unit and the nitro substituents on ending benzene rings would act as electron donor and acceptor, respectively.

1.8 Objective and scope of this research

1) To synthesize and characterize diazo pseudocrown ether derivatives bearing ester and nitro functional groups
2) To study their color expression and optical sensing properties towards metal ions by naked-eye observation and UV-Visible spectrophotometry
3) To study the allosteric effect upon binding with different metal ions

CHAPTER II

EXPERIMENTS

2.1 General procedure

2.1.1 Materials

All chemicals and solvents were of analytical grade from Sigma-Aldrich or Merck and used without further purification. Tetrahydrofuran (THF) was distilled over sodium and benzophenone under nitrogen. Thin-layer chromatography (TLC) was performed on silica gel plates (Kieselgel 60, F_{254}, 1 mm, Merck). Column chromatography was carried out using silica gel (Kieselgel 60, 0.063 - 0.200 mm, Merck) or alumina gel (Aluminium oxide 90 standardized, 0.063 - 0.200 mm, Merck).

2.1.2 Instruments

Nuclear Magnetic Resonance (NMR) spectra were collected via a Varian Mercury Plus 400 NMR and Bruker DRX 400 MHz spectrometers. All chemical shifts were exhibited in part per million (ppm) using the residual proton or carbon signals in deuterated solvents as internal references. Elemental analysis was investigated on Perkin Elmer PE2400 series II (CHNS/O analyzer) by ignition combustion gas chromatography separated by frontal analysis and qualitative detected by thermal conductivity detector. MALDI-TOF mass spectra were recorded on Bruker Daltonics MALDI-TOF using 2-cyano-4-hydroxy cinnamic acid (CCA) as matrix. UV-visible absorption spectra were measured on a Varian Cary 50 UV-Vis spectrophotometer.

2.2 Syntheses

A series of 5 azo dye-based pseudocrown ethers containing either ester or nitro group with different numbers of oxygen atoms in glycol chain was synthesized by coupling of oligoethylenediaminobenzene with ethyl-2-aminobenzoate or 4-nitroaniline as shown in Scheme 2.1 and characterized by ^{1}H, ^{13}C-NMR, mass

spectroscopies and elemental analysis. The synthesis details for each step were described in the following parts (2.2.1.1 - 2.2.3.5).

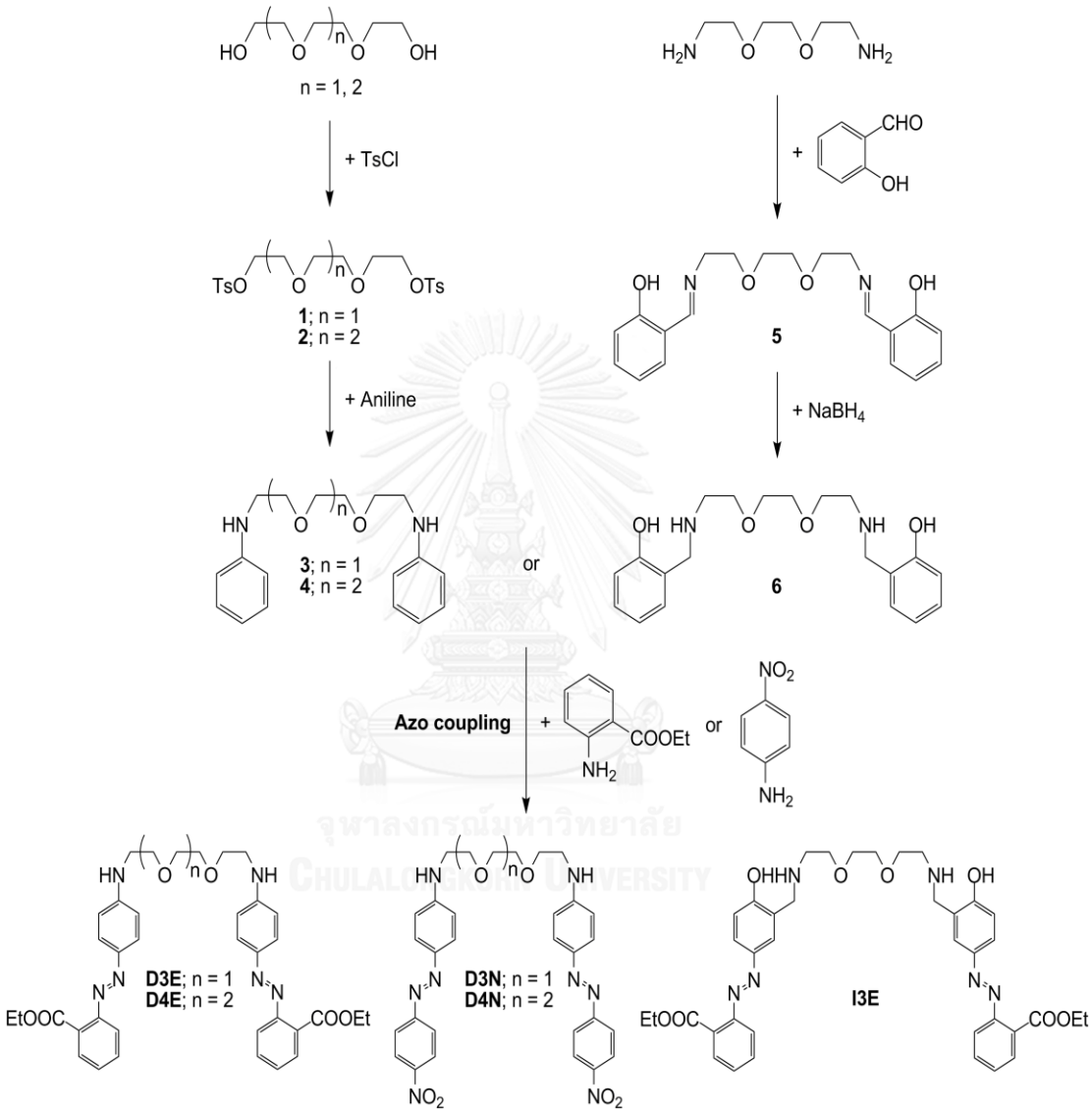

Scheme 2.1 Synthesis pathway of azo dye-based pseudo ether derivatives

2.2.1 Synthesis of oligoethyleneditosylate

2.2.1.1 Synthesis of triethyleneditosylate **1**

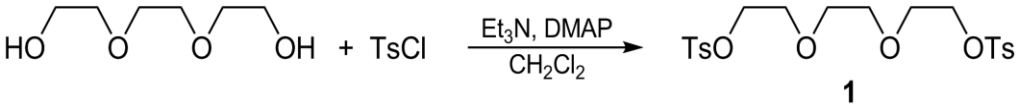

1

Triethyleneglycol (3.754 g, 25 mmol), triethylamine (7.589 g, 75 mmol), and DMAP were mixed in anhydrous dichloromethane (50 mL) in a 100-mL round bottom flask equipped with a magnetic bar and stirred in an iced bath for 30 minutes. Then anhydrous solution of tosylchloride (9.533 g, 50 mmol) was added into the mixture and the stirring continued for 12 hours at room temperature. Later, the pH of this mixture was adjusted to 1 by adding 3 M HCl to eliminate triethylamine residue. It was extracted with water 3 times and only organic phase was collected. CH_2Cl_2 was removed by a rotary evaporator to gain crude product, which was recrystalized in methanol and the white solid was filtered and dried (7.461 g, 62.6 %yield). ^{1}H-NMR: δ 2.44 (s, 6H, C$\underline{H_3}$-Ar), δ 3.53 (s, 4H, O-C$\underline{H_2}$-C$\underline{H_2}$-O), δ 3.65 (t, 4H, O-C$\underline{H_2}$-CH$_2$-OTs), δ 4.13 (t, 4H, CH$_2$-C$\underline{H_2}$-OTs), δ 7.34 (d, 4H, $\underline{Ar}$), δ 7.79 (d, 4H, $\underline{Ar}$)

2.2.1.2 Synthesis of tetraethyleneditosylate **2**

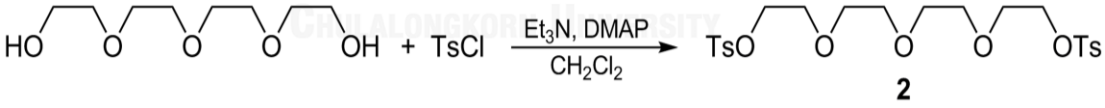

2

Tetrathyleneglycol (4.856 g, 25 mmol), triethylamine (7.589 g, 75 mmol), and DMAP were mixed in anhydrous dichloromethane (50 mL) in a 100-mL round bottom flask equipped with a magnetic bar and stirred in an iced bath for 30 minutes. Then anhydrous solution of tosylchloride (9.533 g, 50 mmol) was added into the mixture, and the stirring continued for 12 hours at room temperature. Later, the pH of this mixture was adjusted to 1 by adding 3 M HCl to eliminate triethylamine residue. It was extracted with water 3 times and only organic phase was collected. CH_2Cl_2 was removed by a rotary evaporator to gain crude product, which was purified by column chromatography using CH_2Cl_2 as eluent and the desired product was obtained as

yellow oil (8.155 g, 64.9 %yield). ^{1}H-NMR: δ 2.23 (s, 6H, C$\underline{H_3}$-Ar), δ 3.41 (s, 8H, O-C$\underline{H_2}$-C$\underline{H_2}$-O), δ 3.53 (t, 4H, O-C$\underline{H_2}$-CH$_2$-OTs), δ 4.21(t, 4H, CH$_2$-C$\underline{H_2}$-OTs), δ 7.22 (d, 4H, $\underline{Ar}$), δ 7.65 (d, 4H, $\underline{Ar}$)

2.2.2 Synthesis of oligoethylenediaminobenzene

2.2.2.1 Synthesis of triethylenedianiline **3**

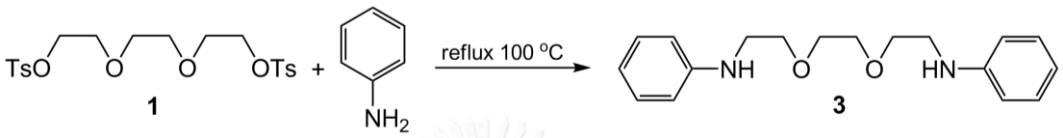

1 **3**

Triethyleneditosylate **1** (0.250 g, 6 mmol) was dissolved in aniline (30 mL) in a 50-mL two-neck round bottom flask equipped with a magnetic bar and refluxed at 100 °C for 6 hours. Then, this solution was transferred into diethyl ether (100 mL) and was filtered to remove the sediment by reduced pressure vacuum. The separated liquid was evaporated to remove diethyl ether by a rotary evaporation and the residue aniline by vacuum distillation. This residue was dissolved in EtOAc and filtered through glass funnel containing alumina gel. The brown solution was collected and evaporated to obtain the crude product, which was purified by column chromatography using 20% EtOAc in hexane as eluent. The desired product was obtained as brown oil (0.145 g, 80.4 %yield). ^{1}H-NMR: δ 3.25 (t, 4H, CH$_2$-C$\underline{H_2}$-N), δ 3.59 (s, 4H, O-C$\underline{H_2}$-C$\underline{H_2}$-O), δ 3.64 (t, 4H, O-C$\underline{H_2}$-CH$_2$-N), δ 6.60 (m, 4H, $\underline{Ar}$), δ 6.71 (m, 2H, $\underline{Ar}$), δ 7.13 (m, 4H, $\underline{Ar}$)

2.2.2.2 Synthesis of tetraethylenedianiline **4**

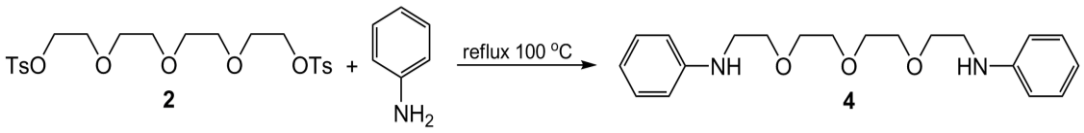

2 **4**

Tetraethyleneditosylate **2** (0.302 g, 6 mmol) was dissolved in aniline (30 mL) in a 50-mL two-neck round bottom flask equipped with a magnetic bar and refluxed

at 100 °C for 6 hours. Then, this solution was transferred into diethyl ether (100 mL) and was filtered to remove the sediment by reduced pressure vacuum. The separated liquid was evaporated to remove diethyl ether by a rotary evaporation and the residue aniline by vacuum distillation. This residue was dissolved in EtOAc and filtered through glass funnel containing alumina gel. The brown solution was collected and evaporated to obtain the crude product, which was purified by column chromatography using 20% EtOAc in hexane as eluent. The desired product was obtained as brown oil and gave 78.4 %yield (0.162 g). ^{1}H-NMR: δ 3.28 (t, 4H, CH_2-C$\underline{H}_2$-N), δ 3.65 (s, 8H, O-C$\underline{H}_2$-C$\underline{H}_2$-O), δ 3.69 (t, 4H, O-C$\underline{H}_2$-CH_2-N), δ 6.61 (d, 4H, $\underline{Ar}$), δ 6.69 (m, 2H, $\underline{Ar}$), δ 7.16 (m, 4H, $\underline{Ar}$)

2.2.2.3 Synthesis of triethylenediaminophenol **5**

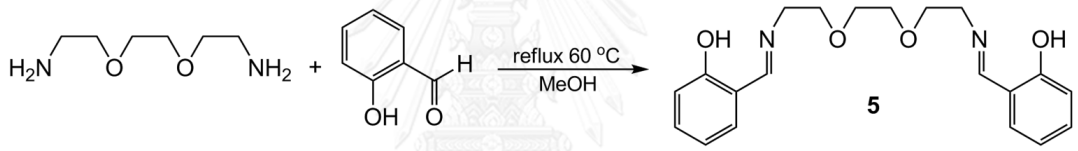

Triethylenediaminophenol **5** was prepared by adding methanol solution (10 mL) of 3, 6-dioxa-1, 8-diaminooctane (1.483 g, 10 mmol) dropwisedly into salicylaldehyde (2.440 g, 20 mmol) in 20 mL MeOH in a 50-mL two-neck round bottom flask equipped with a magnetic bar and refluxed for 5 hours. Then, the mixture was cooled and concentrated using a rotary evaporator before crystallization at −5 °C overnight. The bright yellow crystal product was filtered and dried by reduced pressure vacuum (2.768 g, 77.7 %yield). ^{1}H-NMR: δ 3.60 (s, 4H, CH_2-C$\underline{H}_2$-N), δ 3.72 (s, 8H, CH_2-C$\underline{H}_2$-O), δ 6.88 (t, 2H, $\underline{Ar}$), δ 6.94 (d, 2H, $\underline{Ar}$), δ 7.26 (m, 4H, $\underline{Ar}$), δ 8.32 (s, 2H, C$\underline{H}$-N)

2.2.3 Synthesis of oligoethylenediazobenzene

2.2.3.1 Synthesis of triethylenediesterazobenzene (**D3E**)

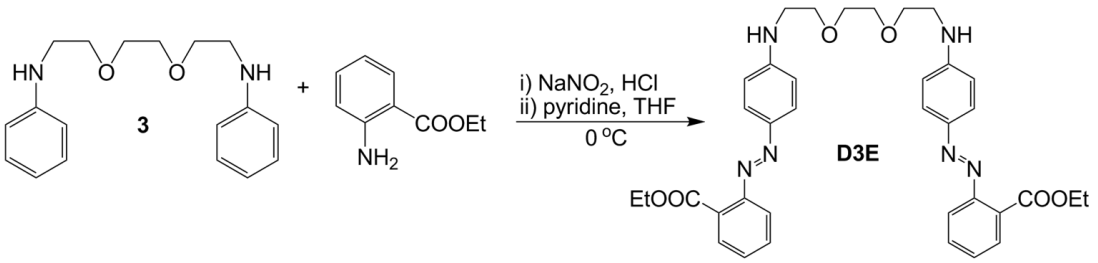

Ethyl-2-amino-benzoate (0.165 g, 1 mmol) was placed in a 50-mL two-neck round bottom flask equipped with a magnetic bar and stirred with $NaNO_2$ (0.104 g, 1.5 mmol) in 4 M HCl (2.4 mL) at 0 °C for 15 minutes before addition of triethylenedianiline **3** (0.100 g, 0.3 mmol) in THF:pyridine (2.4 mL:0.8 mL). After stirring at 0 °C for 6 hours, the mixture was neutralized by 3 M HCl and extracted by CH_2Cl_2. CH_2Cl_2 in collected organic phase was removed using a rotary evaporator. The crude product was purified by column chromatography using 20% EtOAc in hexane as eluent and the resulting product appeared as orange oil (0.059 g, 9.0 %yield).

Characterization of **D3E**

^{1}H-NMR: δ 1.31 (m, 6H, O-CH_2-CH_3), δ 3.61 (s, 4H, O-CH_2-CH_2-O), δ 3.83 (m, 4H, O-CH_2-CH_2-N), δ 4.30 (m, 4H, O-CH_2-CH_3), δ 4.43 (m, 4H, CH_2-CH_2-N), δ 7.09 (m, 2H, Ar), δ 7.24 (m, 2H, Ar), δ 7.34 (m, 4H, Ar), δ 7.45 (m, 2H, Ar), δ 7.53 (t, 4H, Ar), δ 7.68 (d, 2H, Ar)

^{13}C-NMR: δ 14.30 (2C, O-CH_2-CH_3), δ 46.56 (2C, O-CH_2-CH_2-N), δ 61.01 (2C, O-CH_2-CH_3), δ 66.99 (2C, O-CH_2-CH_2-N), δ 70.32 (2C, O-CH_2-CH_2-O), δ 118.00 (4C, Ar), δ 120.02 (4C, Ar), δ 123.83 (2C, Ar), δ 126.18 (2C, Ar), δ 127.45 (2C, Ar), δ 129.06 (2C, Ar), δ 129.54 (2C, Ar), δ 131.67 (2C, Ar), δ 144.87 (2C, N=N-Ar), δ 149.08 (2C, N=N-Ar), δ 168.11 (2C, C=O)

MALDI-TOF: $C_{36}H_{40}N_6O_6$ calcd 652.301 found m/z 652.845 [$M+H^+$]

Elemental Analysis: $C_{36}H_{40}N_6O_6$ calcd C, 66.24; H, 6.18; N, 12.88; O, 14.71 found C, 66.31; H, 6.18; N, 12.54; O, 14.97

2.2.3.2 Synthesis of tetraethylenediesterazobenzene (**D4E**)

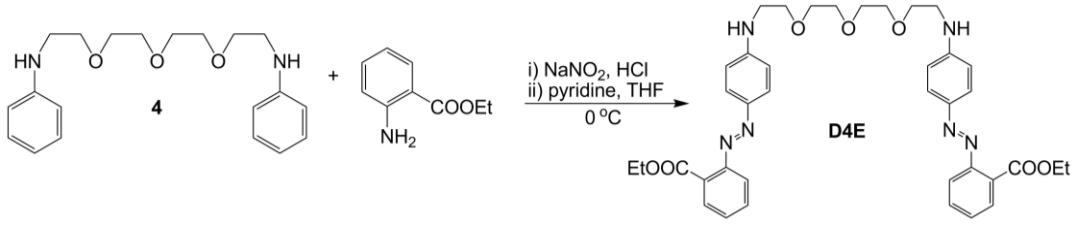

Ethyl-2-amino-benzoate (0.165 g, 1 mmol) was placed in a 50-mL two-neck round bottom flask equipped with a magnetic bar and stirred with $NaNO_2$ (0.104 g, 1.5 mmol) in 4 M HCl (2.4 mL) at 0 °C for 15 minutes before addition of tetraethylenedianiline **4** (0.103 g, 0.3 mmol) in THF:pyridine (2.4 mL:0.8 mL). After stirring at 0 °C for 6 hours, the mixture was neutralized by 3 M HCl and extracted by CH_2Cl_2. CH_2Cl_2 in collected organic phase was removed using a rotary evaporator. The crude product was purified by column chromatography using 20% EtOAc in hexane as eluent and the resulting product appeared as orange oil (0.021 g, 10.3 %yield).

Characterization for **D4E**

^{1}H-NMR: δ 1.31 (m, 6H, O-CH_2-CH_3), δ 3.61 (s, 4H, O-CH_2-CH_2-O), δ 3.83 (m, 4H, O-CH_2-CH_2-N), δ 4.30 (m, 4H, O-CH_2-CH_3), δ 4.43 (m, 4H, CH_2-CH_2-N), δ 7.09 (m, 2H, Ar), δ 7.24 (m, 2H, Ar), δ 7.34 (m, 4H, Ar), δ 7.45 (m, 2H, Ar), δ 7.53 (t, 4H, Ar), δ 7.68 (d, 2H, Ar)

^{13}C-NMR: δ 14.30 (2C, O-CH_2-CH_3), δ 46.55 (2C, O-CH_2-CH_2-N), δ 61.01 (2C, O-CH_2-CH_3), δ 66.90 (2C, O-CH_2-CH_2-N), δ 70.58 (4C, O-CH_2-CH_2-O), δ 117.83 (4C, Ar), δ 119.87 (4C, Ar), δ 123.96 (2C, Ar), δ 126.05 (2C, Ar), δ 127.41 (2C, Ar), δ 128.60 (2C, Ar), δ 129.52 (2C, Ar), δ 131.52 (2C, Ar), δ 144.88 (2C, N=N-Ar), δ 149.06 (2C, N=N-Ar), δ 168.13 (2C, C=O)

MALDI-TOF: $C_{38}H_{44}N_6O_7$ calcd 696.327 found m/z 696.768 [$M+H^+$]

Elemental Analysis: $C_{38}H_{44}N_6O_7$ calcd C, 65.50; H, 6.36; N, 12.06; O, 16.07 found C, 65.63; H, 6.36; N, 11.62; O, 16.39

2.2.3.3 Synthesis of triethylenedinitroazobenzene (**D3N**)

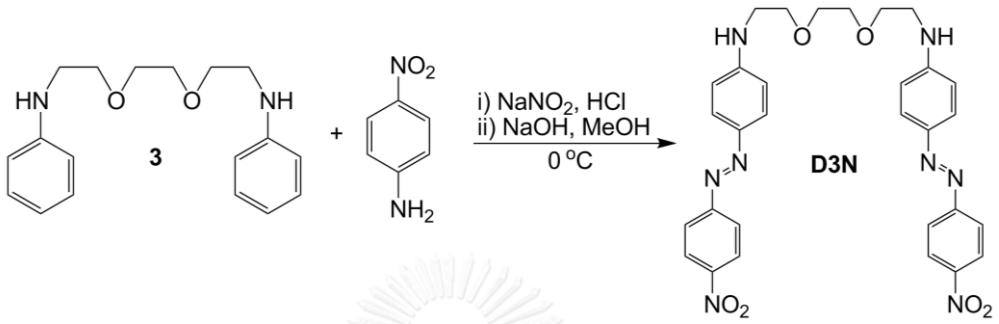

p-nitroaniline (0.138 g, 1 mmol) was placed in a 50-mL two-neck round bottom flask equipped with a magnetic bar and stirred with $NaNO_2$ (0.104 g, 1.5 mmol) in 1 M HCl (6 mL) at 0 ℃ for 30 minutes before addition of triethylenedianiline **3** (0.150 g, 0.5 mmol) with NaOH (0.3 g, 7.5 mmol) in MeOH:H_2O (0.7 mL:1.4 mL). After stirring at 0 ℃ for 2 hours, the mixture was neutralized by 3 M HCl and extracted by CH_2Cl_2. CH_2Cl_2 in collected organic phase was removed using a rotary evaporator. The crude product was precipitated from hexane and purified by column chromatography using 40% EtOAc in hexane as eluent. The resulting product appeared as yellow oil and gave 10.7 %yield (0.064 g).

Characterization of **D3N**

^{1}H-NMR: δ 3.61 (s, 4H, O-C$\underline{H}_2$-C$\underline{H}_2$-O), δ 3.81 (t, 4H, O-C$\underline{H}_2$-CH$_2$-N), δ 4.47 (t, 4H, CH$_2$-C$\underline{H}_2$-N), δ 7.18 (t, 2H, CH$_2$-N$\underline{H}$), δ 7.38 (t, 4H, $\underline{Ar}$), δ 7.56 (d, 4H, $\underline{Ar}$), δ 7.63 (d, 4H, $\underline{Ar}$), δ 8.24 (d, 4H, $\underline{Ar}$)

^{13}C-NMR: δ 47.04 (2C, O-CH$_2$-$\underline{C}$H$_2$-N), δ 66.90 (2C, O-$\underline{C}$H$_2$-CH$_2$-N), δ 70.77 (2C, O-CH$_2$-$\underline{C}$H$_2$-O), δ 118.62 (4C, $\underline{Ar}$), δ 121.56 (4C, $\underline{Ar}$), δ 124.98 (4C, $\underline{Ar}$), δ 125.49 (2C, $\underline{Ar}$), δ 129.38 (4C, $\underline{Ar}$), δ 144.54 (2C, N=N-$\underline{Ar}$), δ 145.78 (2C, N=N-$\underline{Ar}$), δ 154.98 (2C, $\underline{Ar}$-NO$_2$)

MALDI-TOF: $C_{30}H_{30}N_8O_6$ calcd 598.229 found m/z 598.773 [M+H$^+$]

Elemental Analysis: $C_{30}H_{30}N_8O_6$ calcd C, 60.19; H, 5.05; N, 18.72; O, 16.04 found C, 60.95; H, 5.23; N, 17.49; O, 16.33

2.2.3.4 Synthesis of tetraethylenedinitroazobenzene (**D4N**)

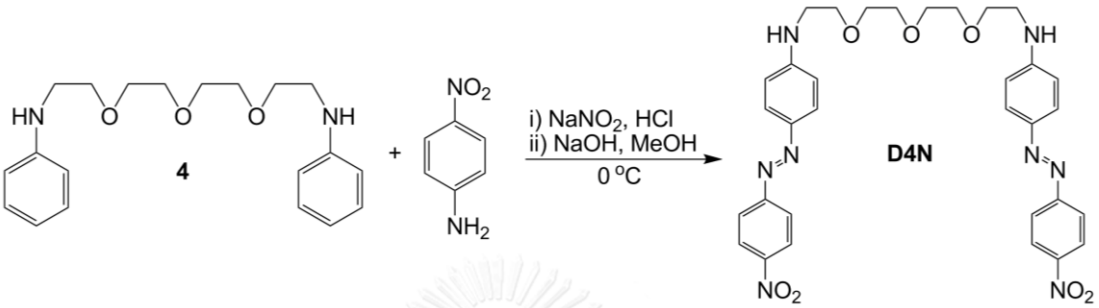

p-nitroaniline (0.138 g, 1 mmol) was placed in a 50-mL two-neck round bottom flask equipped with a magnetic bar and stirred with $NaNO_2$ (0.104 g, 1.5 mmol) in 1 M HCl (6 mL) at 0 °C for 30 minutes before addition of tetraethylenedianiline (0.172 g, 0.5 mmol) with NaOH (0.3 g, 7.5 mmol) in MeOH:H_2O (0.7 mL:1.4 mL). After stirring at 0 °C for 2 hours, the mixture was neutralized by 3 M HCl and extracted by CH_2Cl_2. CH_2Cl_2 in collected organic phase was removed using a rotary evaporator. The crude product was precipitated from hexane and purified by column chromatography using 40% EtOAc in hexane as eluent. The desired product was red oil and gave 12.2 %yield (0.043 g).

Characterization of **D4N**

^{1}H-NMR: δ 3.60 (d, 8H, O-C$\underline{H}_2$-C$\underline{H}_2$-O), δ 3.82 (t, 4H, O-C$\underline{H}_2$-CH_2-N), δ 4.49 (t, 4H, CH_2-C$\underline{H}_2$-N), δ 7.19 (t, 2H, CH_2-N$\underline{H}$), δ 7.39 (t, 4H, $\underline{Ar}$), δ 7.58 (d, 4H, $\underline{Ar}$), δ 7.64 (d, 4H, $\underline{Ar}$), δ 8.24 (d, 4H, $\underline{Ar}$)

^{13}C-NMR: δ 46.26 (2C, O-CH_2-$\underline{C}H_2$-N), δ 66.78 (2C, O-$\underline{C}H_2$-CH_2-N), δ 70.72 (4C, O-CH_2-$\underline{C}H_2$-O), δ 118.62 (4C, $\underline{Ar}$), δ 121.37 (4C, $\underline{Ar}$), δ 124.85 (4C, $\underline{Ar}$), δ 125.04 (2C, $\underline{Ar}$), δ 129.32 (4C, $\underline{Ar}$), δ 144.52 (2C, N=N-$\underline{Ar}$), δ 145.73 (2C, N=N-$\underline{Ar}$), δ 155.00 (2C, $\underline{Ar}$-NO_2)

MALDI-TOF: $C_{32}H_{34}N_8O_7$ calcd 642.255 found m/z 642.855 [$M+H^+$]

2.2.3.5 Synthesis of triethylenediphenol-esterazobenzene (**I3E**)

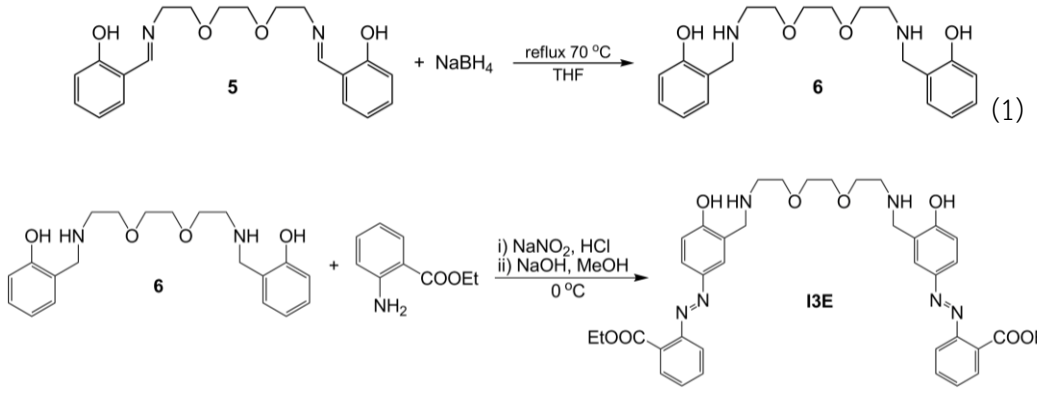

Triethylenediaminophenol **5** (0.180 g, 0.5 mmol) was refluxed with $NaBH_4$ (0.379 g, 10 mmol) in 30 mL THF for 2 days and then the solvent was removed under reduced pressure to gain white sticky gum. This gum was dissolved in the solution of NaOH (7.5 mmol) in MeOH:H_2O (0.7 mL:1.4 mL) before being dropped into the mixture of ethyl-2-aminobenzoate (0.165 g, 1 mmol) and $NaNO_2$ (0.104 g, 1.5 mmol) in 6 mL of 1 M HCl at 0 °C and stirred for 30 minute. After stirring at 0 °C for 2 hours, the mixture was neutralized by 3 M HCl and extracted by CH_2Cl_2. CH_2Cl_2 in collected organic phase was removed using a rotary evaporator. The crude product was purified by column chromatography twice using 20% EtOAc in hexane followed by 70% EtOAc in CH_2Cl_2 as eluents, respectively. The resulting product was orange oil (0.044 g, 12.5 %yield).

Characterization of **I3E**

^{1}H-NMR: δ 1.33 (m, 6H, O-CH_2-C$\underline{H}_3$), δ 3.62 (s, 4H, O-C$\underline{H}_2$-C$\underline{H}_2$-O), δ 3.82 (m, 4H, O-C$\underline{H}_2$-CH_2-N), δ 4.00 (m, 4H, O-CH_2-C$\underline{H}_2$-N), δ 4.35 (m, 4H, O-C$\underline{H}_2$-CH_3), δ 4.95 (s, 4H, N-C$\underline{H}_2$-Ar), δ 6.82 (t, 2H, Ar), δ 6.87 (d, 2H, Ar), δ 7.20 (m, 2H, Ar), δ 7.43 (m, 2H, Ar), δ 7.80 (d, 2H, Ar)

^{13}C-NMR: δ 14.32 (2C, O-CH_2-C$\underline{H}_3$), δ 43.29 (2C, O-CH_2-C$\underline{H}_2$-N), δ 61.18 (2C, Ar-C$\underline{H}_2$-N), δ 61.26 (2C, O-C$\underline{H}_2$-CH_3), δ 69.94 (2C, O-C$\underline{H}_2$-CH_2-N), δ 70.62 (2C, O-CH_2-C$\underline{H}_2$-O), δ 118.68 (2C, Ar), δ 120.28 (2C, Ar), δ 121.69 (2C, Ar), δ 124.28 (2C, Ar), δ 125.80

(2C, Ar), δ 129.66 (2C, Ar), δ 130.60 (2C, Ar), δ 132.02 (2C, Ar), δ 146.21 (2C, Ar), δ 148.38 (2C, Ar), δ 152.19 (2C, N=N-Ar), δ 159.51 (2C, N=N-Ar), δ 167.49 (2C, Ar-NO_2)

MALDI-TOF: $C_{38}H_{44}N_6O_8$ calcd 712.322 found m/z 712.655 [$M+H^+$]

2.3 Study of sensing properties

The concentration of ligand stock solutions were approximately $1x10^{-3}$ M, while metal stock solutions (Li^+, Na^+, K^+, Cs^+, Rb^+, Cu^{2+}, Zn^{2+}, Cd^{2+}, Hg^{2+}, Pb^{2+}) and anion stock solutions (OH^-, F^-, CN^-) were approximately 0.01 M and 0.01 M, respectively. The exact concentration of metal salt stock solutions was determined by complexometric titration with EDTA. Naked eye sensing was studied by addition of guest solutions into 1×10^{-4}, 5×10^{-5}, 2×10^{-5} M ligand solutions at specified ratios. UV-visible spectra were collected by addition of guest solutions into 2×10^{-5} M ligand solutions at specified ratios using a 0.2 or 1 cm path length cuvette.

CHAPTER III

RESULTS AND DISCUSSIONS

3.1 Synthetic procedures

Herein, a general design of a novel series of metal ion chromogenic sensors was originally expected to be ditopic sensors via allosteric effect, which allowed the molecules to rearrange its conformation after binding with a first target to selectively bind with a second target. The chromogenic derivatives in this research consisted of π-conjugated system from benzene rings and azo chromophores, which could be found in most commercial dyes and able to interact with metal ions such as chromium, copper, and mercury [13, 51, 60-63]. The sensing ligands in this study were designed to consist of diaza-pseudocrown ether connecting to aromatic rings and azo bonds. The variation in the ligands would be 1) the connection of nitrogen atoms in diaza-pseudocrown ether to the aromatic rings, 2) number of ethylene glycol units in pseudocrown ether, and 3) the functional group on the ending aromatic rings. This variation is shown in Figure 3.1. Note that the short code for the studied ligands consisted of three components starting with **D** or **I**, which indicated the connection between nitrogen and aromatic rings either being direct (**D**) or indirect (**I**). Next, number **3** or **4** referred to the number of ethylene glycol units in molecule, and last initial **E** or **N** represented the functional group R on the benzene rings as either **E** for ester group or **N** for nitro group. The indirect derivatives also contained hydroxyl group on the aromatic rings next to pseudocrown unit at para position to azo bonds.

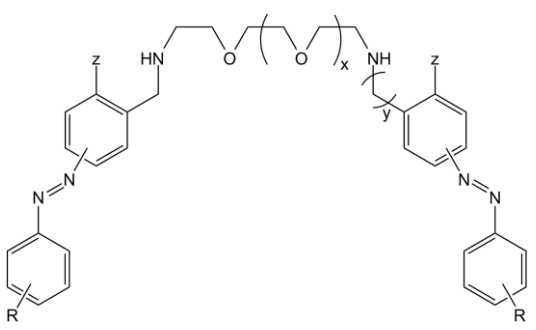

molecules	X	Y	z	R
I3E	1	1	OH	*o*-ester
D3E	1	0	H	*o*-ester
D4E	2	0	H	*o*-ester
I3N	1	1	OH	*p*-nitro
D3N	1	0	H	*p*-nitro
D4N	2	0	H	*p*-nitro

Figure 3.1 The target pseudocrown ether derivatives

3.1.1 Ester derivatives

The first derivative of ester pseudocrown ether ligand, **I3E**, beared the hydroxyl groups on the azobenzene rings to provide lone pairs to enhance the delocalization of π-conjugated system and induce the azo-hydrazone tautomerism by the rotation of proton from hydroxyl group to azo bond, thus promoting a bathochromic shift [38, 39, 51, 60]. The second ester derivative, **D3E**, had its terminal nitrogen atoms in polyethylene chain connected directly to aromatic regions to give lone pairs to π-conjugated system. And the last molecule of ester series, **D4E**, differed from the others by the longest ionophoric chain because of one extra ethylene glycol unit expecting to increase the flexibility of ligand for the efficiency of selective metal ion wrapping.

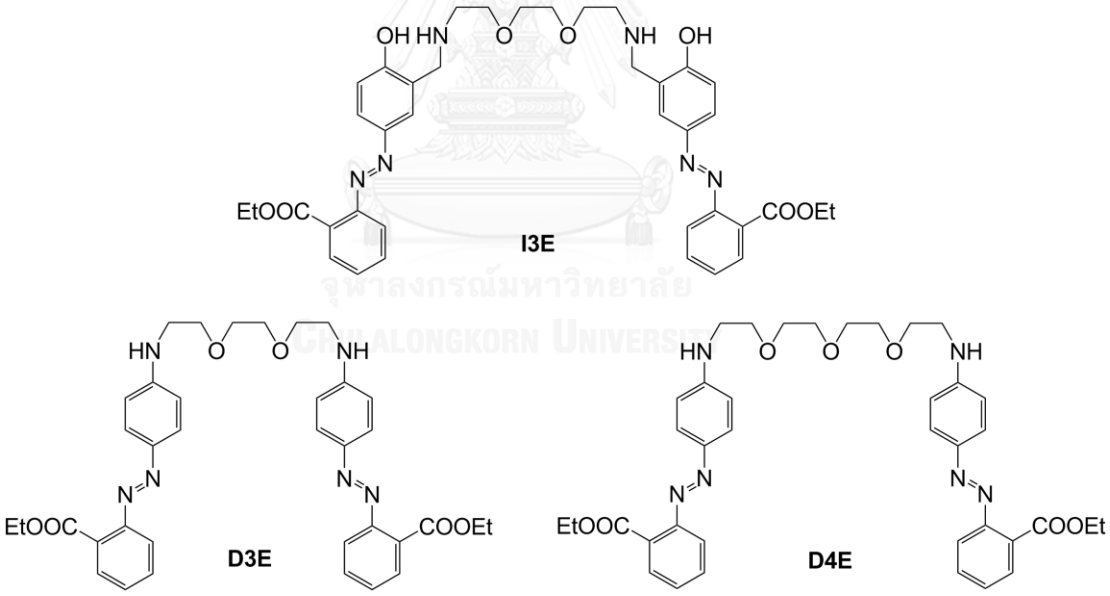

Figure 3.2 Ester pseudocrown ether derivatives

3.1.1.1 Synthesis of **I3E**

I3E, the first ligand to be synthesized in this series, was planned to be generated from initial Scheme 3.1. According to this scheme, the preparation of starting material (**6**) for **I3E** had many steps including the synthesis of

triethyleneditosylate (**1**) and aminophenol (**a**) [64]. Although triethyleneditosylate (**1**) was easy to be generated in high quantity yield, aminophenol (**a**) was quite hard to obtain because of multiple synthetic steps. In addition, the preparation of triethylenediphenol (**6**) via the substitution of aminophenol (**a**) on tosyl group in triethyleneditosylate (**1**) was not successful because hydroxyl group on aminophenol (**a**) was a stronger electrophile than amino group, leading to a preferential interaction of triethyleneditosylate (**1**) and OH group rather than and NH_2 group.

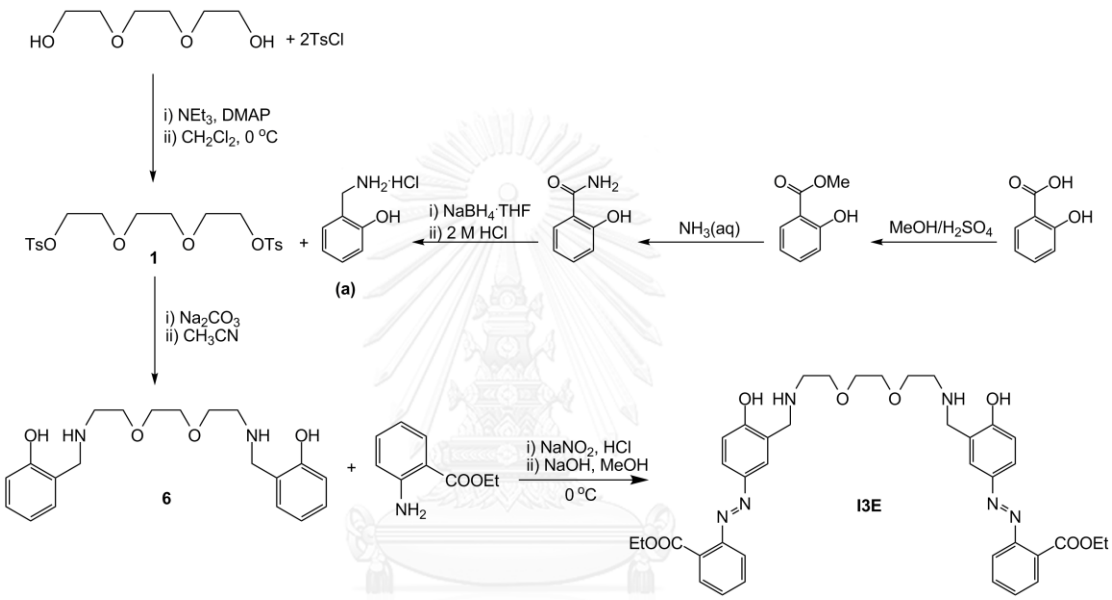

Scheme 3.1 First synthetic pathway of **I3E**

So, **I3E** synthetic plan was changed to Scheme 3.2 by adjusting the synthetic method of triethylenediphenol (**6**) from the substitution reaction between triethyleneditosylate (**1**) and aminophenol (**a**) to the reduction reaction of Schiff base (**5**) [65]. The purification of final product **I3E** was challenging because the crude products contained many by-products, some of them having amino and oxy groups such as one-side arm azobenzene derivative, products of self-coupling esteraniline, which could bind strongly via H-bonding with stationary phase such as silica or alumina gel in column chromatography. This problem was solved by doing separation using silica gel twice: the first round employed 20% EtOAc in hexane as eluents, which was able to elude many by-products, and kept the target product at the baseline because of its high partial charge and strong chromophores. After

exaction the baseline silica gel with methanol, the crudes were purified by the second column chromatography using 70% EtOAc in CH_2Cl_2 as eluents to obtain the desired product.

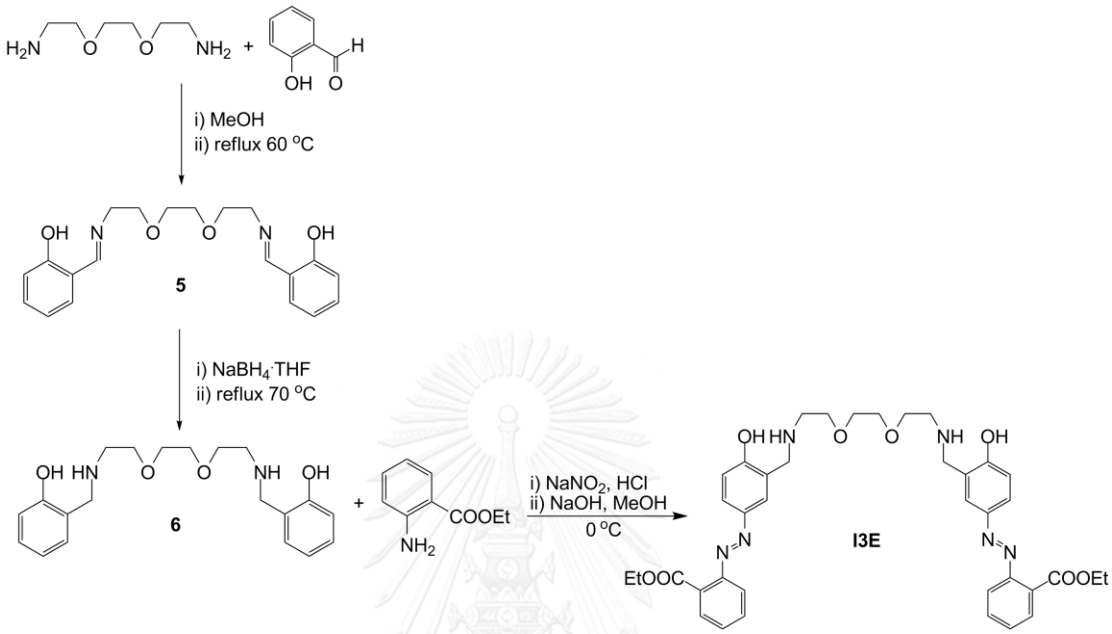

Scheme 3.2 Second synthetic pathway of **I3E**

3.1.1.2 Synthesis of **D3E**

D3E was the second synthesized molecule of the ester based pseudocrown ether derivatives, which was designed for the study of the influence of the shorten space between nitro atom at the chain ends and aryl moieties on the optical behavior. This molecule, differing from **I3E** by the lack of methylene bridge and hydroxyl group to reduce the steric effect, was synthesized through the azo coupling reaction between triethylenedianiline (**3**) [66] and esteraniline as shown in Scheme 3.3. The purification of final products **D3E** was much easier than **I3E** because of the absence of OH groups.

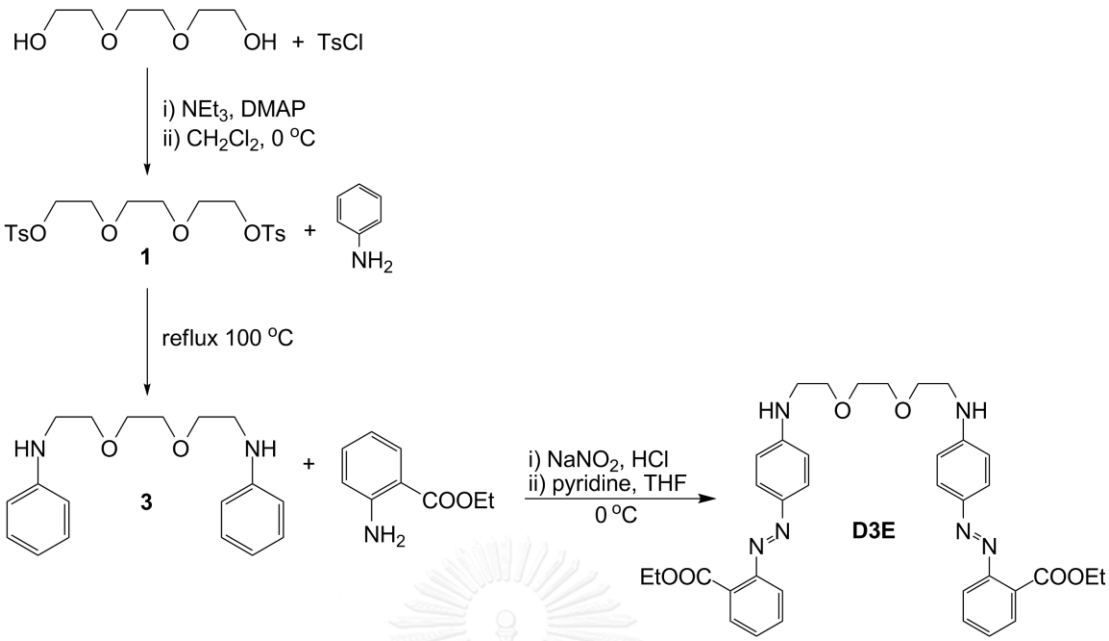

Scheme 3.3 Synthesis pathway of **D3E**

3.1.1.3 Synthesis of **D4E**

D4E was designed based on **D3E** analogue by an extension of the ionophoric chain with a unit of an oxygen atom connected by an ethylene moiety for the study of the effect of the higher flexibility upon the wrapping around metal ion. The synthetic procedure of **D4E** was thus similar to the synthetic procedure of **D3E** in Scheme 3.3 but tetraethylene glycol was used as starting reagent instead of triethylene glycol to yield tetraethyleneditosylate (**2**) and tetraethylenedianiline (**4**), respectively.

3.1.2 Nitro derivatives

The presence of nitro group was introduced into this research via changing the ester substituent in ester pseudocrown ether analogues to the nitro substituent aiming to increase the different partial charge between electron-donating and electron-accepting moiety in the ligand for productive optical properties. Originally, a series of nitro derivatives was planned to have three members as same as in ester derivatives: **I3N**, **D3N**, and **D4N** being analogues to **I3E**, **D3E**, and **D4E**, respectively. Unfortunately, a molecules bearing hydroxyl group, **I3N**, could not be separated

from the mixture products even after several separations under various conditions. The study of **I3N** was thus paused whereas the other nitro ligands, shown in Figure 3.3, were studied.

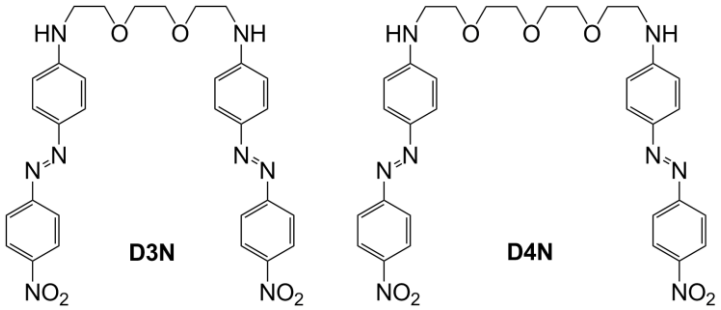

Figure 3.3 Nitro pseudocrown ether derivatives

3.1.2.1 Synthesis of **D3N**

The synthesis of **D3N** was similar to the synthesis of **D3E** but there was a different condition for the azo coupling reaction using nitroaniline as reagent instead of esteraniline. However, the azo coupling reaction of nitroaniline failed when using pyridine as base in THF, which might be caused by the poor promotion of proton abstraction during the azo bond formation as shown in Scheme 3.4 compared to the rate of azo bond formation between two diazonium salts, which inhibited the generation of the desired product. So sodium hydroxide, a stronger base, in methanol was used instead to increase HCl neutralizing rate, thus promoted the azo bonding between triethylenedianiline (**3**) and nitroaniline leading to the successful synthesis of **D3N**.

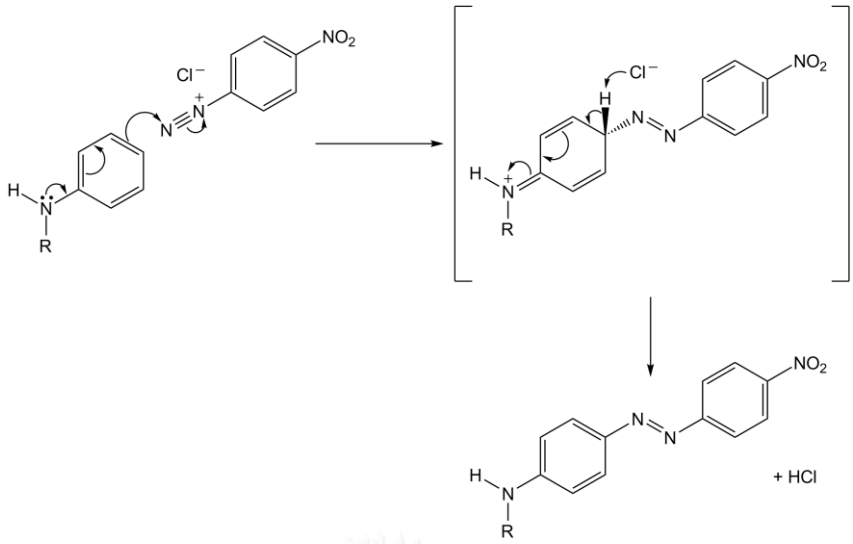

Scheme 3.4 Formation of azo bond in **D3N**

3.1.2.2 Synthesis of **D4N**

D4N was designed to study the influence of the length of ionophoric chain in the nitro pseudocrown ether derivatives via extension of the polyethylene chain with one unit of oxygen atom connected with ethylene moiety. Thus, the synthetic plan of **D4N** was similar to the synthesis of **D3N** by changing the starting reagent from triethylene glycol to tetraethylene glycol to produce tetraethyleneditosylate (**2**) and tetraethylenedianiline (**4**), respectively.

3.2 Studies of sensing properties of pseudocrown ether derivatives

Optical properties of 5 novel pseudocrown ethers bearing azobenzene moieties were studied of which the absorption spectra at 1×10^{-4} M shown in Figure 3.4. The three ester derivatives namely **I3E**, **D3E,** and **D4E**, all dissolved in methanol, yielded a pale yellow, yellow, and slight yellow solution, respectively, corresponding to the wavelength of maximum absorption (λ_{max}) at 325, 406, and 295 nm. The two nitro derivatives, **D3N** and **D4N,** displayed brown and bright yellow solution in DMSO, with the maximum absorption at 404 and 399 nm, respectively. It can be seen that the nitro derivatives showed the higher intensity of absorption than ester ones which could be the results from the distribution of electron density between amino

electron-donating groups and nitro electron-accepting moieties. The comparable maximum absorption for **D3E** and nitro derivatives, supported by intense color appearance, suggests that these ligands were in neutral azo form. Meanwhile the 100 nm shift of **I3E** and **D4E**'s λ_{max} to shorter wavelength suggests protonated-related azo form, similar to what reported in a literature [50]. This might be caused by interaction between MeOH and secondary amine moieties, which could happen in **I3E** and **D4E** because of the extra methyl and ethylene glycol group, respectively.

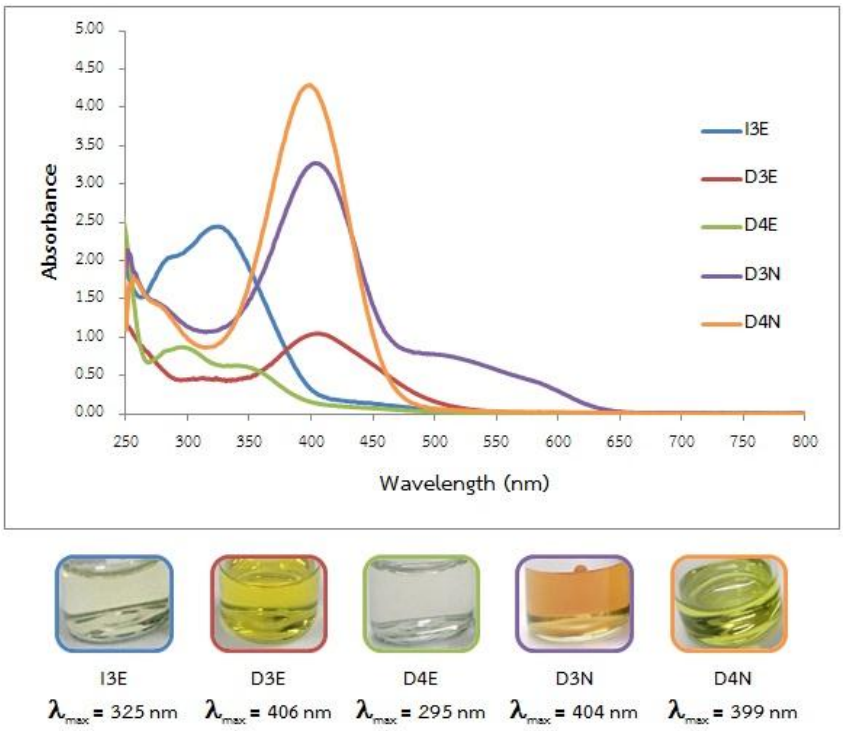

Figure 3.4 UV-visible spectra and colors of five pseudocrown ether derivatives at 1×10^{-4} M in MeOH (ester derivatives **E**) or DMSO (nitro derivatives **N**)

3.2.1 Ester derivatives

3.2.1.1 Study of sensing property of **I3E**

I3E, a pale yellow solution in methanol, displayed the wavelength of maximum absorption (λ_{max}) at 325 nm as can be seen in Figure 3.4 (*vide supra*).

Adding 10 equivalents of alkali metal ions (Li^+, Na^+, K^+, Rb^+, Cs^+) into ligand solution did not bring any change in color and UV-visible absorption spectra. Then,

addition of 10 equivalents of transition or heavy metal ions (Co^{2+}, Ni^{2+}, Cu^{2+}, Zn^{2+}, Cd^{2+}, Hg^{2+}, and Pb^{2+}) was thus investigated. Unfortunately, none of these metal ions could lead to any obvious change in color and UV-visible spectra, which the presence of Cu^{2+} showed a small enhancement of absorption intensity in UV region.

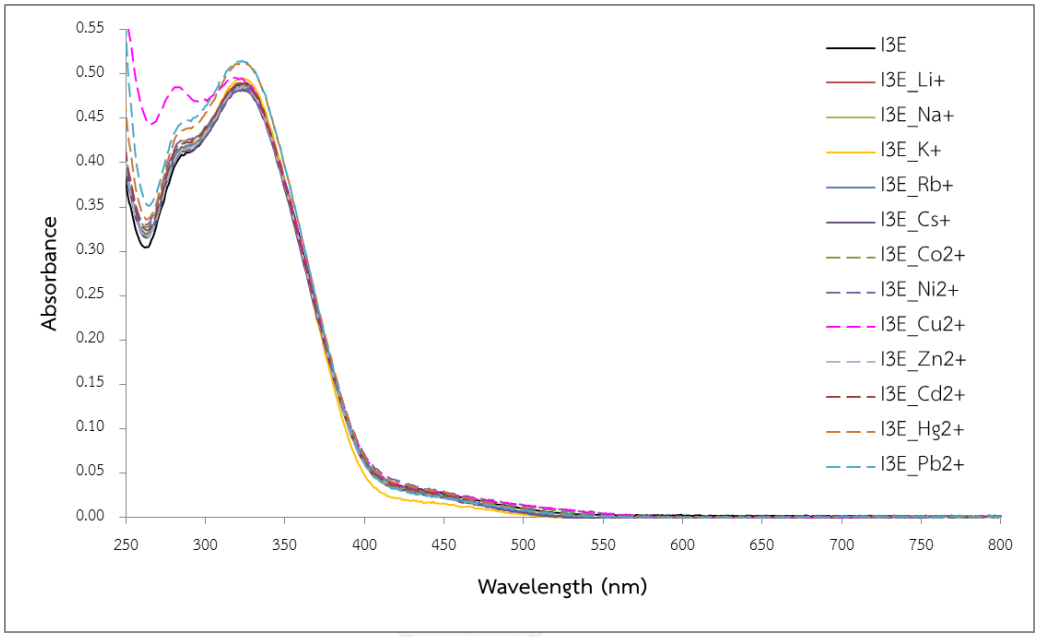

Figure 3.5 UV-visible spectra of 1×10^{-4} M **I3E** upon addition of 10 eq of metal ions

Furthermore, 10 equivalents of hydroxide ions was introduced into **I3E** solution in expectation that deprotonation of H^{+} on phenyl groups in this ligand could disturb the electrons in π-conjugated system leading to color change. It turned out to be the case because color changed from pale yellow without base to bright yellow in basic condition corresponding with an appearance of a new peak around 440 nm.

Hence, the study of metal sensing properties of **I3E** under 10 equivalents of hydroxide ions condition was examined. In case of alkali metal ions, the color and UV-visible spectra change were still similar to the presence of only hydroxide ion in ligand solution, except for the presence of K^{+} induced a small suppression of absorption intensity around 440 nm. Whereas addition of transition or heavy metal ions into this system could convert bright yellow solution to pale yellow mixture

with precipitates as metal-hydroxide complexes, which disturbed the UV-visible spectra.

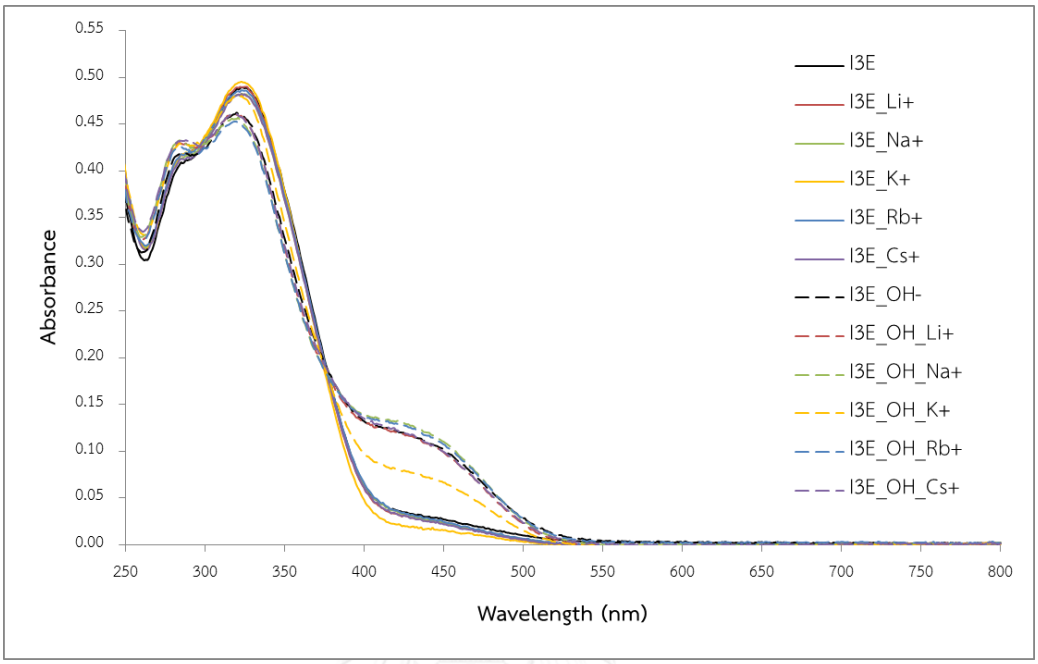

Figure 3.6 UV-visible spectra of 1×10^{-4} M **I3E** upon addition of 10 eq of alkali metal ions under the neutral (solid line) and basic (dash line) conditions

Lastly, the test for proving hypothesis of allosteric effect in designed ligand was studied by addition of two different metal ions, which were expected to bind different ionophores to induce the noticeable color change for naked-eye observation. The first metal ion, Rb^{+}, was chosen to be a target metal ion at pseudocrown ether region by considering from its proper size and character of hard acid allowing Rb^{+} to interact preferably with oxygen atoms. The second metal, Pb^{2+}, expected to be a major target metal ion in this research, was marked as a target metal ion of ester-azobenzene region because of its soft character countering with soft base as carbonyl groups and π-conjugated systems. These studies were carried out under non-hydroxide and hydroxide conditions and looked into sequential addition, *i.e.*, adding Rb^{+} before Pb^{2+}, adding Rb^{+} after Pb^{2+}, and adding Rb^{+} and Pb^{2+} together. The results showed that in non-hydroxide ion system, the alternate adding orders of Rb^{+} and Pb^{2+} could not lead to any color change. In the case of hydroxide

ion systems, the results showed that the color changed from bright yellow solution to pale yellow mixture with white precipitates in any sequential additions, which was similar to the previous result of adding only Pb^{2+} in basic condition. So, the hypothesis of allosteric effect in this designed ligand could not be proved via the addition of these two metal ions because none of color changes was noticed: Rb^{+} and Pb^{2+} were probably unable to invent allosteric conformation involving the chromogenic regions of this ligand.

Figure 3.7 Color change of 1×10^{-4} M **I3E** in MeOH (left) upon addition of 10 eq of hydroxide ions and (right) upon addition of 10 eq of Rb^{+} or/and Pb^{2+} for study of allosteric effect in hydroxide ion system

As mentioned, **I3E** solution could not express any selective changes in color and absorption spectra upon addition of metal ions, which indicated the lack of interaction between this molecule and metal ions. These outcomes could be explained by the following factors: first, polyethylene chain could not wrap around alkali metal ions due to the steric effect from hydroxyl moieties near polyethylene chain, which could repulse each other when they came closer. Second, the transition metal ions could not interact with ester groups and π-conjugated systems because of the inappropriate conformation of **I3E** covering the unsuitable directions and length between transition metal ions and recognition sites.

3.2.1.2 Study of sensing property of **D3E**

D3E, a yellow solution in methanol, displayed the wavelength of maximum absorption (λ_{max}) at 406 nm as can be seen in Figure 3.4 (*vide supra*).

The investigation of complexation behavior of **D3E** toward 10 equivalents of metal ions began from the addition of alkali and alkaline earth metal ions (Li^+, Na^+, K^+, Rb^+, Cs^+, Mg^{2+}, Ca^{2+}) and was found that no obvious color and UV-visible spectral change was observed. Then the addition of transition and heavy metal ions (Cu^{2+}, Zn^{2+}, Cd^{2+}, Hg^{2+}, Pb^{2+}) was studied and any notable change in color was still not observed, except for the case of Cu^{2+} which brought a small colored intensity.

Figure 3.8 Color of 5×10^{-5} M **D3E** upon addition of 10 eq of metal ions

The absorption spectra of **D3E** in the presence of metal ions (alkali, alkaline earth, or transition), shown in Figure 3.9, did not showed any new distinct absorption band but a small shoulder around 550 nm in the case of Cu^{2+}. Small hyperchromic and hypochromic effects (enhancement and suppression of absorption intensity, respectively) were observed for the case of Mg^{2+} and Cu^{2+}, respectively.

The fact that the presence of various metal ions could not bring any pronounced change in color and UV-visible spectra might be explained by two major factors. First, the pseudocrown ether chain contained less binding sites for alkali and alkaline earth metal ions as oxygen atoms leading the lack of stable interaction between **D3E** and these metal ions. Second, the electron accepting group as ester group was too weak to induce the disturbance of the efficient delocalization of electrons from electron donating groups to electron accepting groups upon the interaction of this ligand and metal ions, which caused indistinct color and UV-visible spectral changes.

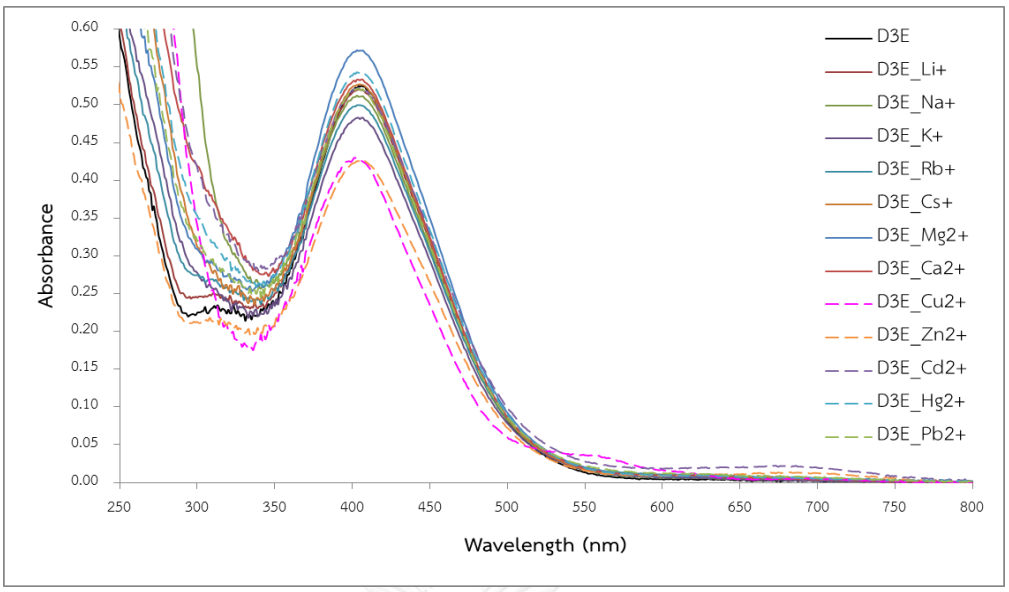

Figure 3.9 UV-visible spectra of 5×10^{-5} M **D3E** upon addition of 10 eq of metal ions

Even if no single ion could make any obvious change, the examination of allosteric effect was still carried on by choosing a couple of metal ions anticipating to fit with each ionophoric regions. Li^{+} was selected for inducing the wrap-around capability of the polyether chain corresponding to the suitable size and hard-soft acid-base relationship between guest and host. Another chosen metal ion was Cu^{2+} because the presence of Cu^{2+} in **D3E** solution increased color intensity. This examination included the order of metal ions addition such as addition of Li^{+} before Cu^{2+} and addition of Li^{+} after Cu^{2+}. The results showed hypochromic effect when Cu^{2+} was presence. However, less effect was observed when Li^{+} was added into copper solution, suggesting that Cu^{2+} somehow helping ligand-Li^{+} interaction. This observed allosteric effect, unfortunately, was too small to be of any use.

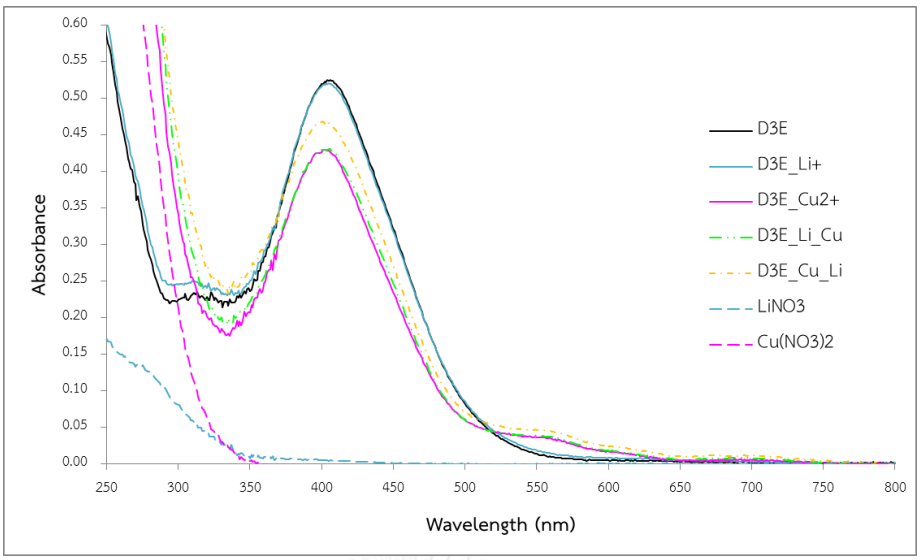

Figure 3.10 UV-visible spectra of 5×10^{-5} M **D3E** in MeOH upon addition of 10 eq of Li^{+} and Cu^{2+} for study of allosteric effect

3.2.1.3 Study of sensing property of **D4E**

D4E, a slight yellow solution in methanol, displayed the wavelength of maximum absorption (λ_{max}) at 295 nm as can be seen in Figure 3.4 (*vide supra*).

The responding of **D4E** upon the addition of 10 equivalents of metal ions showed that addition of alkali and alkaline earth metal ions (Li^{+}, Na^{+}, K^{+}, Rb^{+}, Cs^{+}, Mg^{2+}, Ca^{2+}) could not exhibit any changes in color and UV-visible spectra, similar to the addition of transition and heavy metal ions (Cu^{2+}, Zn^{2+}, Cd^{2+}, Hg^{2+}, Pb^{2+}).

Figure 3.11 Color of 1×10^{-4} M **D4E** upon addition of 10 eq of metal ions

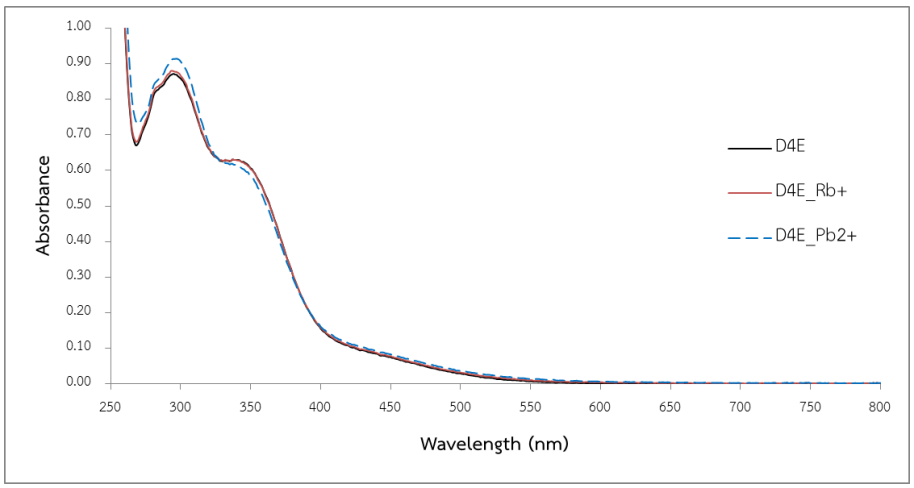

Figure 3.12 UV-visible spectra of 1×10^{-4} M **D4E** upon addition of 10 eq of Rb^{+} or Pb^{2+} ions

According to the results, the absence of optical changing toward the addition of metal ions implied that none of the interaction between this ligand and metal ions was strong enough to disturb the electrons in π-conjugated system to induce color and UV-visible spectral changes due to the lack of degree of organization for metal ions wrapping as pseudocrown ether conformation given by the high flexibility of this ligand.

3.2.2 Nitro derivatives

3.2.2.1 Study of sensing properties of **D3N**

D3N, a brown solution in DMSO, displayed the wavelength of maximum absorption (λ_{max}) at 404 nm as can be seen in Figure 3.4 (*vide supra*).

In a case of addition of 25 equivalents of alkali metal ions (Li^{+}, Na^{+}, K^{+}, Rb^{+}, Cs^{+}), the results exhibited none of the noticeable color and UV-visible spectral changes, excepted K^{+} which showed a slight suppression of the wavelength of maximum absorption of **D3N**. Addition of 25 equivalents of transition and heavy metal ions (Cu^{2+}, Zn^{2+}, Cd^{2+}, Hg^{2+}, Pb^{2+}), however, could exhibit the color change from brown to light orange corresponding to a new absorption peak around 490 nm. The absorption intensity at this new band could be sorted in a descending order

from Cd^{2+} > Zn^{2+} > Cu^{2+} > Hg^{2+} ≈ Pb^{2+}, which related to the presence of Cd^{2+} showing a more intense orange color among the others.

Figure 3.13 Color of 2×10^{-5} M **D3N** upon addition of ions

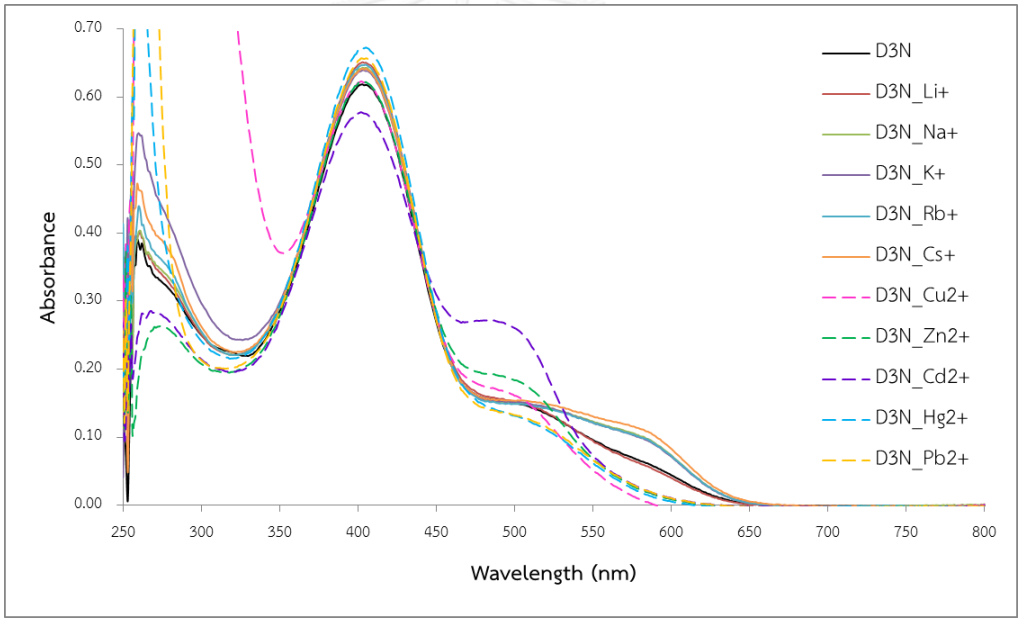

Figure 3.14 UV-visible spectra of 2×10^{-5} M **D3N** upon addition of metal ions

Furthernore, addition of 25 equivalents of hydroxide ion was introduced to this study due to azobenzene compound being known as acid-base indicator, *i.e.* methyl yellow, methyl orange, **D3N** methyl red, alizarine yellow r, etc. [50, 67-69]. The results exhibited the obvious color change from brown to dark purple. A successive titration of hydroxide ion into **D3N** was then performed and the spectral changes were shown in Figure 3.15 starting from 2 OH^- equivalents to deprotonate

two amino protons in this ligand. It can be clearly seen that a new absorption band occurred in a presence of base (*e.g.* 574 nm at 2 OH^- equivalents) and this new peak shifted to a longer wavelength with increasing amount of base. Thus a maximum wavelength difference between the **D3N** and **D3N**+OH^- peaks would be around 170 nm in a presence of 2 OH^- equivalents.

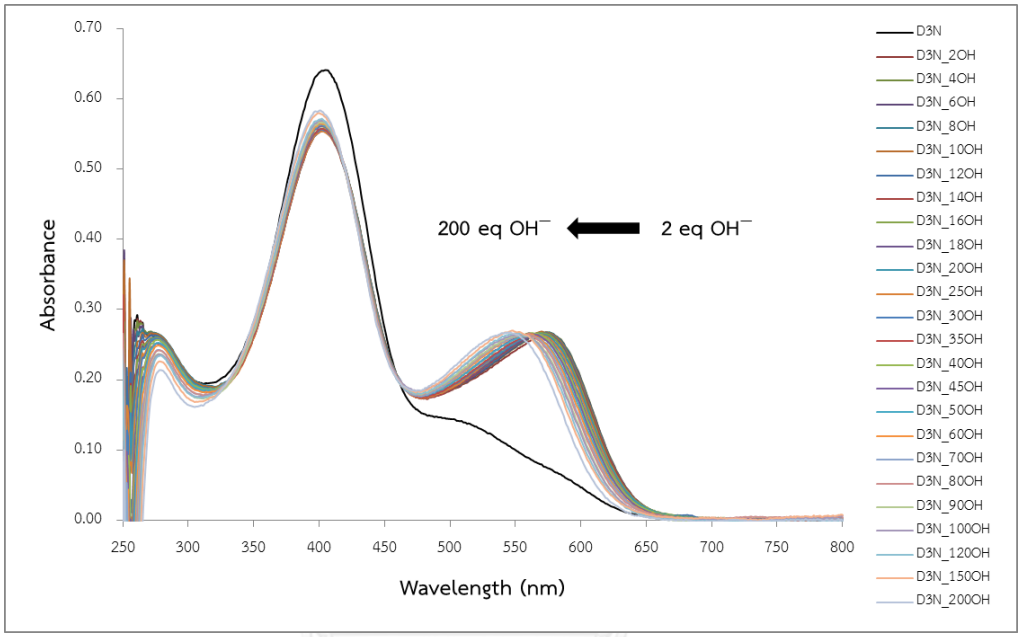

Figure 3.15 UV-visible spectra of 2×10^{-5} M **D3N** upon the presence of various amount of hydroxide ions

To investigate the effect of strong basic anions, addition of F^- and CN^- were performed and the color and UV-visible spectral changes for adding these two anions were found to be similar to the case of OH^- addition. Then a strong nucleophile but a mild basic anion as I^- was examined and none of the changes in color and UV-visible spectrum was obtained. These results indicated that the interaction between **D3N** and these strong basic anions should not involve any nucleophilic addition especially in the case of CN^- addition but it should relate to hydrogen bonding and/or a deprotonation of acidic hydrogen atom in this ligand.

According to the obvious color change upon addition of strong basic anions, the addition of metal ions into basic ligand condition was interesting. The equivalents

of added hydroxide ion were chosen to be 2 since this ratio showed the maximum wavelength difference. It was found that addition of alkali ions into **D3N**+OH^- could not lead to any color or spectral change (Figure 3.16), *i.e.* the color was still dark purple.

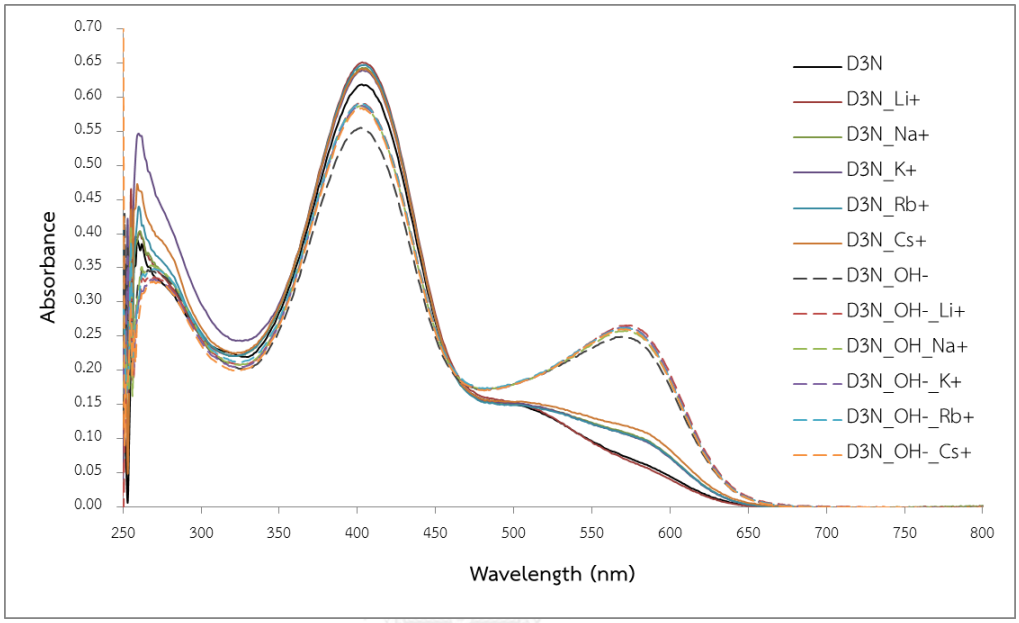

Figure 3.16 UV-visible spectra of 2×10^{-5} M **D3N** upon addition of alkali metal ions under the neutral (solid line) and basic (dash line) conditions

Even if addition of alkali ions to basic **D3N** solution did not show any special results, it was really interesting that the presence of transition or heavy ions could change the dark purple color of basic ligand solution back to orange shade. The UV-visible absorption spectra, shown in Figure 3.18, revealed a wavelength shift from 570-576 nm back to the transition and heavy metal ions absorption band around 490 nm accompanying the enhancement of intensity. The absorption intensity around 490 nm in descending order was found to be Cd^{2+} > Hg^{2+} > Zn^{2+} > Cu^{2+} > Pb^{2+}. This order was slightly different from the order in the absence of base because Hg^{2+}, showing the highest hyperchromic effect, was moved from last to second position. The observed orange color when transition or heavy metal ions were present with hydroxide was independent to the order of metal ions and basic anion addition into **D3N** solution, *i.e.* no matter which ion (metal ion or basic anion) was added first, the

color of the **D3N**+M^{2+}+OH^- mixture was always orange. It should be noted though that even if transition and heavy metal ions could induce color change from yellow (or purple when base was present) to orange, this change was not selective, *i.e.* all transition and heavy metal ions studies yielded orange color. The lack of selective interaction between this ligand and these metal ions might be caused by the flexibility of this molecule and the less steric effect at azobenzene parts, which allowed this host to bind all transition and heavy metal ions without the selectivity of size selection.

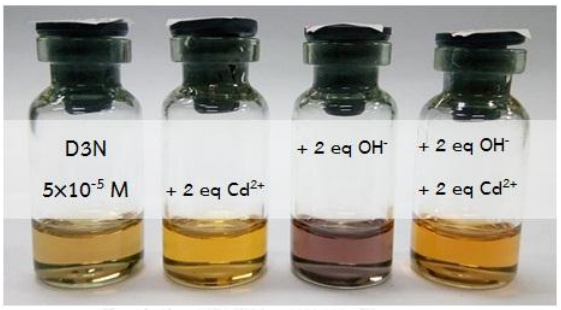

Figure 3.17 Color of 5×10^{-5} M **D3N** upon addition of Cd^{2+} or/and OH^- for the demonstration of the naked-eye sensor for transition and heavy metal ions

The observation of this "always orange" could be applied to a naked-eye sensor for transition or heavy metal ions due to a high contrast change from purple solution of **D3N** and 2 equivalents of hydroxide ions to orange color when metal ion was presented, which will be discussed in section 3.5 (*vide infra*).

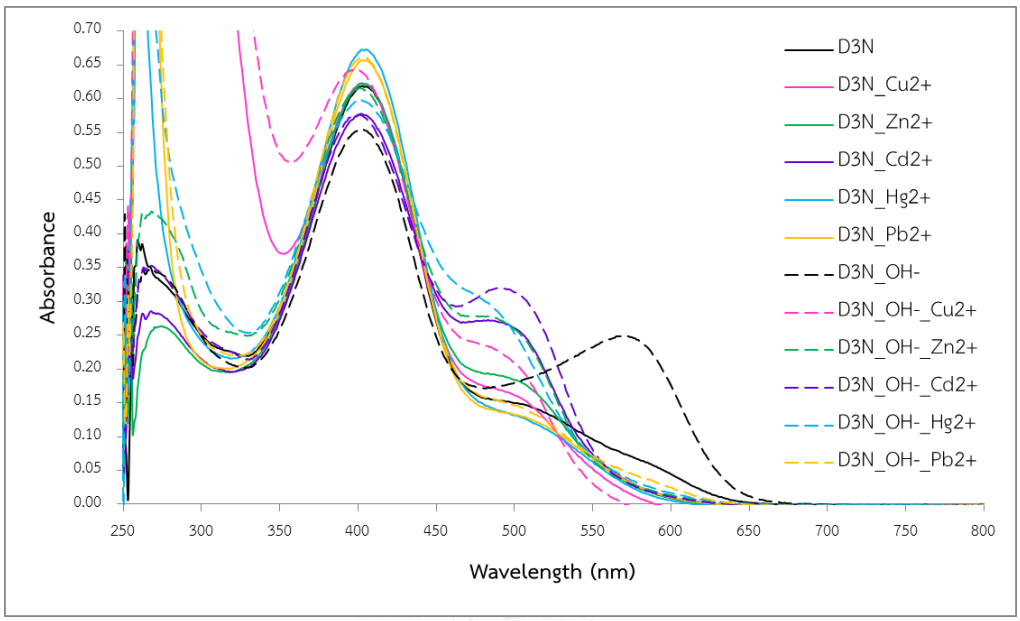

Figure 3.18 UV-visible spectra of 2×10^{-5} M **D3N** upon addition of transition and heavy metal ions under the basic condition under the neutral (solid line) and basic (dash line) conditions

In addition, the occurrence of peak around 490 nm in the presence of transition and heavy metal ions, with or without strong basic anions, suggested that the interaction between **D3N** and transition and heavy metal ions should involve to nitrogen atoms in the two azo bonds. The fact that basic anions could not alter the absorption implied that these basic anions had to interact with the different binding site.

The allosteric effect in **D3N** was also studied by the sequential addition of a couple of metal ions, which was anticipated to be appropriate for different ionophores in this host. The first metal ion being chosen for the ionophoric chain was K^+ due to a slight purple color observed in a preliminary study and the second metal ion being chosen for nitrogen atoms in azo bonds and **π**-electrons on benzene rings was Cd^{2+} due to the most color intense of **D3N**-Cd^{2+} solution. These studies were proceeded under non-hydroxide and hydroxide ions conditions and looked into sequential addition, *i.e.* addition of K^+ first, addition of Cd^{2+} first, and addition of K^+ and Cd^{2+} together. The results showed that the final color observed in the mixture

was always orange, *i.e.* K^{+} could not alter any color at all, and in the presence of base, addition of Cd^{2+} would change purple color back to orange. These outcomes reflected that **D3N** ligand lacked the allosteric effect because none of a dual metal ions condition could exhibit the different optical properties.

3.2.2.2 Study of sensing properties of **D4N**

D4N, a bright yellow solution in DMSO, displayed the wavelength of maximum absorption (λ_{max}) at 399 nm as can be seen in Figure 3.4 (*vide supra*).

The sensing property of this host was studied by addition of 10 equivalents of alkali, alkaline earth, transition or heavy ions (Li^{+}, Na^{+}, K^{+}, Rb^{+}, Cs^{+}, Mg^{2+}, Ca^{2+} Cu^{2+}, Zn^{2+}, Cd^{2+}, Hg^{2+}, Pb^{2+}) into the ligand solution. Unfortunately no metal ion could bring any changes to color or UV-visible spectrum (Figure 3.19 Figure 3.20). Because of some remarkable results of **D3N**, more metal ions (Co^{2+}, Ni^{2+}, Mn^{2+}, Sn^{2+}, Al^{3+}, Eu^{3+}) were also studied in the case of **D4N** hoping that it might have induced some change. However, none of these metal ions could induce any color or UV-visible spectral change. Note that some of metal ions solutions were prepared in methanol, and it was proved that there was no solvatochromic effect from adding 0.1 mL methanol into 1 mL of 1×10^{-4} M **D4N**, *i.e.* there was no color change from using different solvents.

According to the color change of **D3N** analogue solution towards the presence of strong basic anions (OH^{-}, F^{-}, CN^{-}), the addition of strong basic anions into **D4N** was also carried out but no obvious color change was observed because the new shoulder peak around 590 nm was too small. These results might be caused by the flexibility of **D4N** allowing protons in amino groups to form hydrogen bondings with oxygen atoms in pseudocrown ether unit preventing basic anions to interact with these protons. Furthermore, the added ratios of basic anions might be improper due to the influence of the extended polyether chain on the acidity of protons in amino groups.

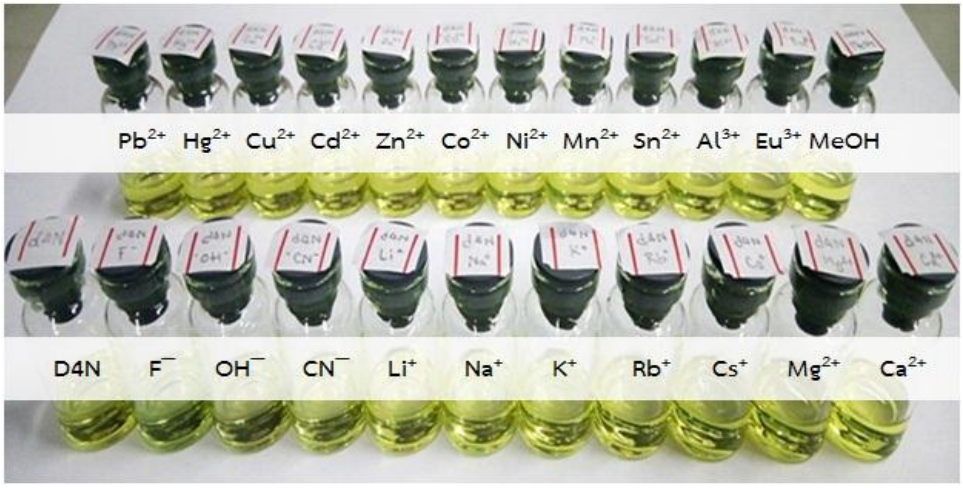

Figure 3.19 Color of 1×10^{-4} M **D4N** upon addition of ions

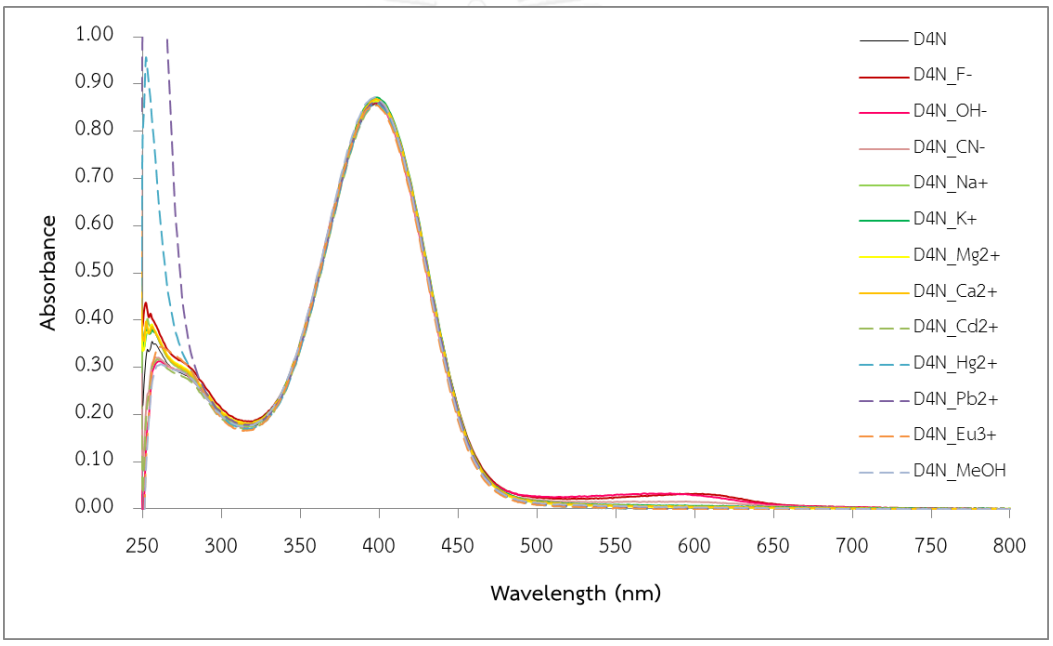

Figure 3.20 UV-visible spectra of 1×10^{-4} M **D4N** upon addition of ions

The lacking of sensing property of **D4N** towards any ion could be explained by the high flexibility of this host, which caused it to lose to form favorable conformation for guests.

3.3 Studies of the interaction of D3N toward strong basic anions

Azobenzene derivatives containing amino substituent in the para position usually display azo-hydrzone tautomerism in solution, of which the hydrazone form always shows a bathochromic shift (the maximum wavelength of absorption moving to a longer wavelength) from the azo form by around 100-150 nm differences [40, 50, 51, 70, 71]. In the case of light brown **D3N** in DMSO with a maximum absorption at

404 nm, addition of strong basic anions (OH^-, F^-, CN^-) led to dark purple color with an appearance of a new peak around 570-575 nm as shown in Figure 3.21. This approximate 170 nm bathochromic shift in **D3N** system is similar to the azo-hydrazone tautomerism. The fact that additions of transition and heavy metal ions into basic ligand solution could retreat the peak maximum of the purple solution to 490 nm of orange solution, as in the case of adding only metal ions, suggests that the interaction between **D3N** and strong base is a reversible reaction.

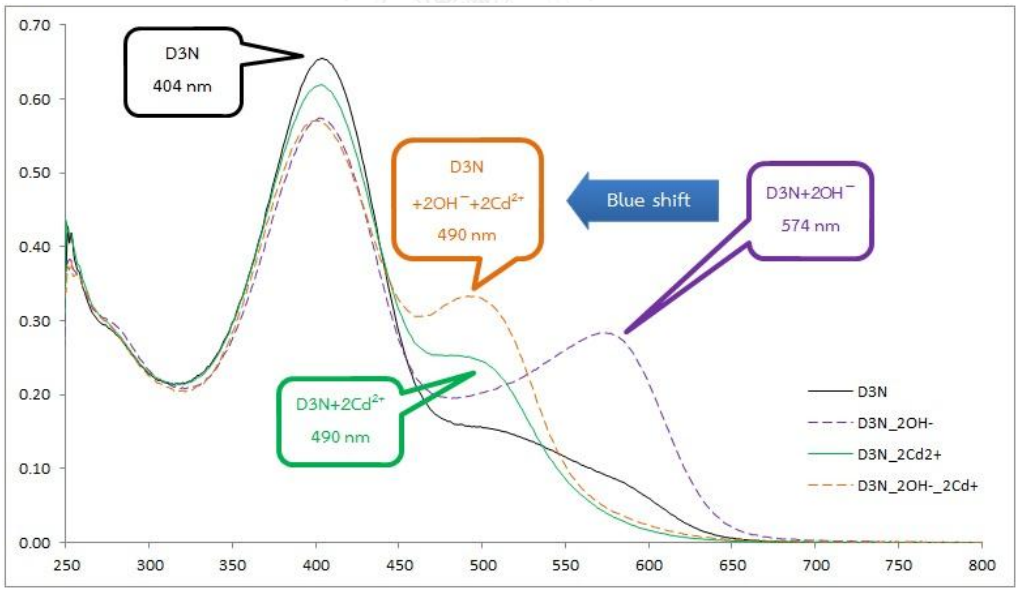

Figure 3.21 UV-visible spectra of 2×10^{-5} M **D3N** upon addition of Cd^{2+} or/and OH^- for the demonstration of the naked-eye sensor for transition and heavy metal ions

The bathochromic shift around 170 nm of **D3N** in the presence of strong basic anions could be a result of an interaction of base with hydrogen at secondary amine

moieties leading to hydrozone-like form. The electron withdrawing groups like nitro groups could increase proton acidity and promote the formation of the strong hydrogen-bonded complexes. The resonance structures for azo-hydrzone tautomers in **D3N** were proposed in Figure 3.22 based on similar results from structures of azo bonds connected to nitro-benzene [40, 50, 67, 72, 73].

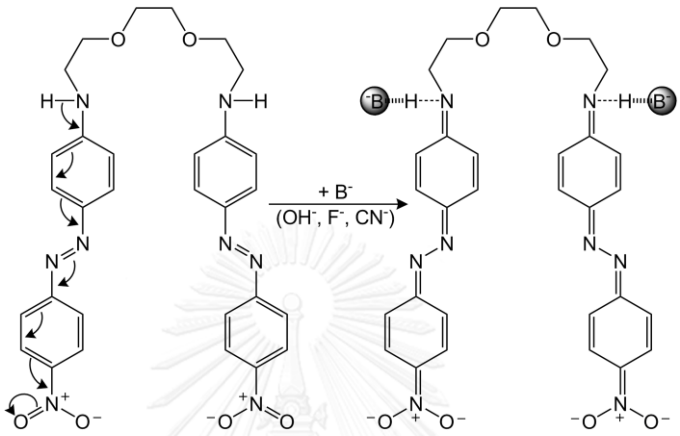

Figure 3.22 Postulated resonance structures

The ^{1}H-NMR spectroscopy was employed to investigate the detail of the interaction between strong basic anions and **D3N** via the addition of the various amount of tetrabutylammonium fluoride solution from 0.1 to 2 equivalents into the [D_6] DMSO solution of 4 mM **D3N**. If the hydrogen bonding or/and the deprotonation at secondary amine moieties occurred, the ^{1}H-NMR spectrum could reveal the change in chemical shift of the related proton or/and the appearance of HF_2^- peak. Unfortunately, the result was inconclusive due to the high intensity of proton in tetrabutylammonium ion compared to the intensity of proton in this ligand, which probably led to a missing of HF_2^- signal.

To confirm the proposed structure, solid potassium fluoride or potassium cyanide which was hardly soluble in DMSO was added into **D3N** solution directly. The resulted ^{1}H-NMR spectra did not show any distinguishable changes in any proton chemical shift nor the presence of HF_2^- or HCN signal. However the solution color did change from yellow brown to dark purple immediately after adding anion salts confirming that some interactions really occurred.

Many publication stated that the appearance of HF_2^- signal around 15-16 ppm [72-76] could be found at high concentration of F^- (up to 10 equivalents) due to acidity of proton [75]. Moreover, some reports showed that neither chemical shift changes in aromatic ring region during the hydrogen bonding complex formation nor the signal of HF_2^- could be seen in the presence of a small amount of F^- [74, 76] The similar results were also observed in the case of low concentration of CN^- of which no chemical shift change in aromatic rings nor free HCN signal around 5-6 ppm could be observed [77]. Thus, it is possible for this study that the absence of HF_2^- or HCN sign and significant chemical shift changes in these ^{1}H-NMR spectral studies might be caused by the low concentration of anions especially the case of solid addition, which could not indicate the exact amount of anions dissolving in [D_6] DMSO.

3.4 Studies of the sensitivity of D3N toward fluoride and cyanide ions

As the presence of fluoride or cyanide ion could cause the obvious change from yellow to dark purple, it was interesting to obtain the calibration curves for these anions via UV-visible spectrophotometric titration between 20 μM **D3N** and tetrabutylammonium fluoride or tetrabutylammonium cyanide in DMSO.

3.4.1 Sensitivity of **D3N** toward fluoride ion

The construction of a calibration curve for F^- was found out that a linearity of a calibration plot of the absorption intensity of 20 μM **D3N** at 569 nm versus [F^-] in DMSO solution showed the correlation coefficient of 0.9832 in the range of the increment amount of F^- from 10 to 40 μM. The slight tint of violet observed at 40 μM F^- addition allowed a naked-eye sensor for F^- as shown in Figure 3.24.

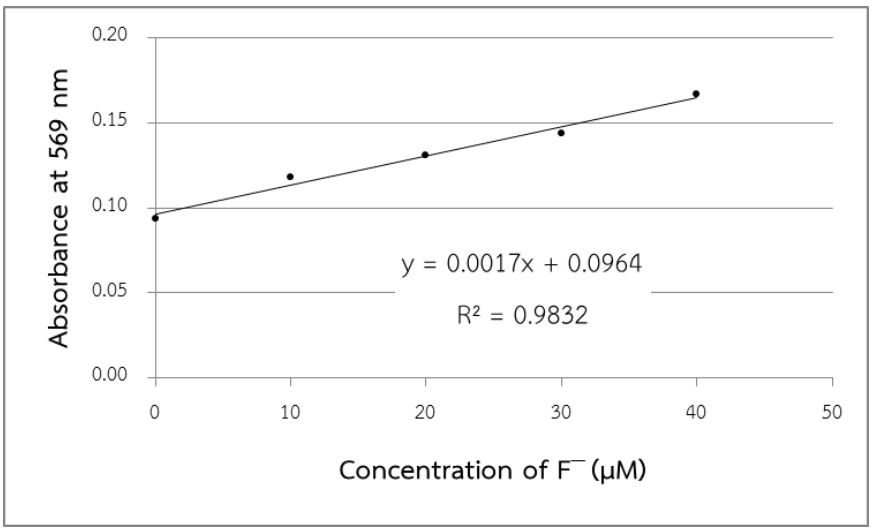

Figure 3.23 Calibration curve of 20 μM **D3N** for the determination of the concentration of F^- in DMSO

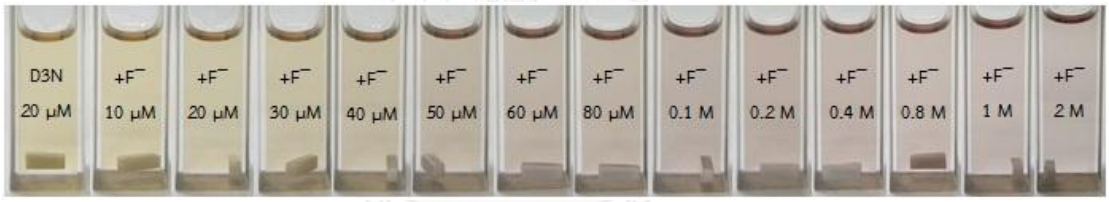

Figure 3.24 Color of 20 μM **D3N** upon the addition of various amount of F^- in DMSO

3.4.2 Sensitivity of **D3N** toward cyanide ion

The construction of a calibration curve for CN^- displayed a linearity of a calibration plot of the absorption intensity of 20 μM **D3N** at 574 nm versus [CN^-] in DMSO solution with the excellent correlation coefficient of 0.9956, which covered the range of the increment amount of CN^- from 2 to 10 μM. The tint of violet could be noticed after the presence of 4 μM CN^- as shown in Figure 3.26.

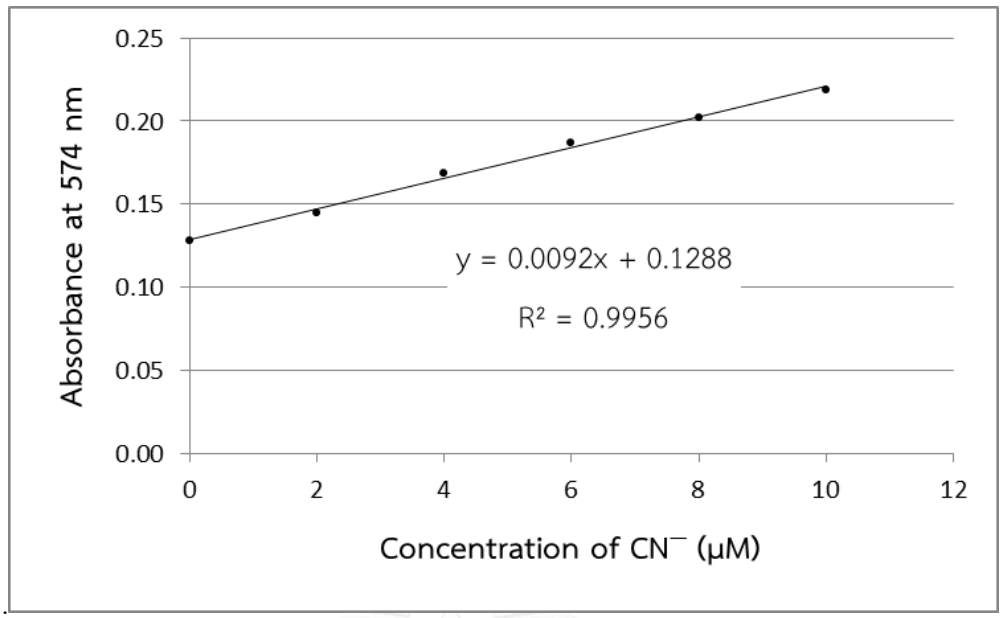

Figure 3.25 Calibration curve of 20 μM **D3N** for the determination of the concentration of CN^- in DMSO

Figure 3.26 Color of 20 μM **D3N** upon the addition of various amount of CN^- in DMSO

Moreover, the scale of linearity for CN^- detection could be extended to a higher concentration range by increasing the concentration of this ligand. For example, a calibration plotting of the absorption intensity of 50 μM **D3N** at 574 nm versus [CN^-] could exhibit a linear fashion with the increment amount of CN^- from 2.5 to 30 μM, which corresponded to the correlation coefficient of 0.998.

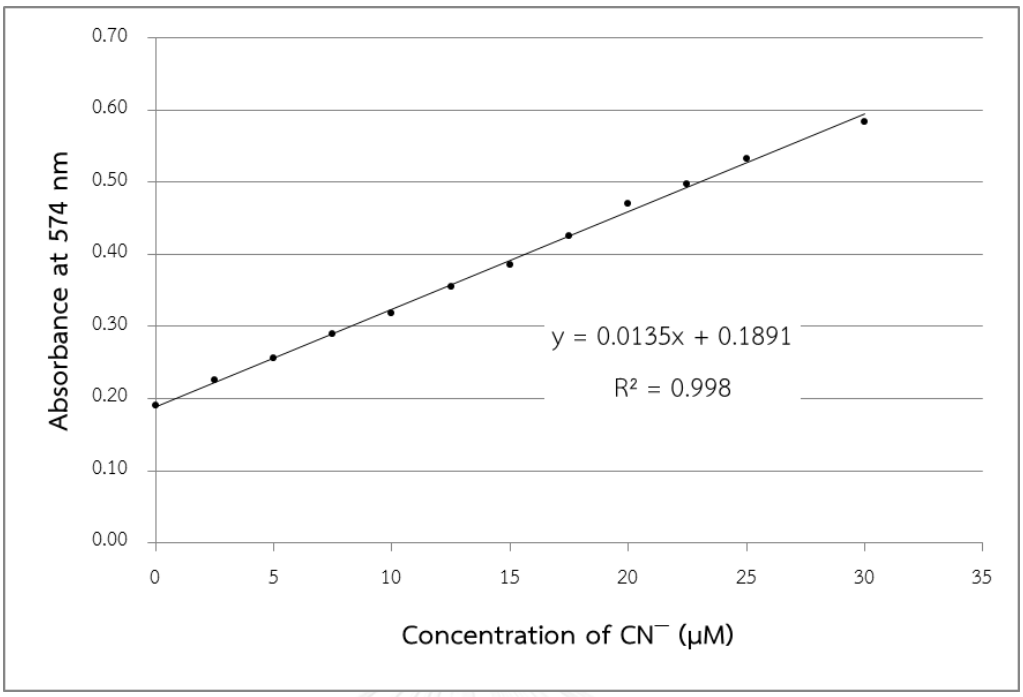

Figure 3.27 Calibration curve of 50 μM **D3N** for the determination of the concentration of CN^- in DMSO

So, **D3N** was able to be used as CN^- optical sensor for a trace and high quantities analysis.

3.5 Studies of the sensitivity of D3N toward transition and heavy metal ions under the basic condition

Although the interaction between **D3N** and transition or heavy metal ions in the absence and the presence of strong basic anions in DMSO could not show any distinguish optical changes toward specific metal ions, the enhancement of absorption intensity in transition and heavy metal ions band caused by the presence of strong basic anions was interesting to use as the condition for the quantitative analysis of these metal ions, which was expected to assist the detection of the signal from a trace amount of these metal ions.

3.5.1 Sensitivity of **D3N** toward cadmium ion

A calibration curve for Cd^{2+} was constructed from the absorption intensity of 20 μM **D3N** with 2 equivalents of hydroxide ions at 575 nm versus [Cd^{2+}] in DMSO solution because the maximum wavelength caused by the presence of hydroxide ions was more consistent than the maximum wavelength of the presence of Cd^{2+}, which moved to the shorter wavelength upon the increment of [Cd^{2+}] as shown in Figure 3.28. A linearity of this calibration plot was found in the range of the increment amount of Cd^{2+} from 2 to 10 μM with the satisfied correlation coefficient of 0.9968 (Figure 3.29), while the color change upon the presence of Cd^{2+} was noticed after the concentration of Cd^{2+} reached 4 μM (Figure 3.30).

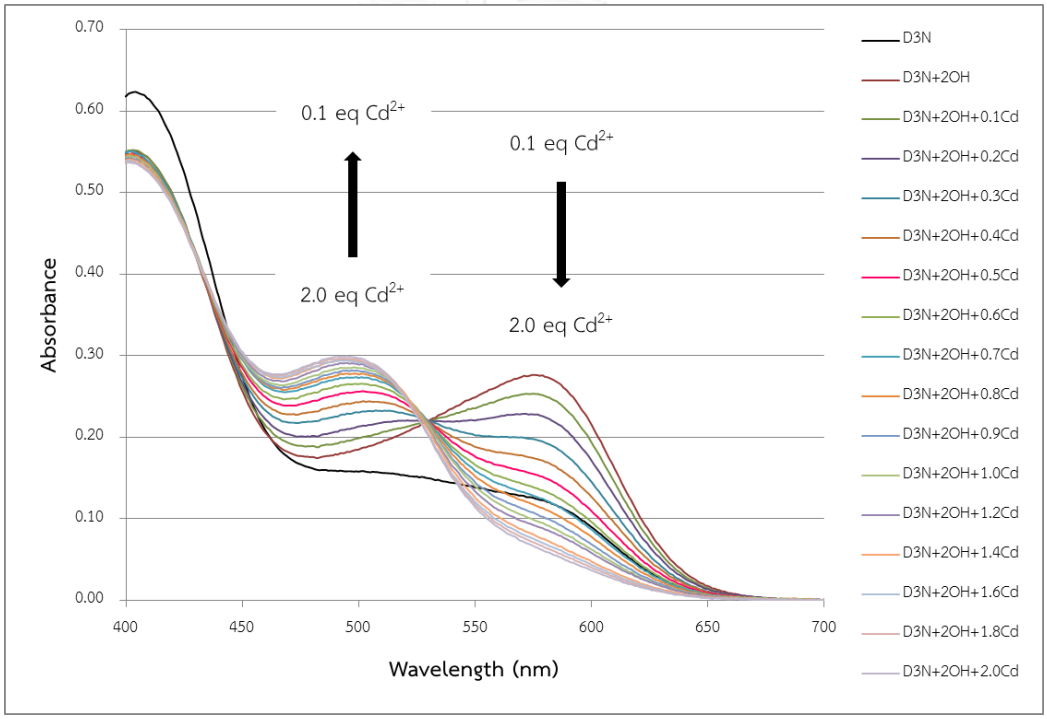

Figure 3.28 UV-visible spectra of 20 μM **D3N** under the basic condition upon the addition of various amount of Cd^{2+} in DMSO.

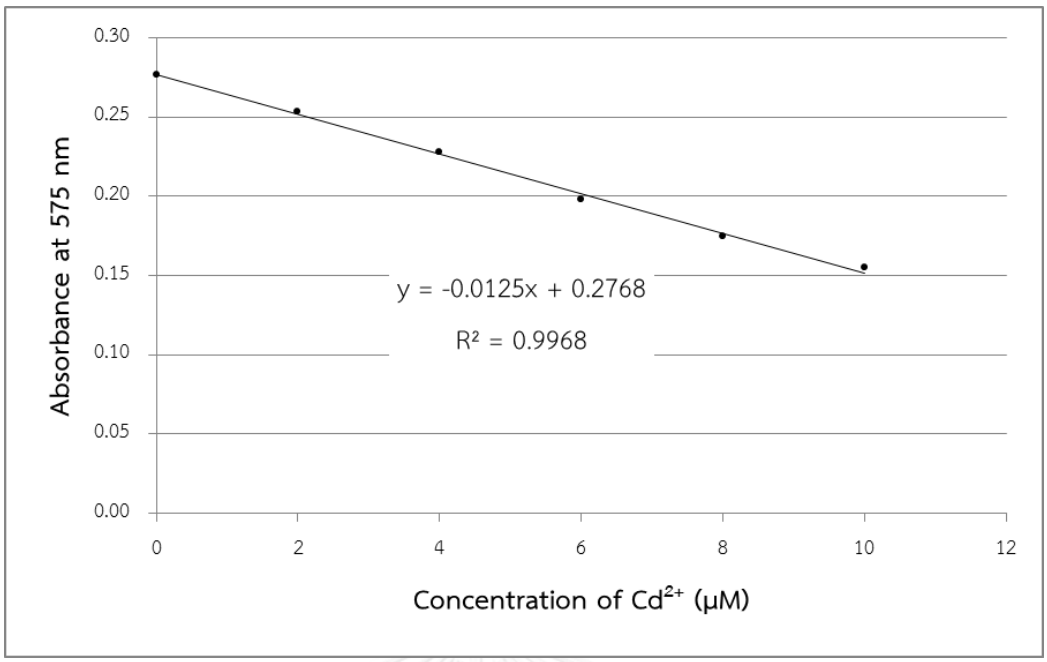

Figure 3.29 Calibration curve of 20 μM **D3N** under the basic condition for the determination of the concentration of Cd^{2+} in DMSO.

Figure 3.30 Color of 20 μM **D3N** under the basic condition upon the addition of various amount of Cd^{2+} in DMSO.

3.5.2 Sensitivity of **D3N** toward mercury ion

The plot of a calibration curve showed the absorption intensity of 20 μM **D3N** with 2 equivalents of hydroxide ions at 574 nm versus [Hg^{2+}] in DMSO solution due to the stable maximum wavelength of the hydroxide ion region comparing with the blue shift maximum wavelength of the Hg^{2+} region. This calibration plot displayed the linearity with the correlation coefficient of 0.9824 in the range of the increment amount of Hg^{2+} from 2 to 8 μM as shown in Figure 3.31.

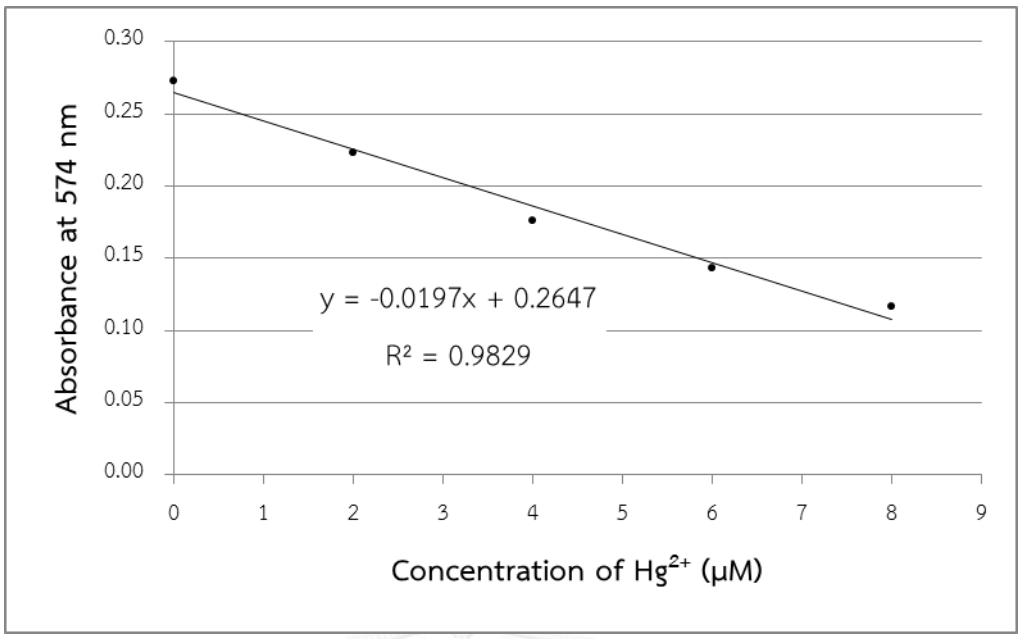

Figure 3.31 Calibration curve of 20 μM **D3N** under the basic condition for the determination of the concentration of Hg^{2+} in DMSO

3.5.3 Sensitivity of **D3N** toward zinc ion

The construction of a calibration curve the absorption intensity of 20 μM **D3N** with 2 equivalents of hydroxide ions versus [Zn^{2+}] in DMSO solution was pointed at 575 nm of the hydroxide ion band because the absorption intensity in the presence of Zn^{2+} was very broad, which was hard to define the maximum absorption. This calibration curve could work in the range of the increment amount of Zn^{2+} from 8 to 20 μM and showed the linearity with the excellent correlation coefficient of 0.999 (Figure 3.32).

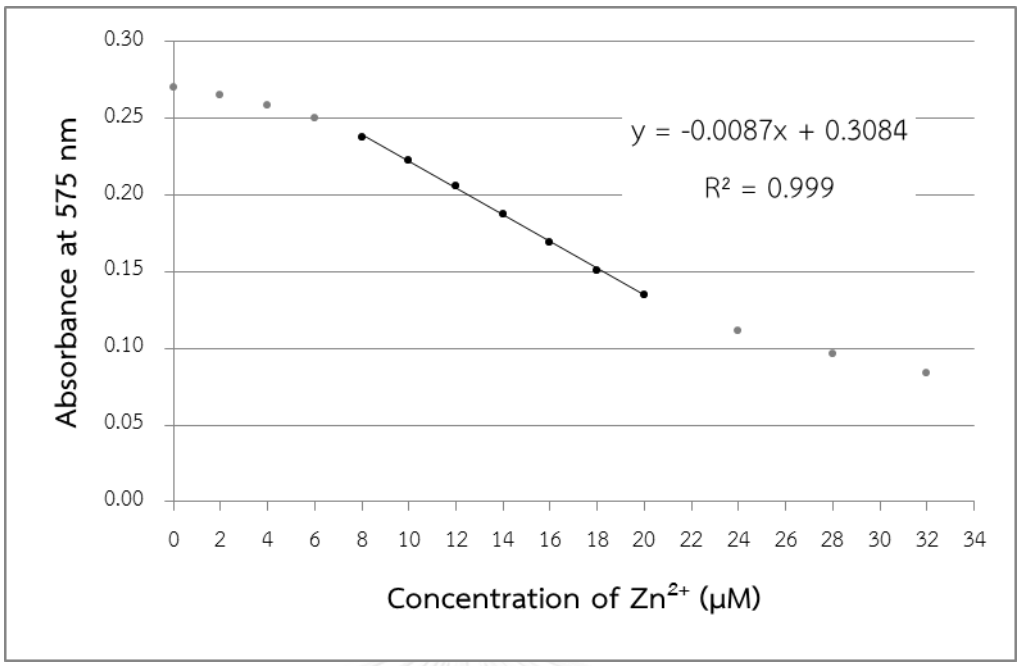

Figure 3.32 Calibration curve of 20 μM **D3N** under the basic condition for the determination of the concentration of Zn^{2+} in DMSO

According to the calibration curves of these metal ions, **D3N** was able to use as the sensor for the quantitative detection of transition and heavy metal ions.

CHAPTER IV
CONCLUSION

4.1 Conclusion

The five novel diazo pseudocrown ether derivatives bearing azo benzene units were successfully synthesized. The sensing properties toward metal ion of ester derivatives showed no obvious color change probably due to the steric effect from ester substituents on terminal benzene rings preventing favorable configuration for metal ion binding. In the case of nitro derivatives, a light brown solution of **D3N** in DMSO (λ_{max} = 404 nm) exhibited a color change from light brown to light orange having a new maximum absorption approximately at 490 nm upon the addition of transition or heavy metal ions (Cu^{2+}, Zn^{2+}, Cd^{2+}, Hg^{2+}, Pb^{2+}). Moreover, the addition of strong basic anions (OH^-, F^-, CN^-) resulted in dark purple color with a new absorption signal around 570-576 nm, a 170 nm shift to a longer wavelength. This solution could turn into orange once transition or heavy metal ions were added. The fact that whenever transition or heavy metal ions were presented, with or without hydroxide ions, the solution would always be orange suggested that these metal ions should interact with nitrogen atoms of azo bonds. Also **D3N,** assisted by addition of 2 equivalents of hydroxide ion, could provide naked-eye detection for transition and heavy metal ions due to the high contrast color change from dark purple to orange. A calibration curve plotted from the absorption intensity of 20 μM **D3N** in DMSO at 574 nm allowed a determination of trace quantity of CN^- in a linear range of 2 – 10 μM with impressive R^2 of 0.9956. In the case of transition and heavy metal ions, the construction of calibration curves was constructed under a basic condition yielding excellent correlation coefficient. Unfortunately, the other nitro derivative **D4N** displayed no color change toward any metal ions, very likely because of the high flexibility of this ligand. Lastly, the expected allosteric effect from these pseudocrown ether derivatives was unfortunately not observed probably because alkali metal ions could not interact with the pseudocrown ether unit well enough to induce the ligand's conformation to suitably bind with transition or heavy metal ions.

4.2 Future works

Future studies for this research will include proving of the ligand's position at which the interaction with guest ions occurs, refining the stability constants of the complexes, and purifying the synthesized **I3N**.

REFERENCES

[1] Ariga, K. and Kunitake, T. Supramolecular Chemistry - Fundamentals and Applications. 1 ed. Germany: Springer-Verlag Berlin Heidelberg, 2006.

[2] Christoph A. Schalley. Analytical Methods in Supramolecular Chemistry. 2 ed. Vol. 1. Germany: John Wiley & Sons, 2012.

[3] Lehn, J.M. Supramolecular Chemistry—Scope and Perspectives Molecules, Supermolecules, and Molecular Devices (Nobel Lecture). Angewandte Chemie International Edition in English 27(1) (1988): 89-112.

[4] Lehn, J.M. Perspectives in Supramolecular Chemistry—From Molecular Recognition towards Molecular Information Processing and Self-Organization. Angewandte Chemie International Edition in English 29(11) (1990): 1304-1319.

[5] Veale, E.B. and Gunnlaugsson, T. Fluorescent sensors for ions based on organic structures. Annual Reports Section "B" (Organic Chemistry) 106 (2010): 376.

[6] Kaur, N. and Kumar, S. Colorimetric metal ion sensors. Tetrahedron 67(48) (2011): 9233-9264.

[7] Ma, D.L., Ma, V.P.Y., Chan, D.S.H., Leung, K.H., He, H.Z., and Leung, C.H. Recent advances in luminescent heavy metal complexes for sensing. Coordination Chemistry Reviews 256(23–24) (2012): 3087-3113.

[8] Carter, K.P., Young, A.M., and Palmer, A.E. Fluorescent sensors for measuring metal ions in living systems. Chem Rev 114(8) (2014): 4564-601.

[9] Quang, D.T. and Kim, J.S. Fluoro- and Chromogenic Chemodosimeters for Heavy Metal Ion Detection in Solution and Biospecimens. Chemical Reviews 110(10) (2010): 6280-6301.

[10] Kim, H.N., Ren, W.X., Kim, J.S., and Yoon, J. Fluorescent and colorimetric sensors for detection of lead, cadmium, and mercury ions. Chem Soc Rev 41(8) (2012): 3210-44.

[11] Kim, T.H., et al. Transition metal ion selective ortho-ester diazophenylcalix[4]arene. Talanta 71(3) (2007): 1294-7.

[12] Loehr, H.G. and Voegtle, F. Chromo- and fluoroionophores. A new class of dye reagents. Accounts of Chemical Research 18(3) (1985): 65-72.

[13] Misra, A. and Shahid, M. Chromo and Fluorogenic Properties of Some Azo-Phenol Derivatives and Recognition of Hg2+ Ion in Aqueous Medium by Enhanced Fluorescence. The Journal of Physical Chemistry C 114(39) (2010): 16726-16739.

[14] Sancenón, F., Martínez-Máñez, R., and Soto, J. Colourimetric detection of Hg2+ by a chromogenic reagent based on methyl orange and open-chain polyazaoxaalkanes. Tetrahedron Letters 42(26) (2001): 4321-4323.

[15] Lee, S.J., et al. A Chromogenic Macrocycle Exhibiting Cation-Selective and Anion-Controlled Color Change: An Approach to Understanding Structure–Color Relationships. Organic Letters 8(8) (2006): 1641-1643.

[16] Antonisse, M.M.G. and Reinhoudt, D.N. Potentiometric Anion Selective Sensors. Electroanalysis 11(14) (1999): 1035-1048.

[17] Bühlmann, P., Pretsch, E., and Bakker, E. Carrier-Based Ion-Selective Electrodes and Bulk Optodes. 2. Ionophores for Potentiometric and Optical Sensors. Chemical Reviews 98(4) (1998): 1593-1688.

[18] Kim, H.J., Park, D.S., Hyun, M.H., and Shim, Y.B. Determination of HgII Ion with a 1,11-Bis(8-quinoyloxy)-3,6,9-trioxaundecane-Modified Glassy Carbon Electrode Using Spin-Coating Technique. Electroanalysis 10(5) (1998): 303-306.

[19] Nabeshima, T., Inaba, T., Furukawa, N., Hosoya, T., and Yano, Y. Artificial allosteric ionophore: regulation of ion recognition of polyethers bearing bipyridine moieties by copper(I). Inorganic Chemistry 32(8) (1993): 1407-1416.

[20] Ushakov, E.N., et al. Sandwich-Type Complexes of Alkaline-Earth Metal Cations with a Bisstyryl Dye Containing Two Crown Ether Units. The Journal of Physical Chemistry A 103(50) (1999): 11188-11193.

[21] Valeur, B. and Leray, I. Design principles of fluorescent molecular sensors for cation recognition. Coordination Chemistry Reviews 205(1) (2000): 3-40.

[22] Wu, J., Kwon, B., Liu, W., Anslyn, E.V., Wang, P., and Kim, J.S. Chromogenic/Fluorogenic Ensemble Chemosensing Systems. Chemical Reviews 115(15) (2015): 7893-7943.

[23] Pedersen, C.J. Cyclic polyethers and their complexes with metal salts. Journal of the American Chemical Society 89(26) (1967): 7017-7036.

[24] Steed, J.W. and Atwood, J.L. Cation-Binding Hosts. in Supramolecular Chemistry, pp. 105-222: John Wiley & Sons, Ltd, 2009.

[25] Pedersen, C.J. Cyclic polyethers and their complexes with metal salts. Journal of the American Chemical Society 89(10) (1967): 2495-2496.

[26] Moore, C. and Pressman, B.C. Mechanism of action of valinomycin on mitochondria. Biochemical and Biophysical Research Communications 15(6) (1964): 562-567.

[27] Vögtle, F. and Weber, E. Multidentate Acyclic Neutral Ligands and Their Complexation. Angewandte Chemie International Edition in English 18(10) (1979): 753-776.

[28] Tuemmler, B., Maass, G., Weber, E., Wehner, W., and Voegtle, F. Noncyclic crown-type polyethers, pyridinophane cryptands, and their alkali metal ion complexes: synthesis, complex stability, and kinetics. Journal of the American Chemical Society 99(14) (1977): 4683-4690.

[29] R. Katritzky, A., A. Belyakov, S., V. Denisko, O., Maran, U., and S. Dalal, N. New podands with terminal chromogenic moieties derived from formazans. Journal of the Chemical Society, Perkin Transactions 2 (3) (1998): 611-616.

[30] Rogers, R.D., Bond, A.H., Aguinaga, S., and Reyes, A. Polyethylene glycol complexation of Cd2+. Structures of triethylene glycol complexes of CdCl2, CdBr2 and CdI2. Inorganica Chimica Acta 212(1–2) (1993): 225-231.

[31] Wen, Y.H., Lahiri, S., Qin, Z., Wu, X.L., and Liu, W.S. Decontamination of radioactive cesium from natural NaCl by amide-type open-chain crown ethers. Journal of Radioanalytical and Nuclear Chemistry 253(2) (2002): 263-265.

[32] Hayashita, T., Qing, D., Bartsch, R.A., Elshani, S., Hanes, R.E., and Teramae, N. Lead Ion Selective Signal Amplification by a Supramolecular Podand Fluoroionophore/Surfactant Complex Sensor in Water. Supramolecular Chemistry 17(1-2) (2005): 141-146.

[33] Abe, A.M.M., Helaja, J., and Koskinen, A.M.P. Novel Crown Ether and Salen Metal Chelation Driven Molecular Pincers. Organic Letters 8(20) (2006): 4537-4540.

[34] Harris, M., et al. Ethylene oxide-bridged bipyridine oligomers that function as selective host molecules for the encapsulation of small alkali cation guests. Journal of Inclusion Phenomena and Macrocyclic Chemistry 60(1-2) (2007): 153-161.

[35] Ruiz-Sanchez, A.J., Vida, Y., Suau, R., and Perez-Inestrosa, E. Cation template assisted oligoethylene glycol desymmetrization by intramolecular Cannizzaro reaction of topologically remote aldehydes. Tetrahedron 64(51) (2008): 11661-11665.

[36] Chen, L., et al. Tridentate lysine-based fluorescent sensor for Hg(II) in aqueous solution. Inorg Chem 50(20) (2011): 10028-32.

[37] Nishimura, Y., Takemura, T., and Arai, S. Li+ Selective Podand-Type Fluoroionophore Based on a Diphenyl Sulfoxide Derivative Bearing Two Pyrene Groups. Molecules 16(8) (2011).

[38] CIEC Promoting Science at the University of York. Colorants [Online]. 2013. Available from: http://www.essentialchemicalindustry.org/materials-and-applications/colorants.html [15 May 2016]

[39] Hunger, K. Industrial Dyes: Chemistry, Properties, Applications. Germany: Verlag GmbH & Co. KGaA, 2003.

[40] Gordon, P.F. and Gregory, P. Azo Dyes. in Organic Chemistry in Colour, pp. 95-162. Berlin, Heidelberg: Springer Berlin Heidelberg, 1987.

[41] R. L. M. Allen. Colour Chemistry. London: Thomas Nelson and Sons Ltd, 1971.

[42] Kovbasyuk, L. and Krämer, R. Allosteric Supramolecular Receptors and Catalysts. Chemical Reviews 104(6) (2004): 3161-3188.

[43] Gianneschi, N.C., Nguyen, S.T., and Mirkin, C.A. Signal Amplification and Detection via a Supramolecular Allosteric Catalyst. Journal of the American Chemical Society 127(6) (2005): 1644-1645.

[44] Kumar, M., Dhir, A., and Bhalla, V. Regulation of metal ion recognition by allosteric effects in thiacalix[4]crown based receptors. Tetrahedron 65(36) (2009): 7510-7515.

[45] Liu, Y., Duan, Z.Y., Zhang, H.Y., Jiang, X.L., and Han, J.R. Selective Binding and Inverse Fluorescent Behavior of Magnesium Ion by Podand Possessing Plural Imidazo[4,5-f]-1,10-phenanthroline Groups and Its Ru(II) Complex. The Journal of Organic Chemistry 70(4) (2005): 1450-1455.

[46] Nishimura, J., Inokuma, S., Nishio, S., Funaki, T., Atarashi, N., and Shirakawa, T. A Pseudo Thiacrown Compound Formed by Hydrophobic Interaction of Its Lipophilic Parts in Water: Ag+Selective Fluorophore in Water. Heterocycles 60(1) (2003).

[47] Cheng, X., Li, Q., Li, C., Qin, J., and Li, Z. Azobenzene-Based Colorimetric Chemosensors for Rapid Naked-Eye Detection of Mercury(II). Chemistry – A European Journal 17(26) (2011): 7276-7281.

[48] Yang, H., Song, H., Zhu, Y., and Yang, S. Single chemosensor for multiple analytes: chromogenic and fluorogenic detection for fluoride anions and copper ions. Tetrahedron Letters 53(16) (2012): 2026-2029.

[49] Lewis, G.E. Structures of the mono-acid cations of 4-aminoazobenzene and its derivatives. Tetrahedron 10(3) (1960): 129-134.

[50] Matazo, D.R.C., Ando, R.A., Borin, A.C., and Santos, P.S. Azo–Hydrazone Tautomerism in Protonated Aminoazobenzenes: Resonance Raman Spectroscopy and Quantum-Chemical Calculations. The Journal of Physical Chemistry A 112(19) (2008): 4437-4443.

[51] Chen, X.C., Tao, T., Wang, Y.G., Peng, Y.X., Huang, W., and Qian, H.-F. Azo-hydrazone tautomerism observed from UV-vis spectra by pH control and metal-ion complexation for two heterocyclic disperse yellow dyes. Dalton Transactions 41(36) (2012): 11107-11115.

[52] Harikrishnan, U. and Menon, S.K. The synthesis, characterization and spectral properties of crown ether based disazo dyes. Dyes and Pigments 77(2) (2008): 462-468.

[53] Caicedo, C., Rivera, E., Valdez-Hernández, Y., and Carreón-Castro, M.d.P. Synthesis and characterization of novel liquid-crystalline azo-dyes bearing two amino-nitro substituted azobenzene units and a well-defined, oligo(ethylene glycol) spacer. Materials Chemistry and Physics 130(1-2) (2011): 471-480.

[54] Solangi, I.B., Memon, S., Memon, N., and Bhanger, M.I. Exploration of Pb2+Selective Behavior of Calix[6]arene Ester Derivative. Journal of Macromolecular Science, Part A 45(12) (2008): 1003-1008.

[55] de Namor, A.F.D., Chahine, S., Kowalska, D., Castellano, E.E., and Piro, O.E. Selective Interaction of Lower Rim Calix[4]arene Derivatives and Bivalent Cations in Solution. Crystallographic Evidence of the Versatile Behavior of Acetonitrile in Lead(II) and Cadmium(II) Complexes. Journal of the American Chemical Society 124(43) (2002): 12824-12836.

[56] Abrahart, E.N. Dyes and Their Intermediates. Edward Arnold, 1977.

[57] García-Amorós, J. and Velasco, D. Recent advances towards azobenzene-based light-driven real-time information-transmitting materials. Beilstein Journal of Organic Chemistry 8 (2012): 1003-1017.

[58] Yen, Y.P. and Ho, K.W. Synthesis of colorimetric receptors for dicarboxylate anions: a unique color change for malonate. Tetrahedron Letters 47(7) (2006): 1193-1196.

[59] Rondino, F., et al. Competition between electron-donor and electron-acceptor substituents in nitrotoluene isomers: a photoelectron spectroscopy and ab initio investigation. RSC Advances 4(10) (2014): 5272-5282.

[60] Encyclopædia Britannica Online. Azo dye [Online]. 2016. Available from: http://global.britannica.com/science/azo-dye [18 May 2016]

[61] Martínez, R., Espinosa, A., Tárraga, A., and Molina, P. New Hg2+ and Cu2+ Selective Chromo- and Fluoroionophore Based on a Bichromophoric Azine. Organic Letters 7(26) (2005): 5869-5872.

[62] Nuriman, Kuswandi, B., and Verboom, W. Selective chemosensor for Hg(II) ions based on tris[2-(4-phenyldiazenyl)phenylaminoethoxy]cyclotriveratrylene in aqueous samples. Analytica Chimica Acta 655(1–2) (2009): 75-79.

[63] Wang, S., Shen, S., and Xu, H. Synthesis, spectroscopic and thermal properties of a series of azo metal chelate dyes. Dyes and Pigments 44(3) (2000): 195-198.

[64] Woods, M. and Sherry, A.D. Synthesis and Luminescence Studies of Aryl Substituted Tetraamide Complexes of Europium(III): A New Approach to pH Responsive Luminescent Europium Probes. Inorganic Chemistry 42(14) (2003): 4401-4408.

[65] Yu, T., et al. Synthesis, crystal structure and electroluminescent properties of a Schiff base zinc complex. Inorganica Chimica Acta 359(7) (2006): 2246-2251.

[66] Ghorbanian, S., Mehta, L.K., Parrick, J., and Robson, C.H. Synthesis of some 24-membered tetralactam derivatives by an unexpectedly simple route, and some macrocyclic polyether dilactams. Tetrahedron 55(50) (1999): 14467-14478.

[67] Dunn, N.J., Humphries, W.H., Offenbacher, A.R., King, T.L., and Gray, J.A. pH-Dependent cis ⟶ trans Isomerization Rates for Azobenzene Dyes in Aqueous Solution. The Journal of Physical Chemistry A 113(47) (2009): 13144-13151.

[68] Escudero, D., Trupp, S., Bussemer, B., Mohr, G.J., and González, L. Spectroscopic Properties of Azobenzene-Based pH Indicator Dyes: A Quantum Chemical and Experimental Study. Journal of Chemical Theory and Computation 7(4) (2011): 1062-1072.

[69] Wang, Y., Tang, B., and Zhang, S. A visible colorimetric pH sensitive chemosensor based on azo dye of benzophenone. Dyes and Pigments 91(3) (2011): 294-297.

[70] Adegoke, O.A., Adesuji, T.E., and Thomas, O.E. Novel colorimetric sensors for cyanide based on azo-hydrazone tautomeric skeletons. Spectrochimica Acta Part A: Molecular and Biomolecular Spectroscopy 128 (2014): 147-152.

[71] Cheon, K.S., Park, Y.S., Kazmaier, P.M., and Buncel, E. Studies of azo–hydrazone tautomerism and H-bonding in azo-functionalized dendrimers and model compounds. Dyes and Pigments 53(1) (2002): 3-14.

[72] Mahapatra, A.K., Manna, S.K., and Sahoo, P. Color response of tri-armed azo host colorimetric sensors and test kit for fluoride. Talanta 85(5) (2011): 2673-2680.

[73] Ros-Lis, J.V., Martínez-Máñez, R., Sancenón, F., Soto, J., Rurack, K., and Weißhoff, H. Signalling Mechanisms in Anion-Responsive Push-Pull Chromophores: The Hydrogen-Bonding, Deprotonation and Anion-Exchange Chemistry of Functionalized Azo Dyes. European Journal of Organic Chemistry 2007(15) (2007): 2449-2458.

[74] Arabahmadi, R. and Amani, S. A new fluoride ion colorimetric sensor based on azo–azomethine receptors. Supramolecular Chemistry 26(5-6) (2014): 321-328.

[75] Khanmohammadi, H. and Rezaeian, K. Naked-eye detection of inorganic fluoride in aqueous media using a new azo-azomethine colorimetric receptor enhanced by electron withdrawing groups. RSC Advances 4(2) (2014): 1032-1038.

[76] Sarkar, A., Bhattacharyya, S., and Mukherjee, A. Colorimetric detection of fluoride ions by anthraimidazoledione based sensors in the presence of Cu(ii) ions. Dalton Transactions 45(3) (2016): 1166-1175.

[77] Balamurugan, G. and Velmathi, S. Novel chromogenic selective sensors for aqueous cyanide ions under high water content and real sample analysis. Analytical Methods 8(7) (2016): 1705-1710.

APPENDIX

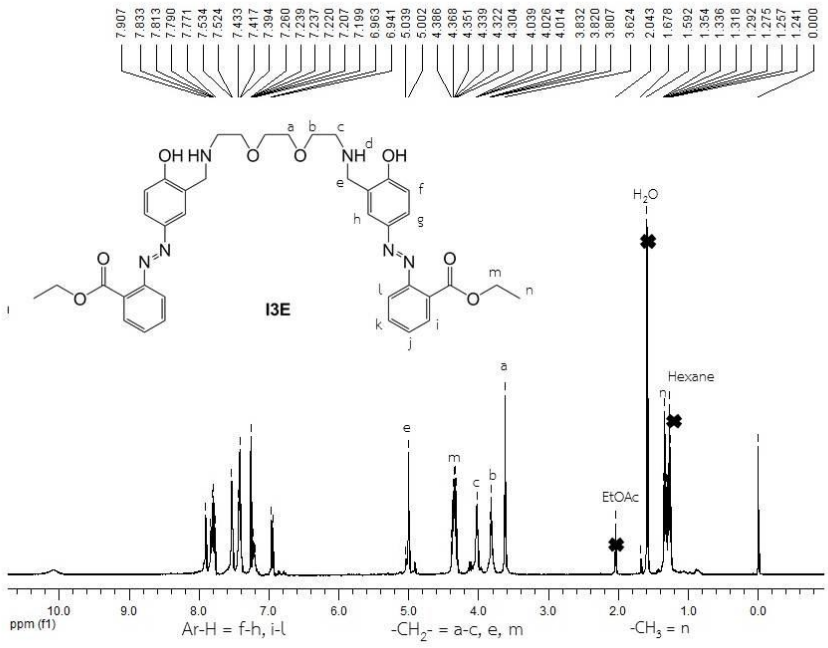

Figure A1 ^{1}H-NMR spectrum of **I3E** in $CDCl_3$ at 400 MHz

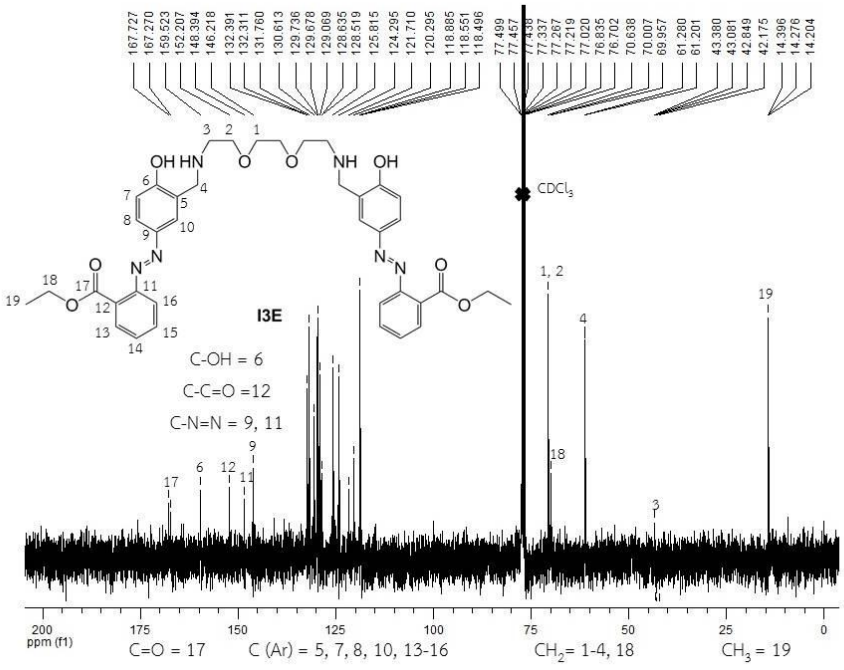

Figure A2 ^{13}C-NMR spectrum of **I3E** in $CDCl_3$ at 400 MHz

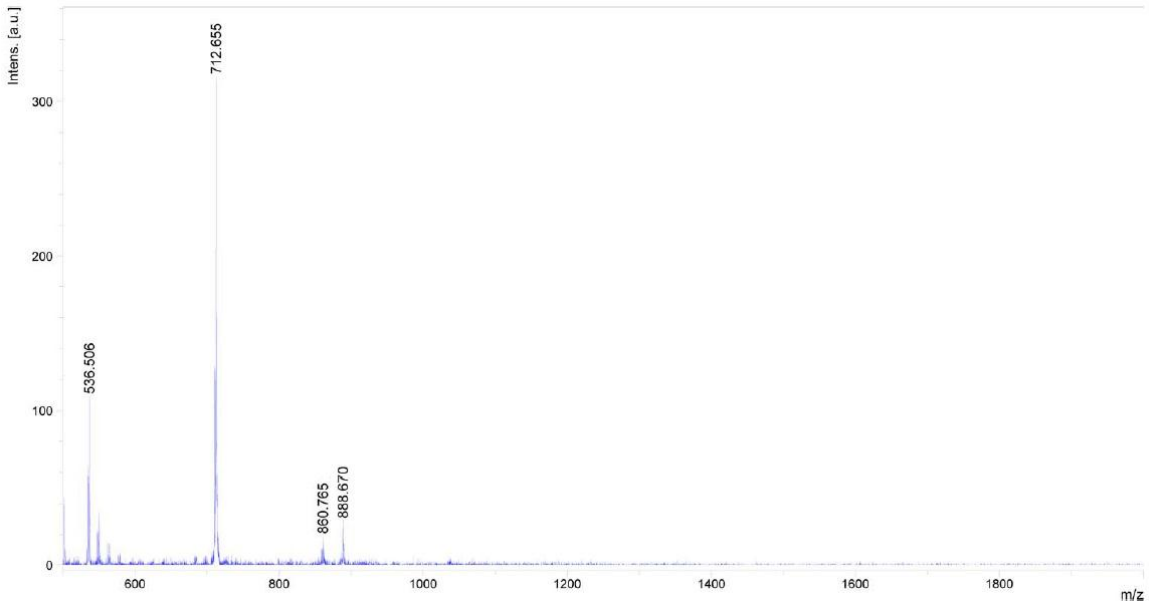

Figure A3 MALDI-TOF mass spectrum of **I3E** at 712.655 m/z

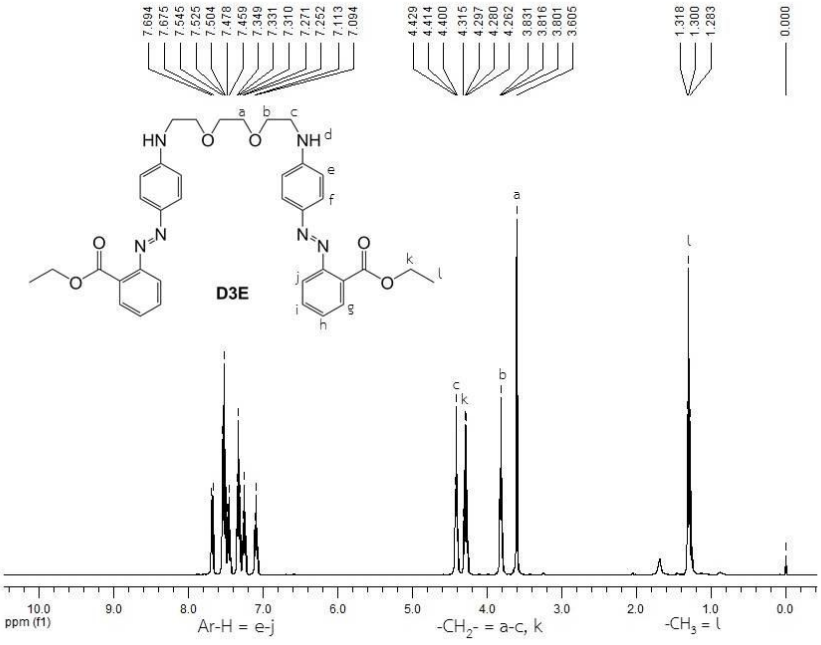

Figure A4 ^{1}H-NMR spectrum of **D3E** in $CDCl_3$ at 400 MHz

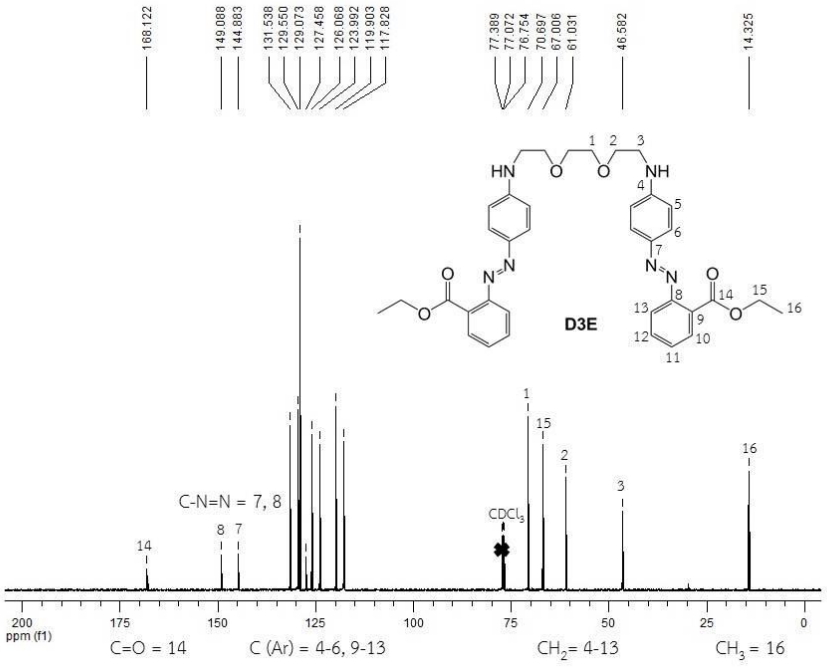

Figure A5 ^{13}C-NMR spectrum of **D3E** in $CDCl_3$ at 400 MHz

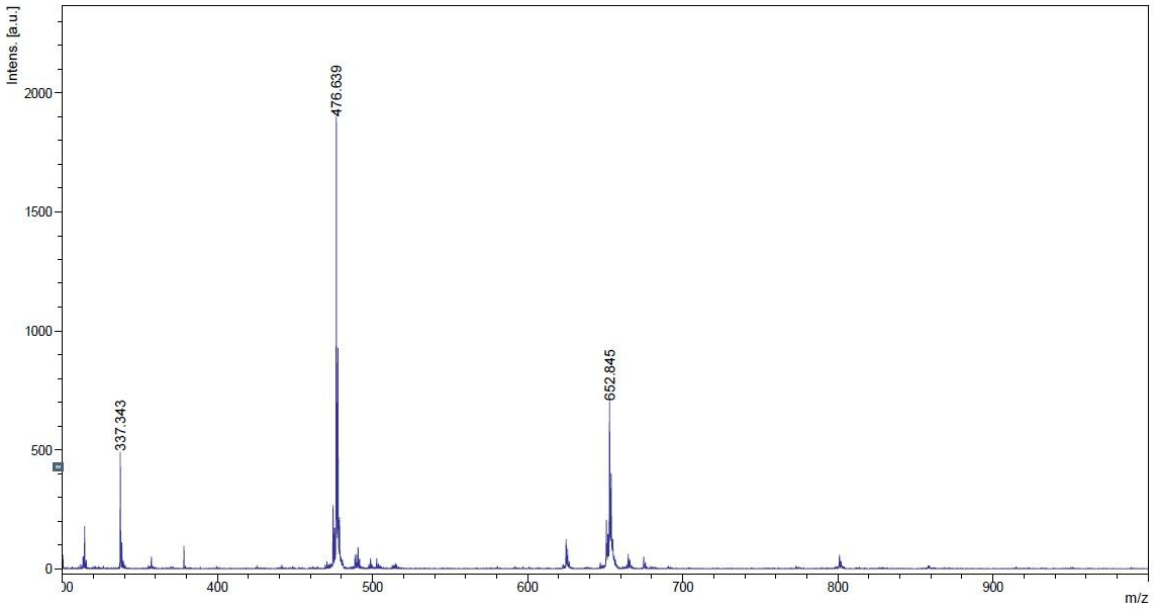

Figure A6 MALDI-TOF mass spectrum of **D3E** at 652.845 m/z

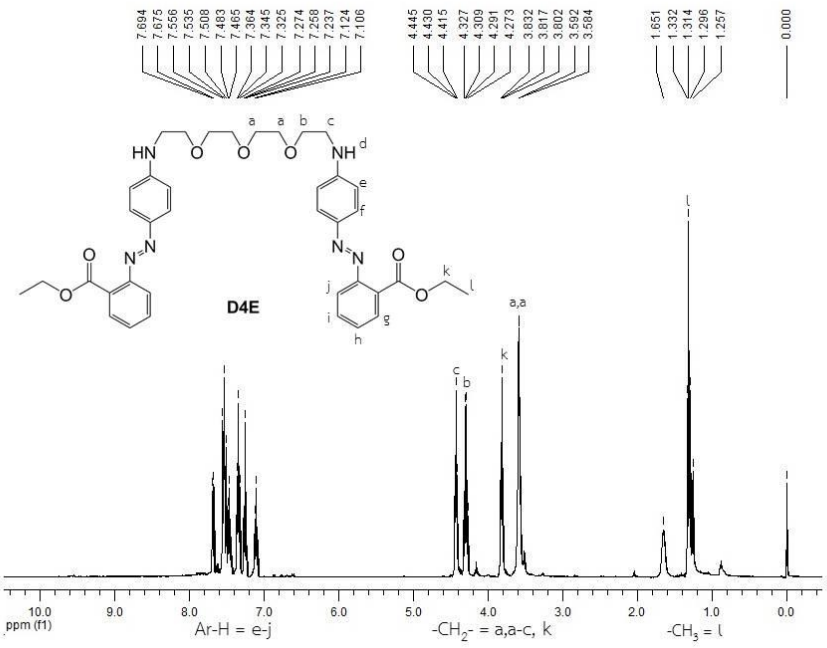

Figure A7 ^{1}H-NMR spectrum of **D4E** in $CDCl_3$ at 400 MHz

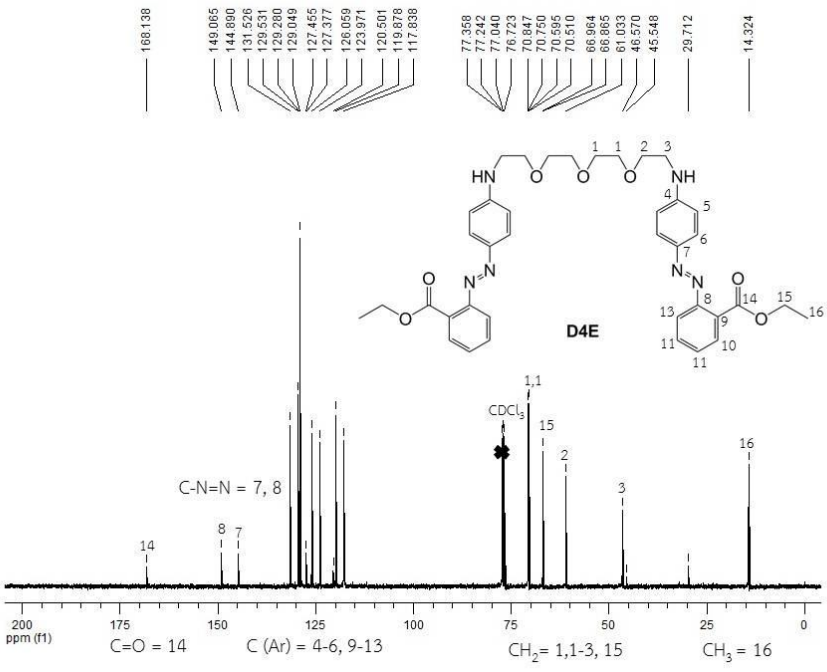

Figure A8 ^{13}C-NMR spectrum of **D4E** in $CDCl_3$ at 400 MHz

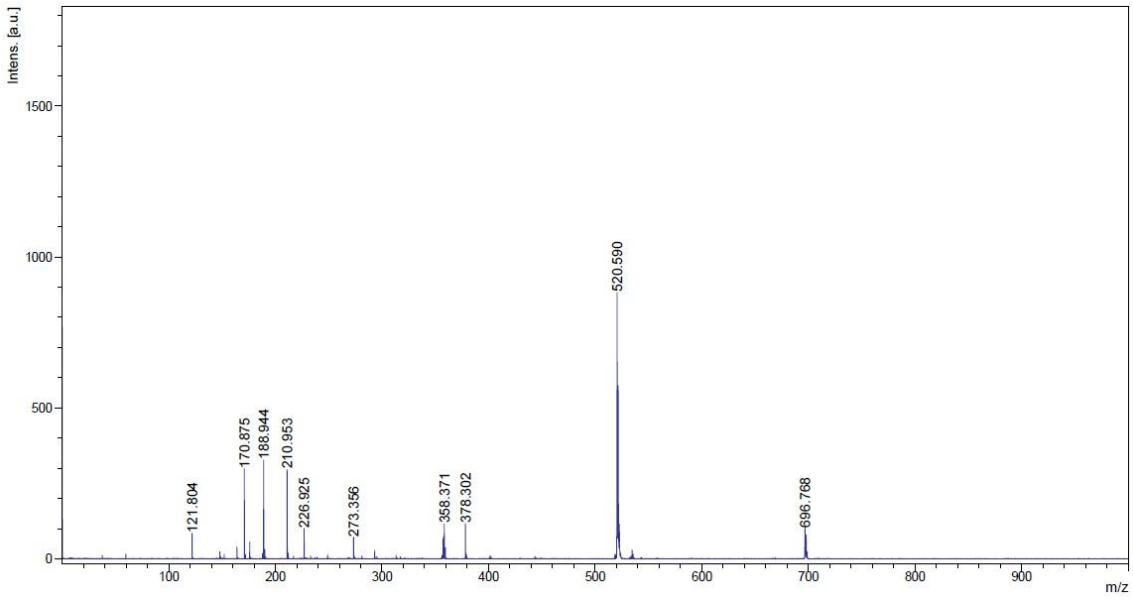

Figure A9 MALDI-TOF mass spectrum of **D4E** at 696.768 m/z

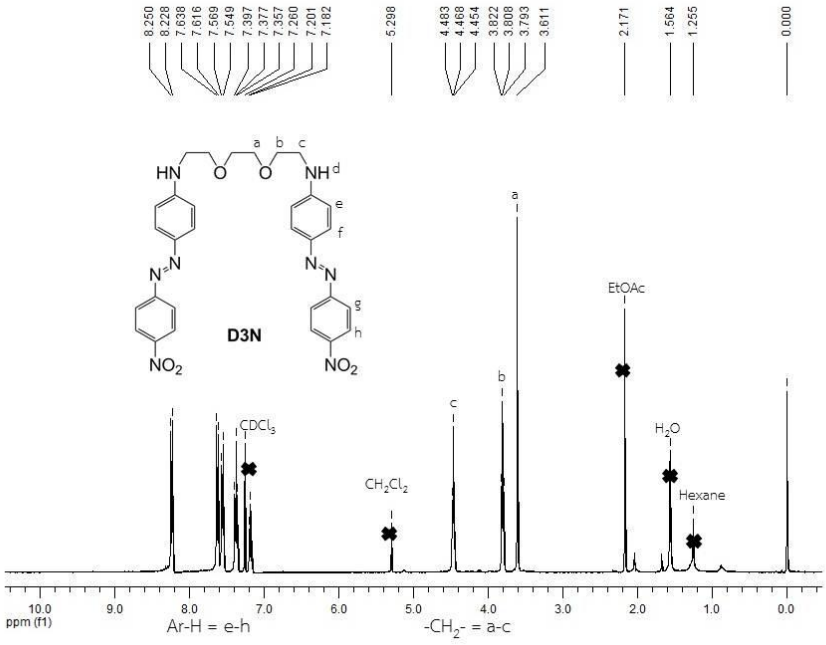

Figure A10 ^{1}H-NMR spectrum of **D3N** in $CDCl_3$ at 400 MHz

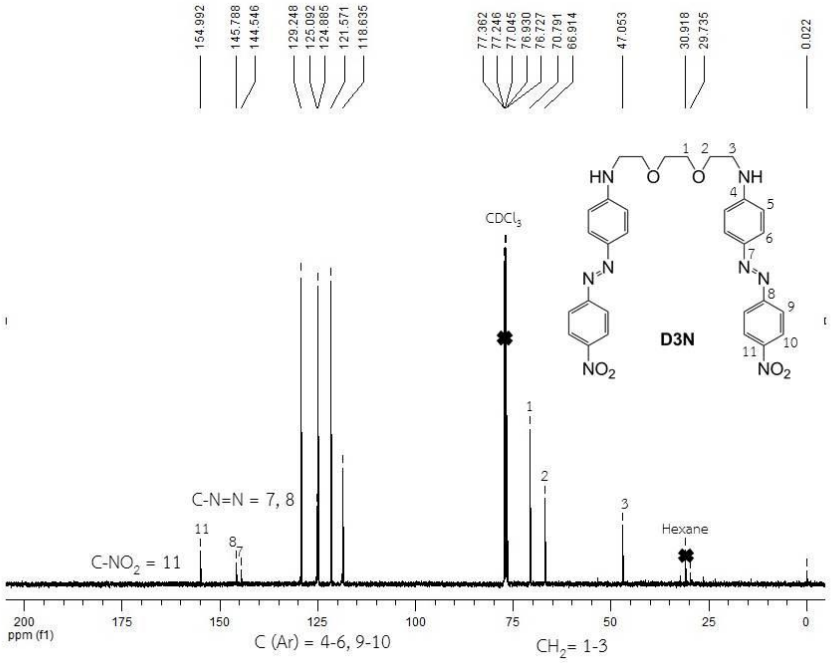

Figure A11 ^{13}C-NMR spectrum of **D3N** in $CDCl_3$ at 400 MHz

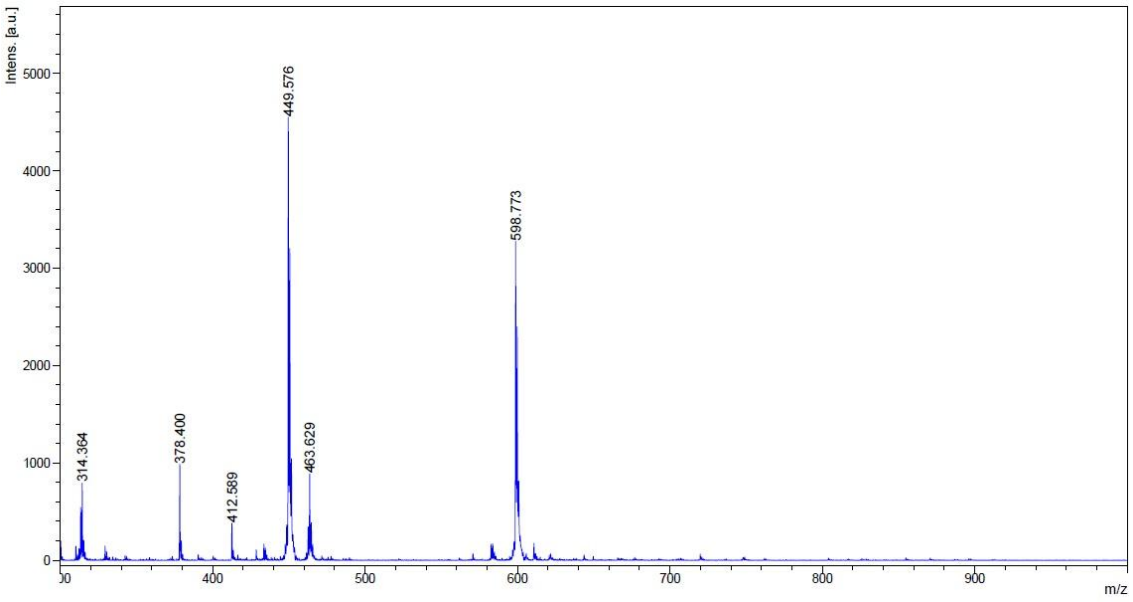

Figure A12 MALDI-TOF mass spectrum of **D3N** at 598.773 m/z

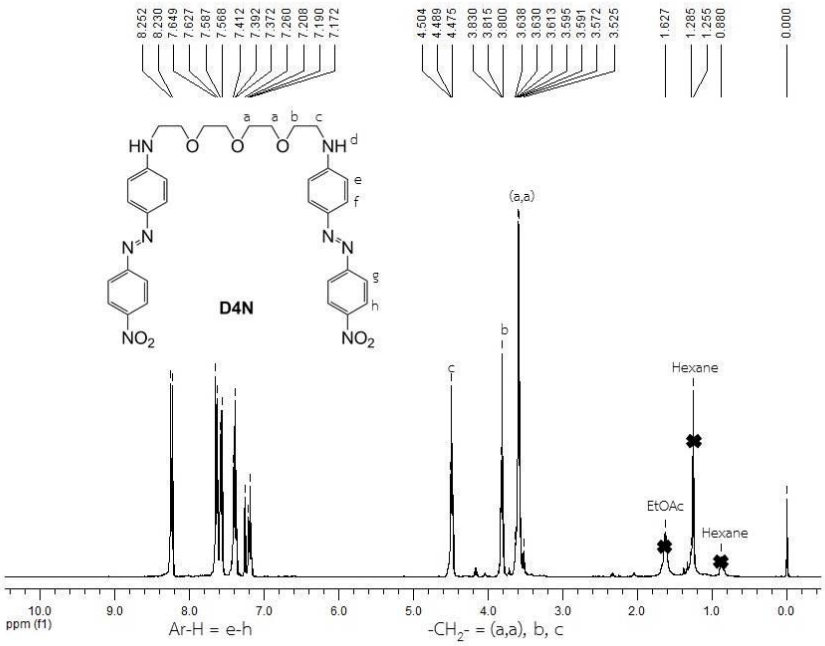

Figure A13 ^{1}H-NMR spectrum of **D4N** in $CDCl_3$ at 400 MHz

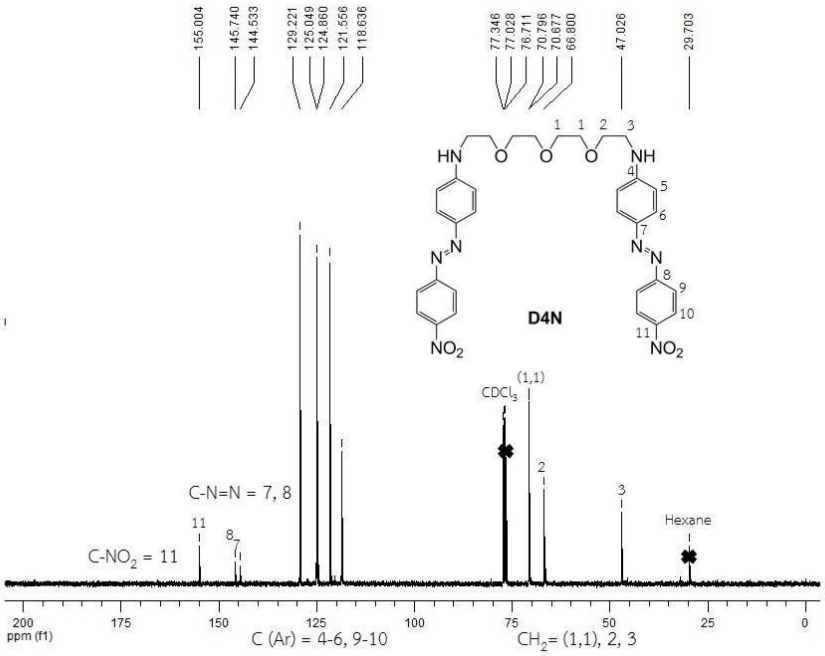

Figure A14 ^{13}C-NMR spectrum of **D4N** in $CDCl_3$ at 400 MHz

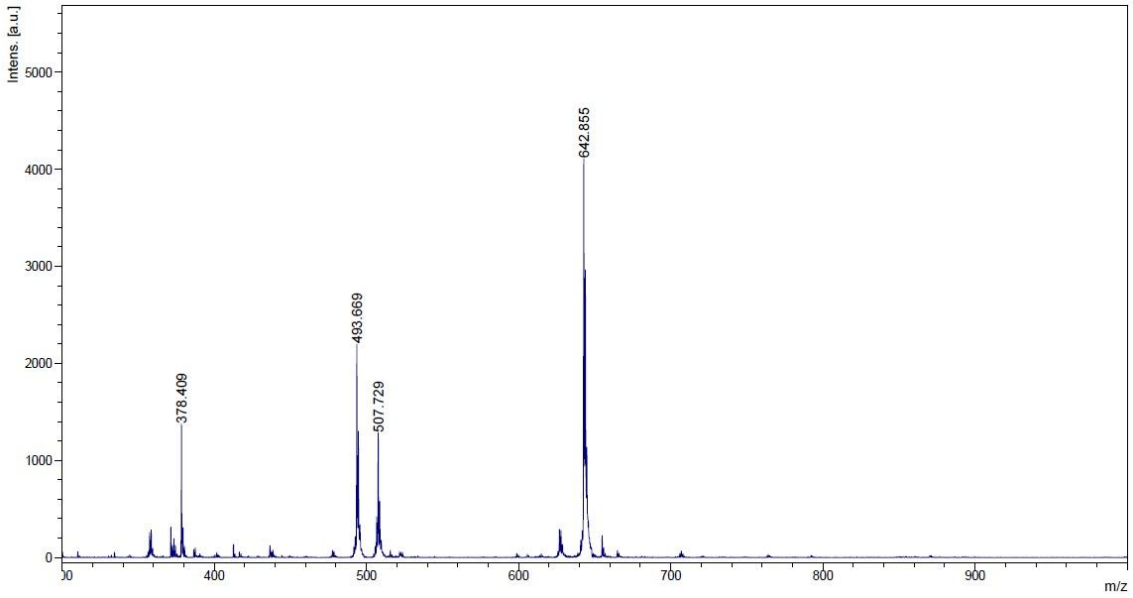

Figure A15 MALDI-TOF mass spectrum of **D4N** at 642.855 m/z

VITA

General Biographical Information

Mister Athip Anupan was born on 6th October 1989 in Lampang, Thailand. He has graduated with a high school diploma from Bunyawat Witthayalai School (Mathematics and Science Programme), Lampang in 2008. Then, he has graduated with the Bachelor's degree from department of Chemistry, faculty of Science, Chulalongkorn University in 2011. Afterwards, he was a Master degree student of Inorganic Chemistry and a member of Supramolecular Chemistry Research Unit (SCRU) at Chulalongkorn University under supervision of Assistant Professor Dr. Saowarux Fuangswasdi

Scholarship

2012-2013 Teaching Assistant Scholarship, Chulalongkorn University

Academic Experience

2016 Poster presentation at The 10th Pure and Applied Chemistry International Conference 2016 (PACCON2016), 9-11 February 2016, BITEC, Bangkok, Thailand